Supplementary Information (SI) for Organic Chemistry Frontiers.
This journal is © the Partner Organisations 2025

Supporting Information

Solvation and Temperature-Modulated Supramolecular Assembly of Amphiphilic Water-soluble Schiff Base-Containing Platinum(II) Complexes

Huilan Zhang,[a,b] Michael Ho-Yeung Chan,[b] Jonathan Lam,[b] Ming-Yi Leung,[b] Lixin Wu*[a] and Vivian Wing-Wah Yam*[a,b]

[a]State Key Laboratory of Supramolecular Structure and Materials and College of Chemistry, Jilin University, Changchun 130012, P. R. China.

[b]Institute of Molecular Functional Materials and Department of Chemistry, The University of Hong Kong, Pokfulam Road, Hong Kong SAR, P. R. China.

Photophysical Measurements and Instrumentation

^{1}H NMR and ^{13}C{^{1}H} NMR spectra were obtained on a Bruker DRX 500 (500 MHz) spectrometer at 298 K with chemical shifts reported relative to tetramethylsilane (Me_4Si). 2D ^{1}H–^{1}H NOESY NMR spectra were recorded on a Bruker DRX 600 (600 MHz) spectrometer at 298 K with chemical shifts reported relative to tetramethylsilane (Me_4Si). All MALDI-TOF mass spectra were recorded on a Autoflex speed TOF/TOF mass spectrometer. Elemental analysis was carried out on a Vario micro cube analyzer from Elementar. The single crystal structure was obtained on a R-AXIS RAPID X-ray single crystal diffractometer. UV−Vis absorption spectra were recorded using a Varian Cary 50 UV−vis spectrophotometer. Steady-state excitation and emission spectra at room temperature were obtained on an Edinburgh Instruments FS5 spectrofluorometer. The temperature-dependent UV−vis absorption spectra were obtained using a Varian Cary S-1 50 UV−vis spectrophotometer equipped with a Varian Cary single cell peltier thermostat. FT-IR spectra were collected on Bruker Vertex 80V Fourier transform infrared spectrometer. Dynamic light scattering (DLS) experiments were performed on a Malvern Zetasizer NanoZS instrument. TEM images were obtained with a JEM-2100F electron microscope operating at 200 kV. Cryo-TEM images were obtained with a FEI Talos F200C electron microscope operating at 20−100 kV. Atomic force

microscope (AFM) measurements were carried out on a Bruker FastScan atomic force microscope. X-Ray diffraction (XRD) data were recorded on a Rigaku X-ray diffractometer using Cu-Kα radiation at a wavelength of 1.542 Å.

Computational Details

All calculations were performed using the Gaussian16 suite of programs[1] on research computing facilities offered by Information Technology Services at the University of Hong Kong.

Geometries for **1** and **7** were optimized in dichloromethane using the Perdew-Burke-Ernzerhof parameter-free hybrid functional[2,3] (PBE0) in conjunction with the Solvation Model based on Density (SMD)[4]. This was followed by the calculation of vibrational frequencies at the same level of theory to verify that each is a minimum (NIMAG = 0) on the potential energy surface. The Stuttgart effective core potentials (ECPs) and the associated basis set were used to describe platinum[5] with an f-type polarization function ($\zeta = 0.993$),[6] whereas the remainder of the complex was described using the 6-31G (d,p) basis set.[7–10] These calculations were performed on the ground state (S_0) and lowest-lying triplet excited state (T_1) of **1** and **7**.

For the case of the dimer $\mathbf{7}_2$, geometry optimization was performed at the same level in three different solvents (*n*-hexane, dichloromethane and water). Furthermore, platinum centers were described using the Stuttgart ECPs and the associated basis set, with two f-type polarization functions ($\zeta = 0.70$ and 0.14).[11] All remaining atoms were described using 6-31G (d,p) basis set, as in the monomer case. Both S_0 and T_1 states of dimer $\mathbf{7}_2$ were fully optimized in this way.

On the basis of the optimized ground-state geometries, time-dependent DFT (TDDFT)[12–14] calculations were performed at the same level of theory, with the number of states (singlet only) set to 50. Using the calculated singlet–singlet transitions, simulated UV−Vis spectra were generated by the wavefunction analysis software Multiwfn.[15] In principle, emission maximal wavelength should be simulated using the optimized T_1 geometry. However, due to the poor performance of TDDFT in describing the triplet states of transition metal complexes at their optimized T_1 structure, the phosphorescence emission energy is usually calculated at the S_0 state geometry to better correlate with experimental results. As such, the emission energies of **1** and **7** were also calculated using their S_0 structures.[16]

Non-covalent interactions were calculated with NCI plot,[17–19] which makes use of the electron

density and its gradient at critical points between molecules, and the resulting isosurfaces were modelled using Visual Molecular Dynamics (VMD) 1.9.3.[20] The interactions between monomers are depicted in NCI plot on a color spectrum, using blue for strong attractive interactions, green for weak van der Waals interactions and red for strong repulsive interactions. Cartesian coordinates of the S_0 and T_1 states of **1**, **7** and dimer $\mathbf{7}_2$ in their optimized geometries are given in **Tables S8–S17**. All DFT and TDDFT calculations were performed with a pruned (99,590) grid for numerical integration.

Temperature-Dependent Nucleation–Elongation Model in Curve Fitting

Temperature-dependent nucleation–elongation model[21,22] was developed by Meijer and coworkers and has been applied to fit the experimental data in the variable temperature UV−vis spectroscopic studies for complexes **2**–**4** in DMSO−water mixtures. All cooling curves obtained are performed at a slow cooling rate of 0.5 K min^{-1} to ensure that the self-assembly processes were under thermodynamic control.

Nucleation–Elongation Model

The nucleation and elongation regime are governed by the following equations (1) and (2) respectively.

$$\phi_n = K_a^{1/3} exp\left[\left(2/3\, K_a^{-1/3} - 1\right)\frac{h_e}{RT_e^2}(T - T_e)\right] \quad (1)$$

$$\phi_n = \phi_{SAT}\left(1 - exp\left[-\frac{h_e}{RT_e^2}(T - T_e)\right]\right) \quad (2)$$

ϕ_n is the degree of aggregation, and ϕ_{SAT} is a factor introduced to the equation such that ϕ_n/ϕ_{SAT} does not exceed unity. h_e is the molecular enthalpy released due to non-covalent interactions during elongation process, T_e is the elongation temperature, K_a is the dimensionless equilibrium constant of the nucleation process at T_e and R is the universal gas constant.

Moreover, the number-averaged degree of polymerization averaged over all active species in the elongation regime at a temperature T, $\langle N_n \rangle$, is given by equation (3) below:

$$\langle N_n(T) \rangle = \frac{1}{\sqrt{K_a}}\frac{\phi_n}{\phi_{SAT} - \phi_n} \quad (3)$$

Whereas the number-averaged degree of polymerization averaged over all active nucleated species at T_e, and is given by equation (4) as follows.

$$\langle N_n(T_e) \rangle = \frac{1}{\sqrt[3]{K_a}} \quad (4)$$

Determination of Distances Between Protons by ^{1}H–^{1}H NOESY Spectroscopy

For the ^{1}H–^{1}H NOESY spectra of complexes **2**–**5** in 10 % D_2O–DMSO-d_6, the integrals of the cross peaks in the NOESY spectra were extracted. Then the distance between H_b and H_e on the Schiff base ligand is assumed to be 2.30 Å based on the X-ray crystal structure of complex **1**, which is used as a standard. The distances between protons in close proximities were determined using the relation:[23]

$$\frac{A_1}{A_2} = \frac{r_2^6}{r_1^6} \quad (5)$$

Experimental Section

Materials and Reagent: 2-Hydroxy-4-methoxybenzaldehyde, 1,2-diaminobenzene, 2,4-dihydroxybenzaldehyde, 18-crown-6 and potassium tetrachloroplatinate(II) ($K_2[PtCl_4]$) (Chem. Pur., 98 %) were purchased from Energy Chemical Co, Ltd. Ethanol (C_2H_5OH), dimethyl sulfoxide (DMSO), tetrahydrofuran (THF), dichloromethane (CH_2Cl_2), acetonitrile (CH_3CN), potassium carbonate (K_2CO_3) and sodium sulphate (Na_2SO_4) were the products of Beijing Chemical Reagent Company. All commercially available reagents were of analytical grade and were used as received. All solvents were purified and distilled using standard procedures before use. 1,2-Diaminobenzene with different oxyalkyl chain[24] and triethylene glycol-pendant,[25] 13-(2,5,8,11-tetraoxadodecyl)-2,5,8,11-tetraoxatradecan-14-yl-4-methylbenzenesulfonate) (molecule A)[26,27] were synthesized according to previously reported literature procedures.

Sample Preparation

The samples for single crystal structure were prepared by layering of *n*-hexane into a concentrated dichloromethane solution of the complex **1**. The samples for TEM measurements were prepared by drop-casting the solutions onto a carbon grid, allowing the remaining solvent to evaporate. The samples for cryo-TEM measurements were prepared by drop-casting the solutions onto copper mesh and froze by liquid nitrogen. The samples for X-ray diffraction (XRD) pattern of a thin film were obtained by prepared by drop-casting the solutions onto the carbon grid, and the solvent was allowed to evaporate. Samples for FT-IR spectra were prepared by dropping the solutions onto CaF_2 pallet and allowing the remaining solvent to evaporate.

Synthesis

Experimental Procedures

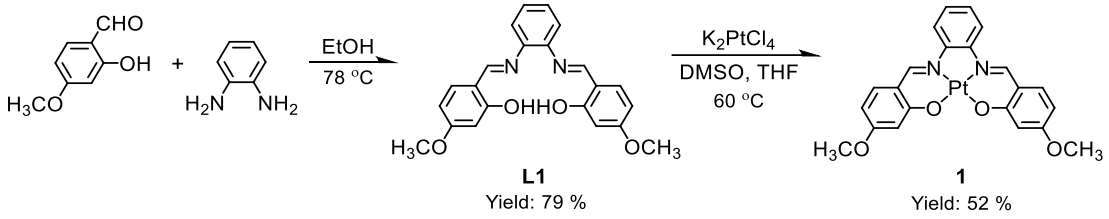

Scheme S1. Synthetic route for complex **1**.

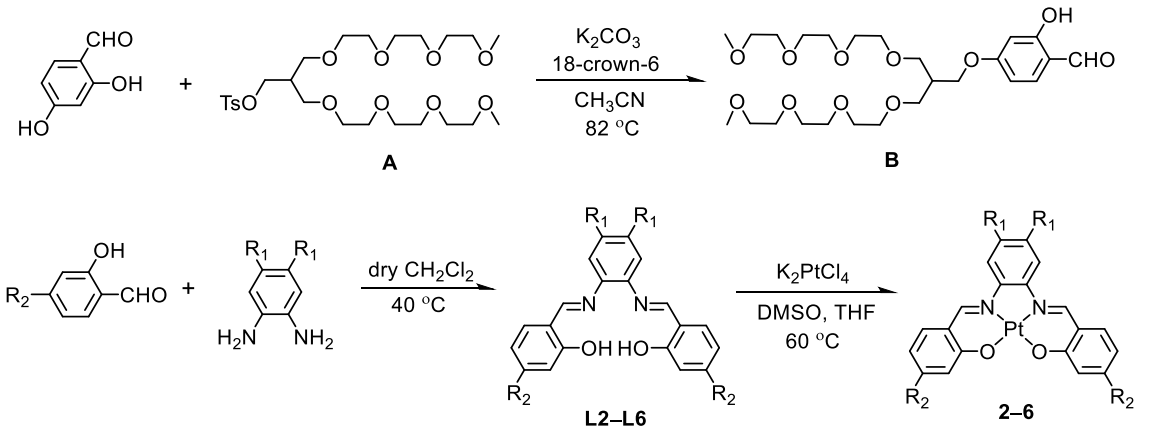

Scheme S2. Synthetic route for complexes **2–6**.

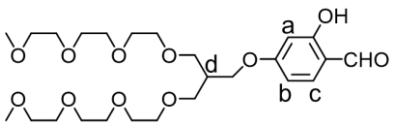

Molecule B. A mixture of 2,4-dihydroxybenzaldehyde (5.0 g, 36.2 mmol), **A** (12.6 g, 24.1 mmol), K_2CO_3 (5.0 g, 36.2 mmol) and a catalytic amount of 18-crown-6 were refluxed in 150 mL of acetonitrile for 24 h. The reaction mixture was then cooled to room temperature before pouring water (100 mL) into it. The reaction mixture was extracted with CH_2Cl_2 (3 × 100 mL) and washed with water several times. The organic layer was further washed with brine and dried over Na_2SO_4.

The residue after solvent evaporation was purified by silica-gel column chromatography with ethyl acetate-methanol (20:1 v/v) to give a yellow oil. Yield: 11.6 g (62 %). ^{1}H NMR (500 MHz, $CDCl_3$, 298 K) δ / ppm = 11.44 (s, 1H; –OH), 9.73 (s, 1H; –CHO), 7.44 (d, J = 8.7 Hz, 1H; H_a), 6.56 (dd, J = 8.7, 2.2 Hz, 1H; H_b), 6.47 (d, J = 2.2 Hz, 1H; H_c), 4.13 (d, J = 5.8 Hz, 2H; –OCH_2–), 3.65 (m, 16H; –OCH_2–), 3.61 (m, 8H; –OCH_2–), 3.56 (m, 4H; –OCH_2–), 3.40 (s, 6H; –OCH_3), 2.44 (m, 1H; H_d); ^{13}C{^{1}H} NMR (125 MHz, $CDCl_3$, 298 K) δ / ppm = 194.27, 166.30, 164.37, 135.19, 115.09, 108.51, 101.30, 71.85, 70.54, 70.43, 68.99, 66.54, 58.91, 39.70. Elemental analysis calcd (%) for $C_{25}H_{42}O_{11}$: C 57.90, H 8.16. Found: C 58.13, H 8.11. MALDI-TOF MS: calcd m/z = 518.27, found m/z = 518.69 $[M]^+$.

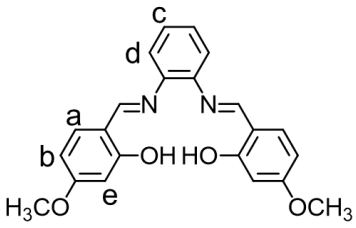

L1. A solution of the 1,2-diaminobenzene (1.0 g, 9.3 mmol) and 2-hydroxy-4-methoxybenzaldehyde (2.8 g, 18.5 mmol) was refluxed in ethanol under nitrogen for 12 h. The reaction mixture was then cooled to room temperature. The yellow precipitate was filtered and recrystallized from ethanol to give a yellow solid. Yield: 2.8 g (79 %). ^{1}H NMR (500 MHz, $CDCl_3$, 298 K) δ / ppm = 13.61 (s, 2H; –OH), 8.57 (s, 2H; –NCH–), 7.32 (m, 2H; H_d), 7.28 (d, J = 8.6 Hz, 2H; H_a), 7.24 (m, 2H; H_c), 6.57 (d, J = 2.4 Hz, 2H; H_e), 6.50 (dd, J = 8.6, 2.4 Hz, 2H; H_b), 3.85 (s, 6H; –OCH_3); ^{13}C{^{1}H} NMR (125 MHz, $CDCl_3$, 298 K) δ / ppm = 164.29, 164.14, 162.20, 142.30, 133.57, 127.15, 119.48, 113.26, 107.28, 101.24, 55.45. Elemental analysis calcd (%) for $C_{22}H_{20}N_2O_4$: C 70.20, H 5.36, N 7.44. Found: C 70.51, H 5.59, N 7.23. MALDI-TOF MS: calcd m/z = 376.14, found m/z = 377.38 $[M]^+$.

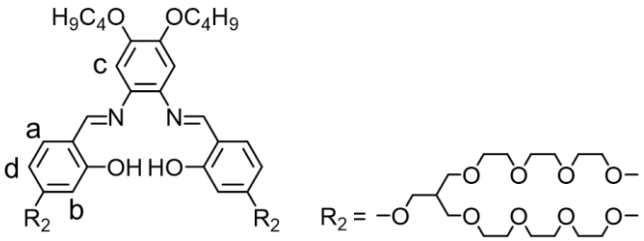

L2. A solution of the **B** (2.1 g, 4.0 mmol), 1,2-diamino-4,5-dibutoxybenzene (500 mg, 2.0 mmol) and a few drops of glacial acetic acid was refluxed for about 12 h in dry CH_2Cl_2 under nitrogen. The

reaction mixture was then cooled to room temperature and washed with brine and dried over Na_2SO_4. The residue after solvent evaporation was purified by silica-gel column chromatography with ethyl acetate-methanol (15:1 v/v) to give an orange oil. Yield: 2.1 g (85 %). ^{1}H NMR (500 MHz, $CDCl_3$, 298 K) δ / ppm = 13.54 (s, 2H; –OH), 8.48 (s, 2H; –NCH–), 7.21 (d, J = 8.6 Hz, 2H; H_a), 6.77 (s, 2H; H_c), 6.51 (d, J = 2.3 Hz, 2H; H_b), 6.45 (dd, J = 8.6, 2.3 Hz, 2H; H_d), 4.05 (t, J = 6.0 Hz, 8H; –OCH_2–), 3.63 (m, 32H; –OCH_2–), 3.58 (m, 16H; –OCH_2–), 3.51 (m, 8H; –OCH_2–), 3.34 (s, 12H; –OCH_3), 2.39 (m, 2H; –$CH(OCH_2)_2$–), 1.83 (m, 4H; –CH_2–), 1.52 (m, 4H; –CH_2–), 0.98 (t, J = 7.4 Hz, 6H; –CH_3); ^{13}C{^{1}H} NMR (125 MHz, $CDCl_3$, 298 K) δ / ppm = 163.72, 163.31, 160.85, 148.57, 135.27, 133.27, 113.35, 107.14, 105.40, 102.04, 71.92, 70.62, 70.50, 70.47, 69.52, 69.21, 66.20, 59.00, 39.82, 31.36, 19.24, 13.88. Elemental analysis calcd (%) for $C_{64}H_{104}N_2O_{22}$: C 61.32, H 8.36, N 2.23. Found: C 61.54, H 8.19, N 2.47. MALDI-TOF MS: calcd m/z = 1252.71, found m/z = 1252.64 $[M]^+$.

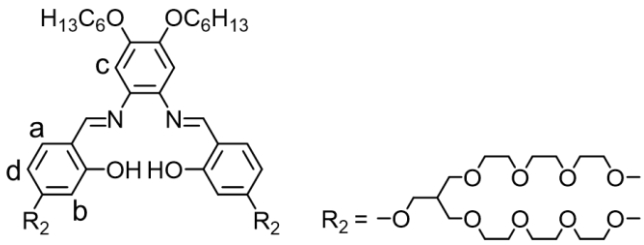

L3. The procedure was similar to that described for the synthesis of **L2**, except 1,2-diamino-4,5-dihexyloxybenzene (617 mg, 2.0 mmol) was used in place of 1,2-diamino-4,5-dibutoxybenzene. The crude product was purified by silica-gel column chromatography with ethyl acetate-methanol (15:1 v/v) to give an orange oil. Yield: 2.3 g (87 %). ^{1}H NMR (500 MHz, $CDCl_3$, 298 K) δ / ppm = 13.58 (s, 2H; –OH), 8.52 (s, 2H; –NCH–), 7.25 (d, J = 8.6 Hz, 2H; H_a), 6.80 (s, 2H; H_c), 6.54 (d, J = 2.4 Hz, 2H; H_b), 6.48 (dd, J = 8.6, 2.4 Hz, 2H; H_d), 4.07 (m, 8H; –OCH_2–), 3.65 (m, 48H; –OCH_2–), 3.56 (m, 8H; –OCH_2–), 3.38 (s, 12H; –OCH_3), 2.43 (m, 2H; –$CH(OCH_2)_2$–), 1.87 (m, 4H; –CH_2–), 1.52 (m, 4H; –CH_2–), 1.37 (m, 8H; –CH_2–), 0.94 (t, J = 6.9 Hz, 6H; –CH_3); ^{13}C{^{1}H} NMR (125 MHz, $CDCl_3$, 298 K) δ / ppm = 163.73, 163.31, 160.85, 148.55, 135.26, 133.26, 113.36, 107.14, 105.37, 102.05, 71.93, 70.63, 70.51, 70.48, 69.82, 69.22, 66.21, 59.01, 39.83, 31.59, 29.28, 25.71, 22.61, 14.03. Elemental analysis calcd (%) for $C_{68}H_{112}N_2O_{22}$: C 62.36, H 8.62, N 2.14. Found: C 62.08, H 8.49, N 2.17. MALDI-TOF MS: calcd m/z = 1308.77, found m/z = 1308.56 $[M]^+$.

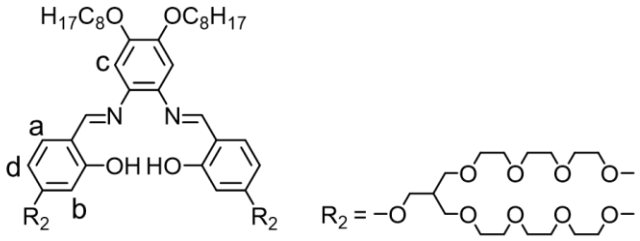

L4. The procedure was similar to that described for the synthesis of **L2**, except 1,2-diamino-4,5-dioctyloxybenzene (729 mg, 2.0 mmol) was used in place of 1,2-diamino-4,5-dibutoxybenzene. The crude product was purified by silica-gel column chromatography with ethyl acetate-methanol (15:1 v/v) to give an orange oil. Yield: 2.3 g (84 %). ^{1}H NMR (500 MHz, $CDCl_3$, 298 K) δ / ppm = 13.57 (s, 2H; –OH), 8.52 (s, 2H; –NCH–), 7.25 (d, J = 8.6 Hz, 2H; H_a), 6.80 (s, 2H; H_c), 6.55 (d, J = 2.3 Hz, 2H; H_b), 6.48 (dd, J = 8.6, 2.3 Hz, 2H; H_d), 4.09 (m, 8H; –OCH_2–), 3.65 (m, 48H; –OCH_2–), 3.56 (m, 8H; –OCH_2–), 3.38 (s, 12H; –OCH_3), 2.43 (m, 2H; –$CH(OCH_2)_2$–), 1.87 (m, 4H; –CH_2–), 1.52 (m, 4H; –CH_2–), 1.35 (m, 16H; –CH_2–), 0.91 (t, J = 7.1 Hz, 6H; –CH_3); ^{13}C{^{1}H} NMR (125 MHz, $CDCl_3$, 298 K) δ / ppm = 163.72, 163.30, 160.82, 148.55, 135.24, 133.26, 113.34, 107.15, 105.35, 102.03, 71.90, 70.60, 70.48, 69.81, 69.20, 66.20, 58.99, 39.81, 31.81, 29.37, 29.31, 29.27, 26.04, 22.66, 14.10. Elemental analysis calcd (%) for $C_{72}H_{120}N_2O_{22}$: C 63.32, H 8.86, N 2.05. Found: C 63.11, H 8.93, N 2.34. MALDI-TOF MS: calcd m/z = 1364.83, found m/z = 1364.98 $[M]^+$.

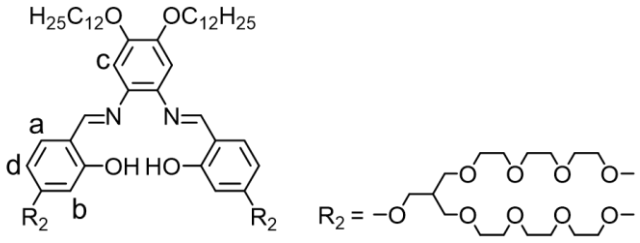

L5. The procedure was similar to that described for the synthesis of **L2**, except 1,2-diamino-4,5-didodecyloxybenzene (954 mg, 2.0 mmol) was used in place of 1,2-diamino-4,5-dibutoxybenzene. The crude product was purified by silica-gel column chromatography with ethyl acetate-methanol (15:1 v/v) to give an orange oil. Yield: 2.4 g (82 %). ^{1}H NMR (500 MHz, $CDCl_3$, 298 K) δ / ppm = 13.57 (s, 2H; –OH), 8.51 (s, 2H; –NCH–), 7.24 (d, J = 8.6 Hz, 2H; H_a), 6.80 (s, 2H; H_c), 6.54 (d, J = 2.3 Hz, 2H; H_b), 6.48 (dd, J = 8.6, 2.3 Hz, 2H; H_d), 4.09 (m, 8H; –OCH_2–), 3.63 (m, 48H; –OCH_2–), 3.56 (m, 8H; –OCH_2–), 3.38 (s, 12H; –OCH_3), 2.43 (m, 2H; –$CH(OCH_2)_2$–), 1.87 (m, 4H; –CH_2–), 1.52 (m, 4H; –CH_2–), 1.36 (m, 32H; –CH_2–), 0.90 (t, J = 7.1 Hz, 6H; –CH_3); ^{13}C{^{1}H} NMR (125 MHz, $CDCl_3$, 298 K) δ / ppm = 163.74, 163.32, 160.84, 148.57, 135.26, 133.43, 113.36,

107.15, 105.39, 102.05, 71.93, 70.63, 70.51, 70.48, 69.84, 69.22, 69.09, 66.21, 29.66, 29.52, 29.44, 29.37, 26.16, 26.06, 22.69, 14.12. Elemental analysis calcd (%) for $C_{80}H_{136}N_2O_{22}$: C 65.01, H 9.28, N 1.90. Found: C 65.28, H 9.13, N 2.02. MALDI-TOF MS: calcd *m/z* = 1476.96, found *m/z* = 1477.07 $[M]^+$.

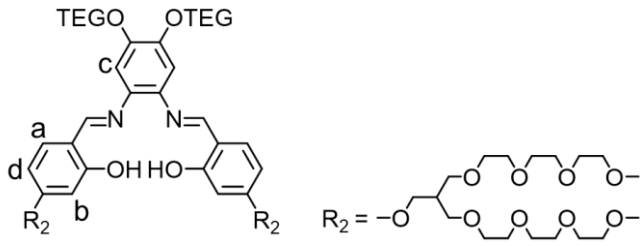

L6. The procedure was similar to that described for the synthesis of **L2**, except 1,2-diamino-4,5-bis(2-(2-(2-methoxyethoxy)ethoxy)ethoxy)benzene (865 mg, 2.0 mmol) was used in place of 1,2-diamino-4,5-dibutoxybenzene. The crude product was purified by silica-gel column chromatography with ethyl acetate-methanol (10:1 v/v) to give an orange oil. Yield: 2.2 g (78 %). ^{1}H NMR (500 MHz, $CDCl_3$, 298 K) δ / ppm = 13.52 (s, 2H; –OH), 8.51 (s, 2H; –NCH–), 7.26 (d, J = 8.6 Hz, 2H; H_a), 6.87 (s, 2H; H_c), 6.55 (d, J = 2.4 Hz, 2H; H_b), 6.49 (dd, J = 8.6, 2.4 Hz, 2H; H_d), 4.26 (t, J = 4.8 Hz, 4H; –OCH_2–), 4.09 (d, J = 5.6 Hz, 4H; –OCH_2–), 3.92 (t, J = 4.9 Hz, 4H; –OCH_2–), 3.78 (m, 4H; –OCH_2–), 3.71 (m, 4H; –OCH_2–), 3.66 (m, 36H; –OCH_2–), 3.62 (m, 16H; –OCH_2–), 3.56 (m, 12H; –OCH_2–), 3.39 (s, 18H; –OCH_3), 2.43 (m, 2H; –$CH(OCH_2)_2$–); ^{13}C{^{1}H} NMR (125 MHz, $CDCl_3$, 298 K) δ / ppm = 163.74, 163.38, 161.11, 148.26, 135.87, 133.36, 113.32, 107.21, 106.34, 102.02, 71.92, 70.85, 70.62, 70.56, 70.50, 70.48, 69.80, 69.42, 69.21, 66.21, 59.01, 39.81. Elemental analysis calcd (%) for $C_{70}H_{116}N_2O_{28}$: C 58.64, H 8.16, N 1.95. Found: C 58.79, H 8.01, N 1.73. MALDI-TOF MS: calcd *m/z* = 1432.77 found *m/z* = 1433.14 $[M]^+$.

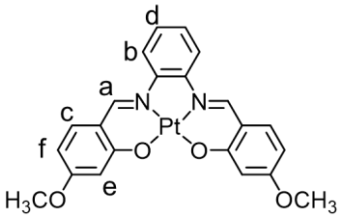

1. A solution of the Schiff base ligand **L1** (45 mg, 0.12 mmol) and K_2CO_3 (50 mg, 0.36 mmol) was stirred for about 0.5 h in dry THF under nitrogen at 60 ºC. Then, a DMSO (2 mL) solution of $K_2[PtCl_4]$ (50 mg, 0.12 mmol) was added to the reaction mixture, which was continuously stirred for 3 days under nitrogen at 60 ºC. The reaction mixture was extracted with CH_2Cl_2 and washed

with water several times. The organic layer was further washed with brine and dried over Na_2SO_4. The residue after solvent evaporation was recrystallized using dichloromethane/hexane to give an orange solid. Yield: 36 mg (52 %). ^{1}H NMR (500 MHz, $CDCl_3$, 298 K) δ / ppm = 8.68 (s, 2H; H_a), 7.92 (dd, J = 6.2, 3.2 Hz, 2H; H_b), 7.44 (d, J = 8.9 Hz, 2H; H_c), 7.30 (d, J = 3.2 Hz, 2H; H_d), 6.90 (d, J = 2.4 Hz, 2H; H_e), 6.45 (dd, J = 8.9, 2.4 Hz, 2H; H_f), 3.88 (s, 6H; –OCH_3); ^{13}C{^{1}H} NMR (125 MHz, $CDCl_3$, 298 K) δ / ppm = 167.98, 166.13, 147.22, 135.70, 126.82, 116.37, 114.91, 109.37, 103.26, 55.54, 29.72. Elemental analysis calcd (%) for $C_{22}H_{18}N_2O_4Pt$: C 46.40, H 3.19, N 4.92. Found: C 46.11, H 3.28, N 5.14. MALDI-TOF MS: calcd m/z = 569.09, found m/z = 569.52 $[M]^+$.

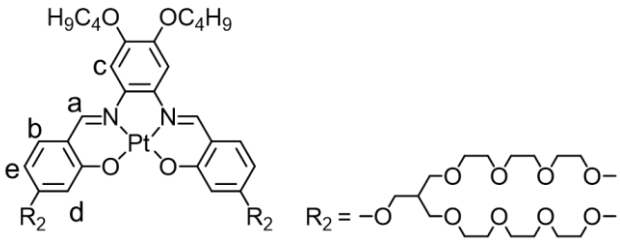

2. A solution of the Schiff base ligand **L2** (150 mg, 0.12 mmol) and K_2CO_3 (50 mg, 0.36 mmol) was stirred for about 0.5 h in dry THF under nitrogen at 60 ºC. Then, a DMSO (2 mL) solution of $K_2[PtCl_4]$ (50 mg, 0.12 mmol) was added to the reaction mixture, which was continuously stirred for 3 days under nitrogen at 60 ºC. The reaction mixture was extracted with CH_2Cl_2 and washed with water several times. The organic layer was further washed with brine and dried over Na_2SO_4. The residue after solvent evaporation was purified by silica-gel column chromatography with ethyl acetate-methanol (10:1 v/v) and subsequent purification by layering of hexane into a concentrated dichloromethane solution of **2** afforded a yellow oil. Yield: 101 mg (58 %). ^{1}H NMR (500 MHz, $CDCl_3$, 298 K) δ / ppm = 8.33 (s, 2H; H_a), 7.35 (d, J = 8.9 Hz, 2H; H_b), 7.21 (s, 2H; H_c), 6.81 (d, J = 2.0 Hz, 2H; H_d), 6.35 (dd, J = 8.8, 2.1 Hz, 2H; H_e), 4.05 (m, 8H; –OCH_2–), 3.62 (m, 48H; –OCH_2–), 3.54 (m, 8H; –CH_2–), 3.36 (s, 12H; –OCH_3), 2.43 (m, 2H; –$CH(OCH_2)_2$–), 1.83 (m, 4H; –CH_2–), 1.53 (m, 4H; –CH_2–), 1.01 (t, J = 7.4 Hz; –CH_3); ^{13}C{^{1}H} NMR (125 MHz, $CDCl_3$, 298 K) δ / ppm = 166.99, 165.16, 148.44, 145.87, 138.31, 135.49, 116.44, 108.72, 103.86, 99.06, 71.93, 70.70, 70.64, 70.51, 69.56, 69.25, 66.22, 59.02, 40.99, 39.80, 31.29, 19.24, 13.94. Elemental analysis calcd (%) for $C_{64}H_{102}N_2O_{22}Pt$: C 53.14, H 7.11, N 1.94. Found: C 53.41, H 7.32, N 2.07. MALDI-TOF MS: calcd m/z = 1445.66, found m/z = 1445.13 $[M]^+$.

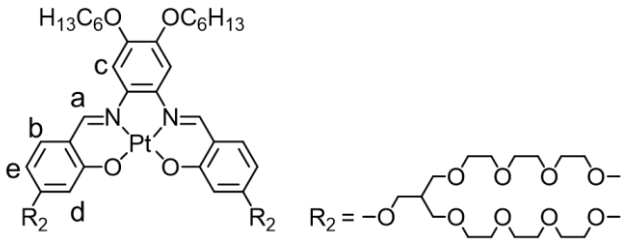

3. The procedure was similar to that described for the synthesis of complex **2**, except Schiff base ligand **L3** (157 mg, 0.12 mmol) was used in place of Schiff base ligand **L2**. The crude product was purified by silica-gel column chromatography with ethyl acetate-methanol (10:1 v/v) and subsequent purification by layering of hexane into a concentrated dichloromethane solution of **3** afforded a yellow oil. Yield: 99 mg (55 %). ^{1}H NMR (500 MHz, $CDCl_3$, 298 K) δ / ppm = 8.40 (s, 2H; H_a), 7.41 (d, J = 8.9 Hz, 2H; H_b), 7.29 (s, 2H; H_c), 6.86 (d, J = 2.1 Hz, 2H; H_d), 6.41 (dd, J = 8.9, 2.2 Hz, 2H; H_e), 4.10 (m, 8H; –OCH_2–), 3.66 (m, 48H; –OCH_2–), 3.57 (m, 8H; –CH_2–), 3.39 (s, 12H; –OCH_3), 2.45 (m, 2H; –$CH(OCH_2)_2$–), 1.89 (m, 4H; –CH_2–), 1.53 (m, 4H; –CH_2–), 1.40 (m, 8H; –CH_2–), 0.96 (t, J = 6.8 Hz, 6H; –CH_3); ^{13}C{^{1}H} NMR (125 MHz, $CDCl_3$, 298 K) δ / ppm = 167.11, 165.22, 148.53, 145.93, 138.42, 135.46, 120.03, 116.45, 108.80, 103.95, 99.08, 71.94, 70.71, 70.64, 70.51, 69.90, 69.28, 66.26, 59.03, 39.80, 31.61, 29.21, 25.70, 22.62, 14.05. Elemental analysis calcd (%) for $C_{68}H_{110}N_2O_{22}Pt$: C 54.35, H 7.38, N 1.86. Found: C 54.09, H 7.55, N 1.78. MALDI-TOF MS: calcd *m/z* = 1501.72, found *m/z* = 1501.21 $[M]^+$.

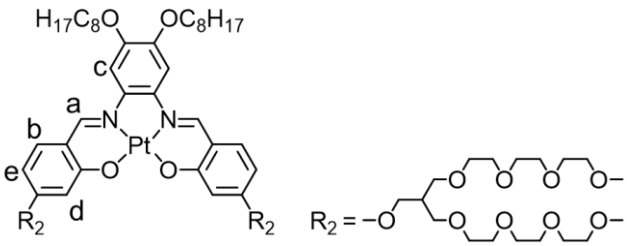

4. The procedure was similar to that described for the synthesis of complex **2**, except Schiff base ligand **L4** (164 mg, 0.12 mmol) was used in place of Schiff base ligand **L2**. The crude product was purified by silica-gel column chromatography with ethyl acetate-methanol (10:1 v/v) and subsequent purification by layering of hexane into a concentrated dichloromethane solution of **4** afforded a yellow oil. Yield: 107 mg (57 %). ^{1}H NMR (500 MHz, $CDCl_3$, 298 K) δ / ppm = 8.41 (s, 2H; H_a), 7.41 (d, J = 8.9 Hz, 2H; H_b), 7.30 (s, 2H; H_c), 6.86 (d, J = 2.1 Hz, 2H; H_d), 6.42 (dd, J =

8.9, 2.1 Hz, 2H; H_e), 4.11 (m, 8H; –OCH_2–), 3.68 (m, 48H; –OCH_2–), 3.54 (m, 8H; –OCH_2–), 3.39 (s, 12H; –OCH_3), 2.45 (m, 2H; –$CH(OCH_2)_2$–), 1.91 (m, 4H; –CH_2–), 1.56 (m, 4H; –CH_2–), 1.36 (m, 16H; –CH_2–), 0.96 (t, J = 6.4 Hz, 6H; –CH_3); $^{13}C\{^1H\}$ NMR (125 MHz, $CDCl_3$, 298 K) δ / ppm = 167.17, 165.24, 148.59, 145.96, 138.50, 135.43, 116.43, 108.82, 103.99, 99.16, 71.93, 70.70, 70.64, 70.51, 69.94, 69.27, 66.26, 59.03, 39.79, 31.84, 29.40, 29.29, 26.05, 22.69, 14.12. Elemental analysis calcd (%) for $C_{72}H_{118}N_2O_{22}Pt$: C 55.48, H 7.63, N 1.80. Found: C 55.73, H 7.59, N 1.59. MALDI-TOF MS: calcd m/z = 1557.78, found m/z = 1557.24 $[M]^+$.

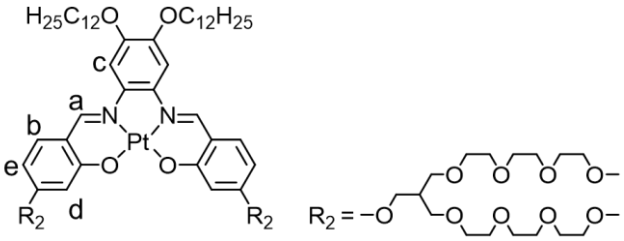

5. The procedure was similar to that described for the synthesis of complex **2**, except Schiff base ligand **L5** (177 mg, 0.12 mmol) was used in place of Schiff base ligand **L2**. The crude product was purified by silica-gel column chromatography with ethyl acetate-methanol (10:1 v/v) and subsequent purification by layering of hexane into a concentrated dichloromethane solution of **5** afforded a yellow oil. Yield: 112 mg (56 %). ^1H NMR (500 MHz, $CDCl_3$, 298 K) δ / ppm = 8.39 (s, 2H; H_a), 7.40 (d, J = 8.9 Hz, 2H; H_b), 7.28 (s, 2H; H_c), 6.85 (d, J = 2.3 Hz, 2H; H_d), 6.40 (dd, J = 8.9, 2.3 Hz, 2H; H_e), 4.10 (m, 8H; –OCH_2–), 3.65 (m, 48H; –OCH_2–), 3.56 (m, 8H; –OCH_2–), 3.39 (s, 12H; –OCH_3), 2.45 (m, 2H; –$CH(OCH_2)_2$–), 1.89 (m, 4H; –CH_2–), 1.54 (m, 4H; –CH_2–), 1.41 (m, 4H; –CH_2–), 1.31 (m, 28H; –CH_2–), 0.90 (t, J = 6.7 Hz, 6H; –CH_3); $^{13}C\{^1H\}$ NMR (125 MHz, $CDCl_3$, 298 K) δ / ppm = 167.04, 165.18, 148.45, 145.89, 138.35, 135.46, 116.44, 108.77, 103.89, 99.05, 71.92, 70.70, 70.63, 70.50, 69.85, 69.24, 66.24, 59.01, 39.79, 31.93, 29.73, 29.67, 29.47, 29.38, 29.24, 26.04, 22.69, 14.12. Elemental analysis calcd (%) for $C_{80}H_{134}N_2O_{22}Pt$: C 57.50, H 8.08, N 1.68. Found: C 57.74, H 7.89, N 1.77. MALDI-TOF MS: calcd m/z = 1669.91, found m/z = 1669.57 $[M]^+$.

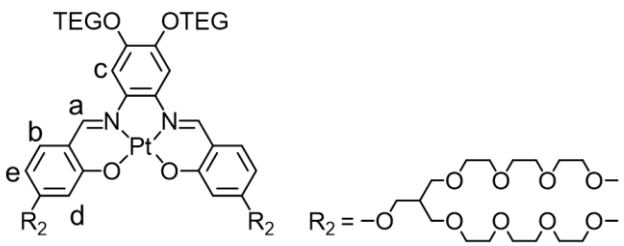

6. The procedure was similar to that described for the synthesis of complex **2**, except Schiff base ligand **L6** (172 mg, 0.12 mmol) was used in place of Schiff base ligand **L2**. The crude product was purified by silica-gel column chromatography with ethyl acetate-methanol (10:1 v/v) and subsequent purification by layering of hexane into a concentrated dichloromethane solution of **6** afforded a yellow oil. Yield: 105 mg (54 %). ^{1}H NMR (500 MHz, $CDCl_3$, 298 K) δ / ppm = 8.43 (s, 2H; H_a), 7.43 (d, J = 8.9 Hz, 2H; H_b), 7.41 (s, 2H; H_c), 6.85 (d, J = 2.1 Hz, 2H; H_d), 6.39 (dd, J = 8.9, 2.1 Hz, 2H; H_e), 4.28 (t, J = 4.5 Hz, 4H; –OCH_2–), 4.09 (d, J = 5.5 Hz, 4H; –OCH_2–), 3.94 (t, J = 4.5 Hz, 4H; –OCH_2–), 3.79 (m, 4H; –OCH_2–), 3.72 (m, 4H; –OCH_2–) 3.65 (m, 48H; –OCH_2–), 3.56 (m, 12H; –OCH_2–), 3.39 (s, 12H; –OCH_3), 3.36 (s, 6H; –OCH_3), 2.45 (m, 2H; –$CH(OCH_2)_2$–); ^{13}C{^{1}H} NMR (125 MHz, $CDCl_3$, 298 K) δ / ppm = 166.94, 165.17, 147.98, 146.42, 138.59, 135.61, 116.53, 108.78, 103.78, 99.94, 71.93, 70.85, 70.70, 70.64, 70.51, 69.67, 69.37, 69.25, 66.24, 59.01, 58.93, 39.80. Elemental analysis calcd (%) for $C_{70}H_{114}N_2O_{28}Pt$: C 51.68, H 7.06, N 1.72. Found: C 51.41, H 7.34, N 1.69. MALDI-TOF MS: calcd m/z = 1625.72, found m/z = 1625.56 $[M]^+$.

NMR Spectra

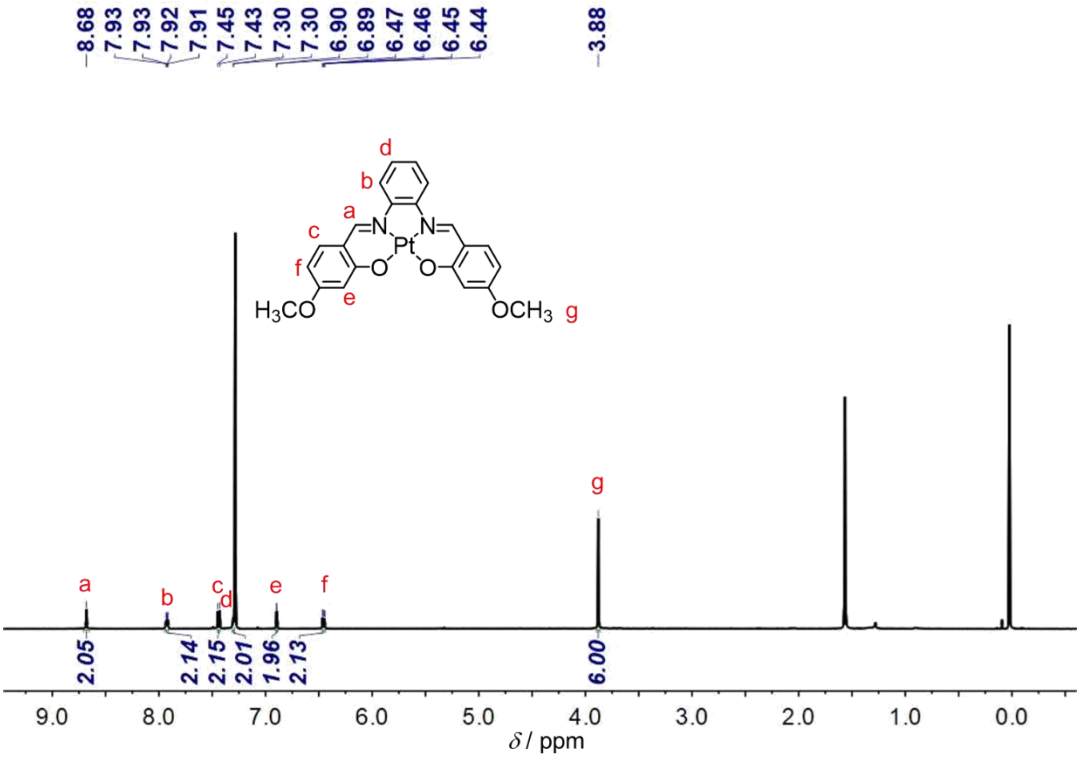

Figure S1. ^{1}H NMR spectrum of **1** in $CDCl_3$ at 298 K.

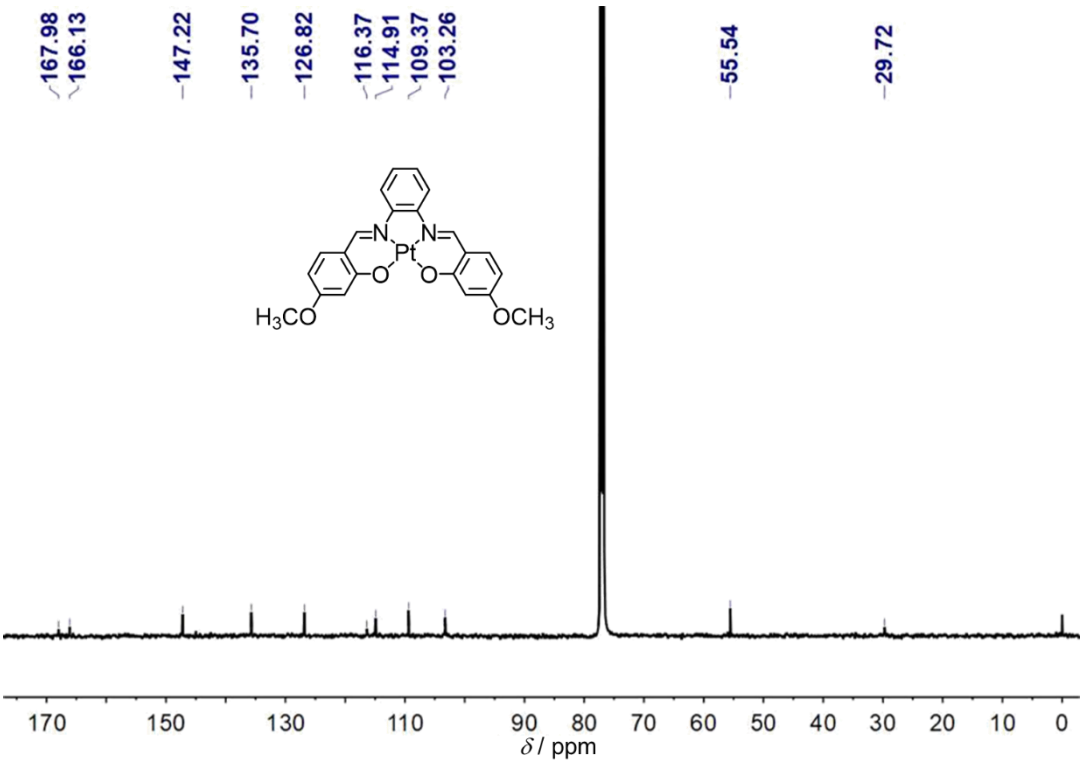

Figure S2. $^{13}C\{^{1}H\}$ NMR spectrum of **1** in $CDCl_3$ at 298 K.

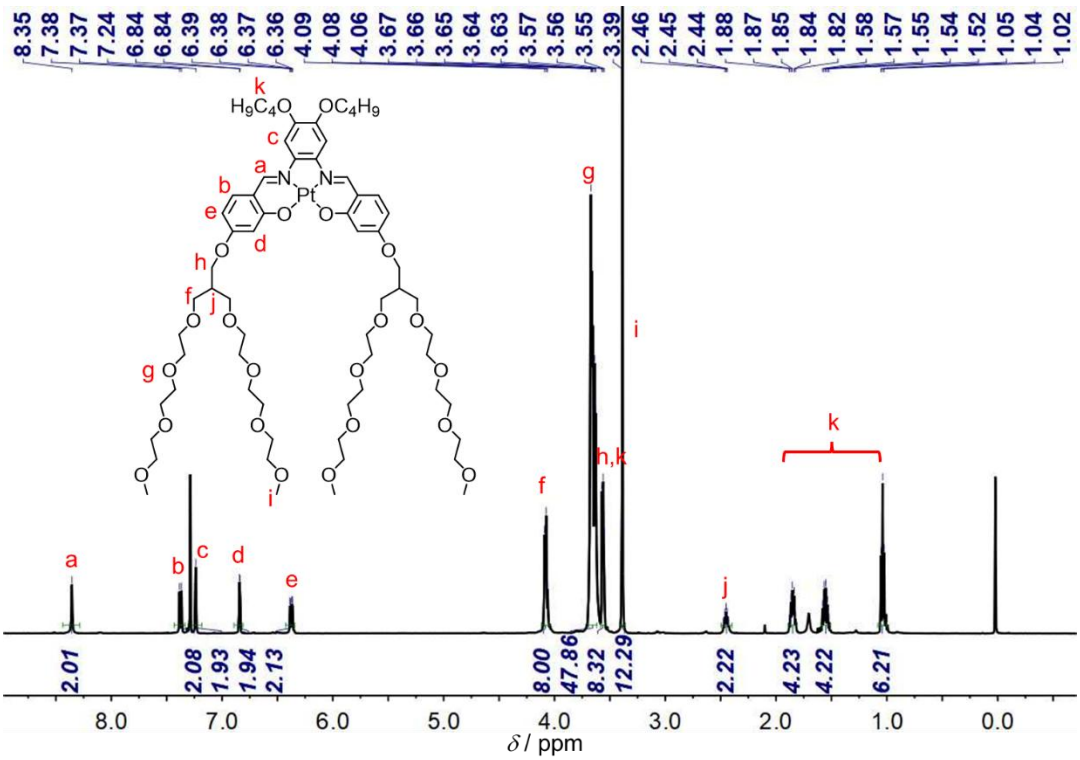

Figure S3. ^{1}H NMR spectrum of **2** in $CDCl_3$ at 298 K.

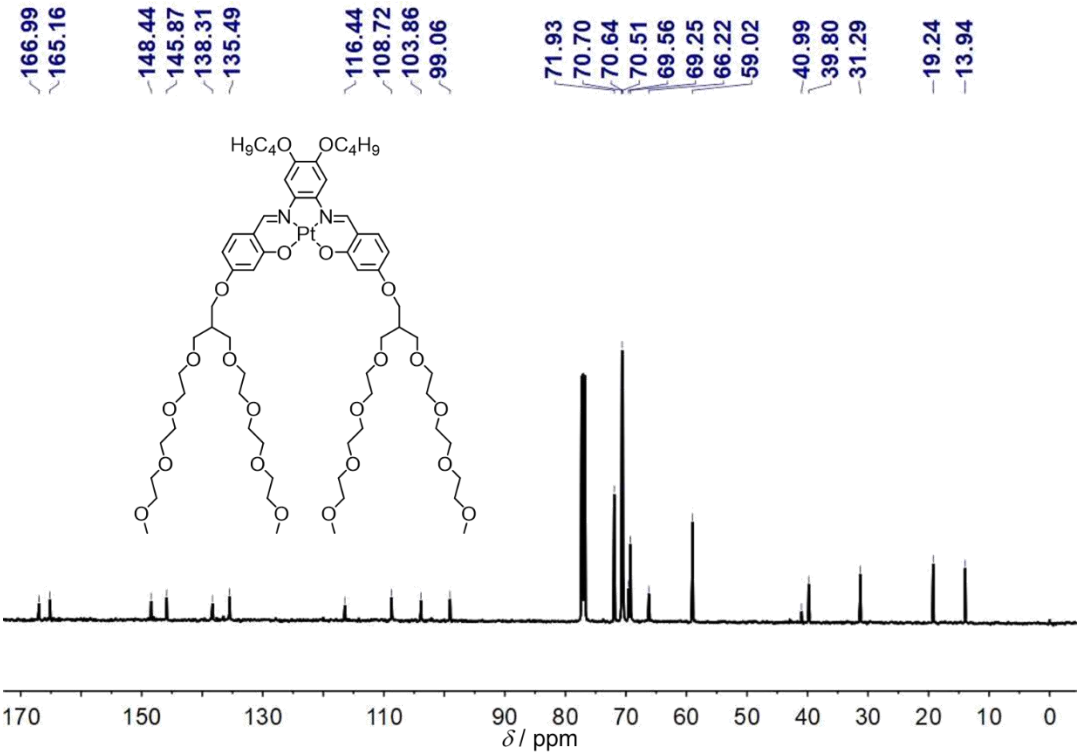

Figure S4. $^{13}C\{^{1}H\}$ NMR spectrum of **2** in $CDCl_3$ at 298 K.

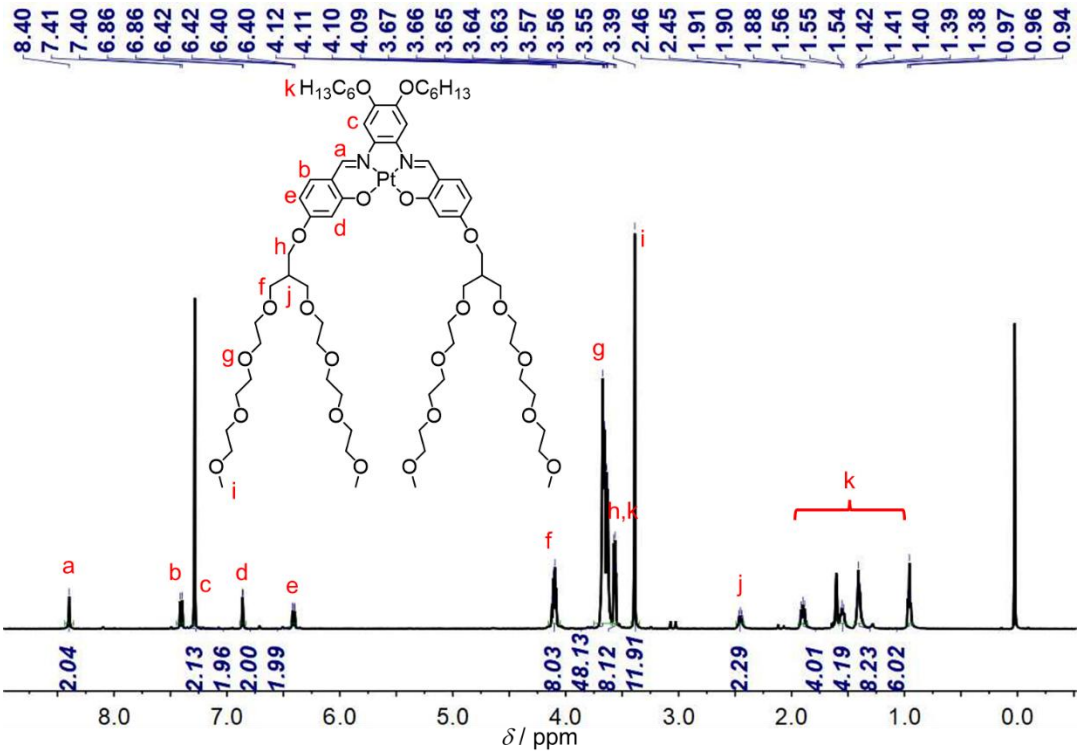

Figure S5. ^{1}H NMR spectrum of **3** in $CDCl_3$ at 298 K.

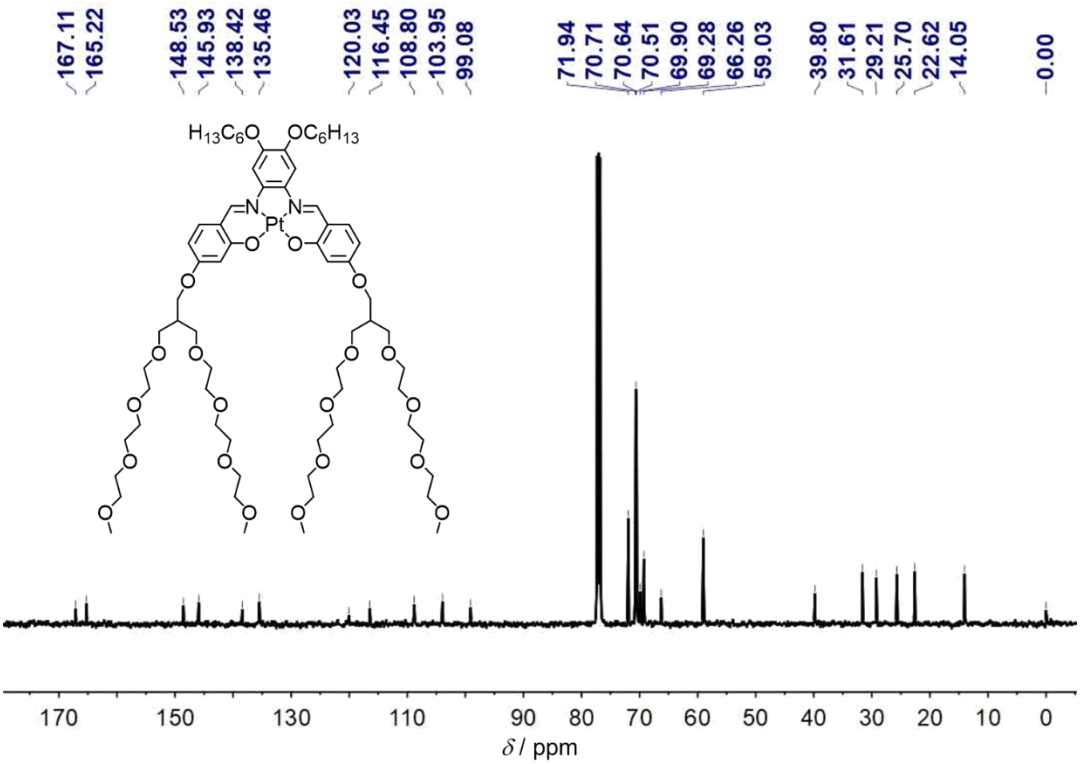

Figure S6. $^{13}C\{^{1}H\}$ NMR spectrum of **3** in $CDCl_3$ at 298 K.

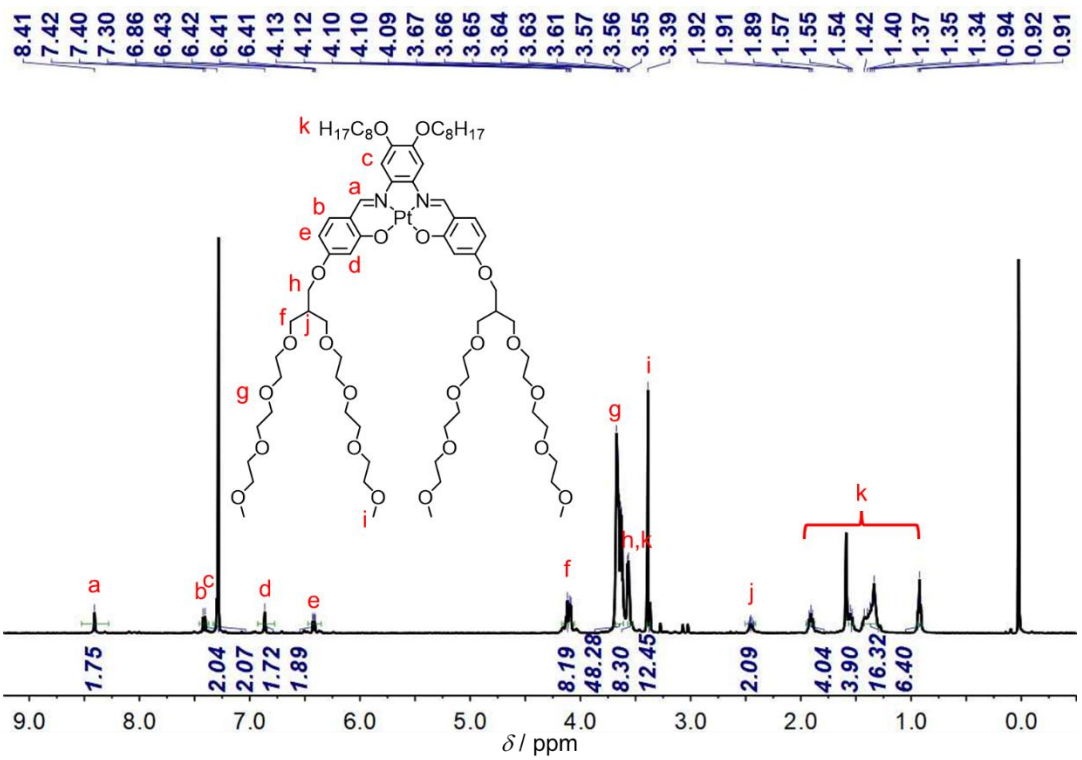

Figure S7. ^{1}H NMR spectrum of **4** in $CDCl_3$ at 298 K.

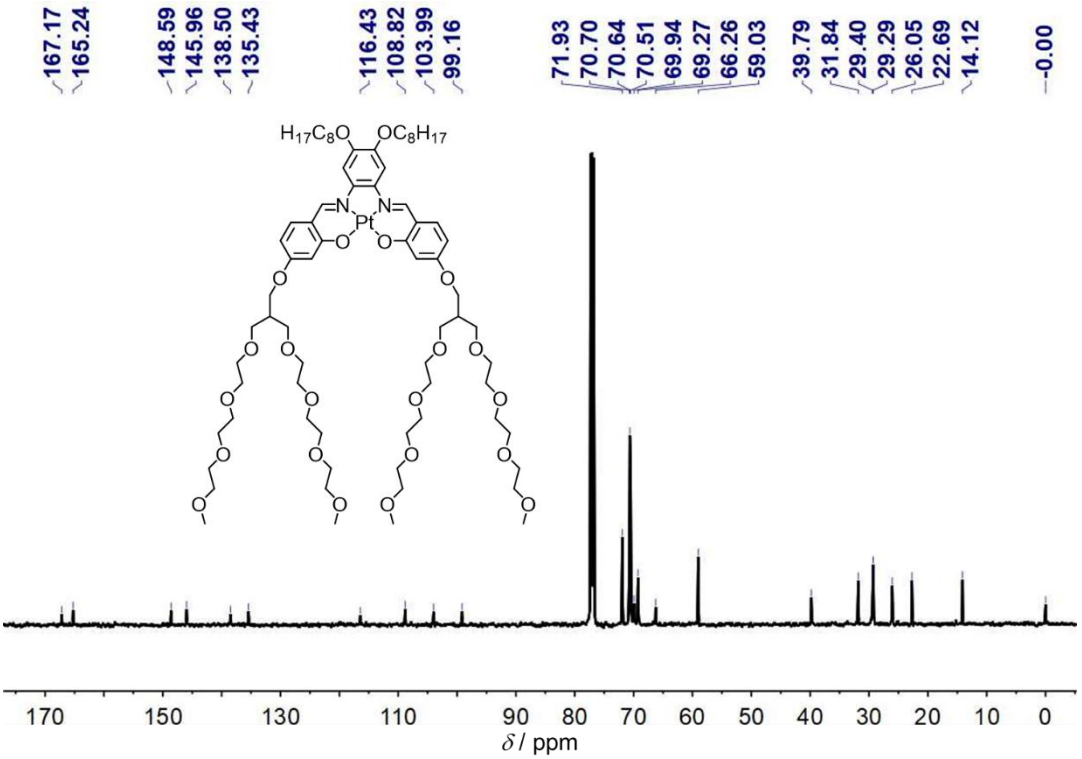

Figure S8. $^{13}C\{^{1}H\}$ NMR spectrum of **4** in $CDCl_3$ at 298 K.

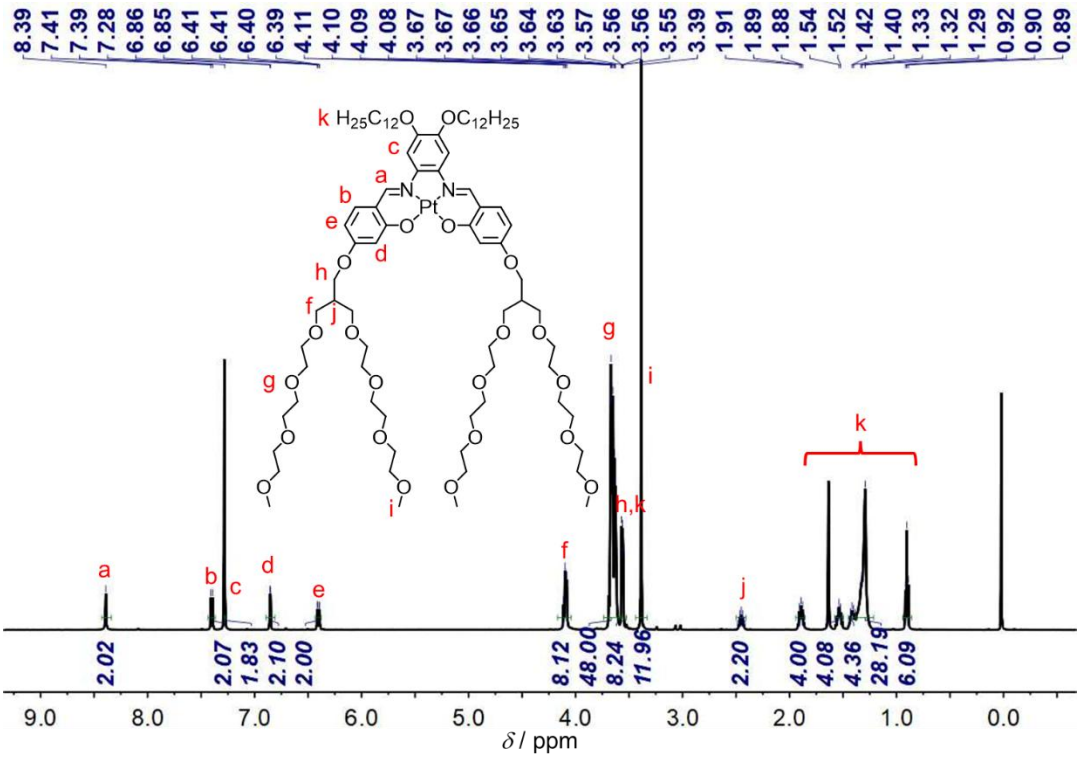

Figure S9. ^{1}H NMR spectrum of **5** in $CDCl_3$ at 298 K.

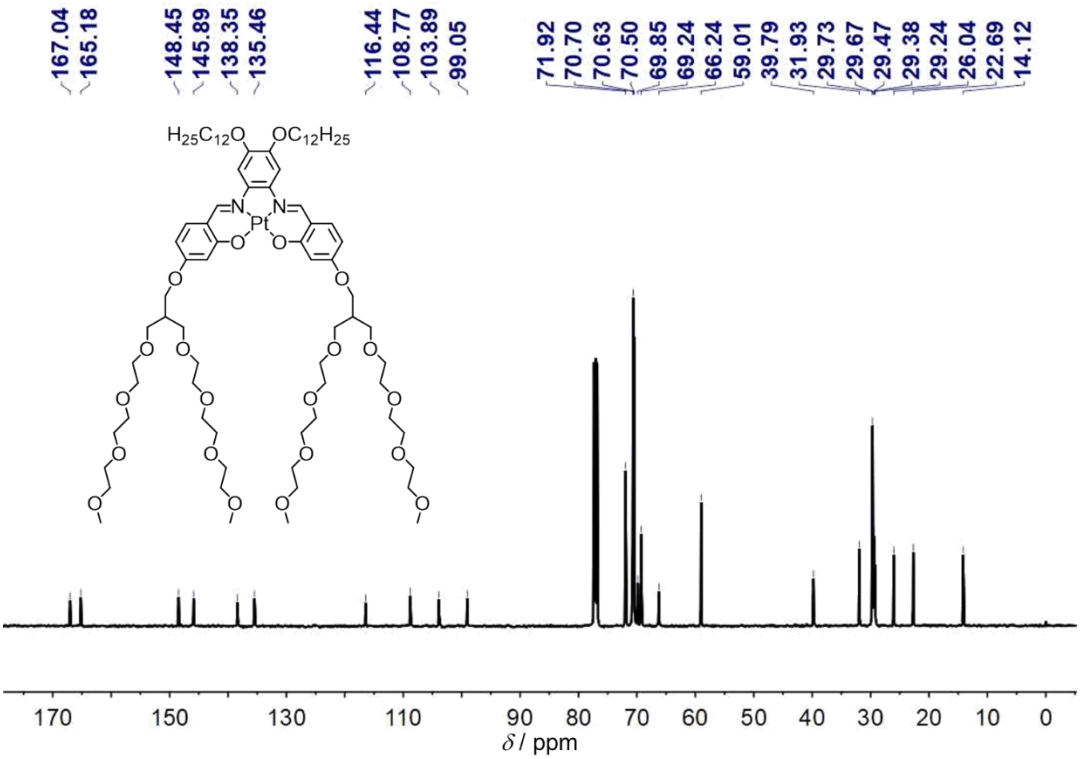

Figure S10. $^{13}C\{^{1}H\}$ NMR spectrum of **5** in $CDCl_3$ at 298 K.

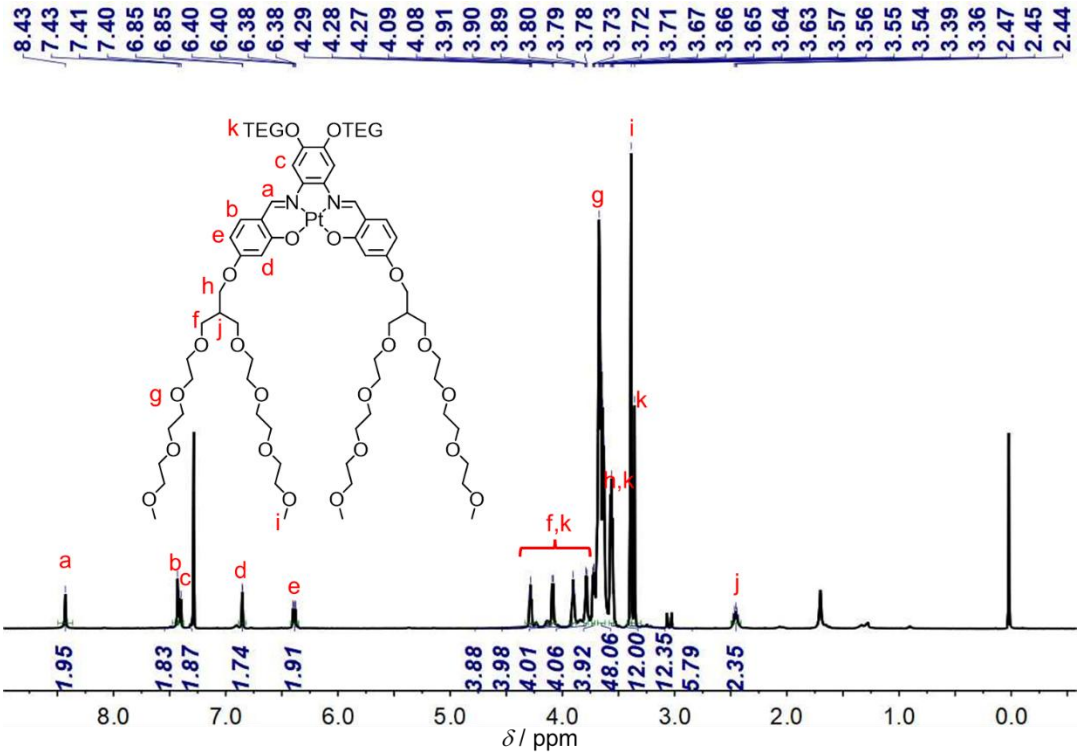

Figure S11. ^{1}H NMR spectrum of **6** in $CDCl_3$ at 298 K.

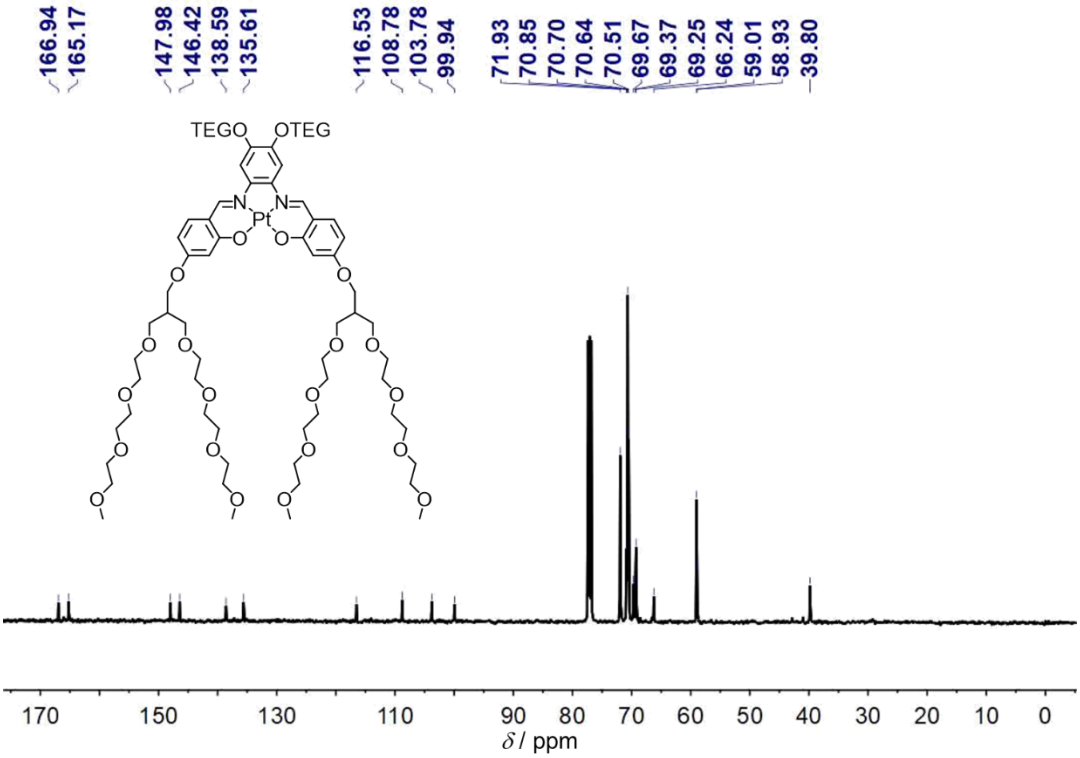

Figure S12. $^{13}C\{^{1}H\}$ NMR spectrum of **6** in $CDCl_3$ at 298 K.

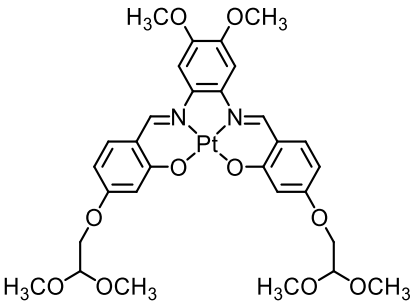

Figure S13. Structure of complex **7** used in the computational study.

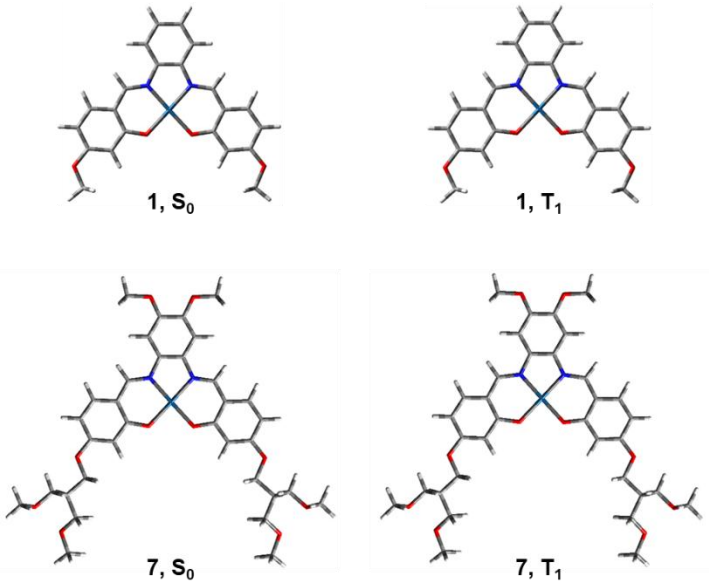

Figure S14. Optimized ground state (S_0) and lowest energy triplet excited state (T_1) geometries for **1** and **7**.

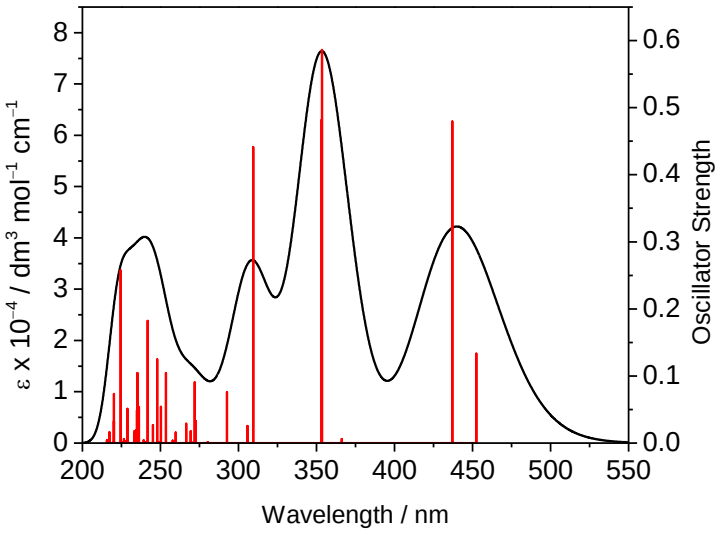

Figure S15. Simulated absorption spectrum of **7**. The heights of the vertical straight lines are the calculated oscillator strengths of the corresponding vertical transitions.

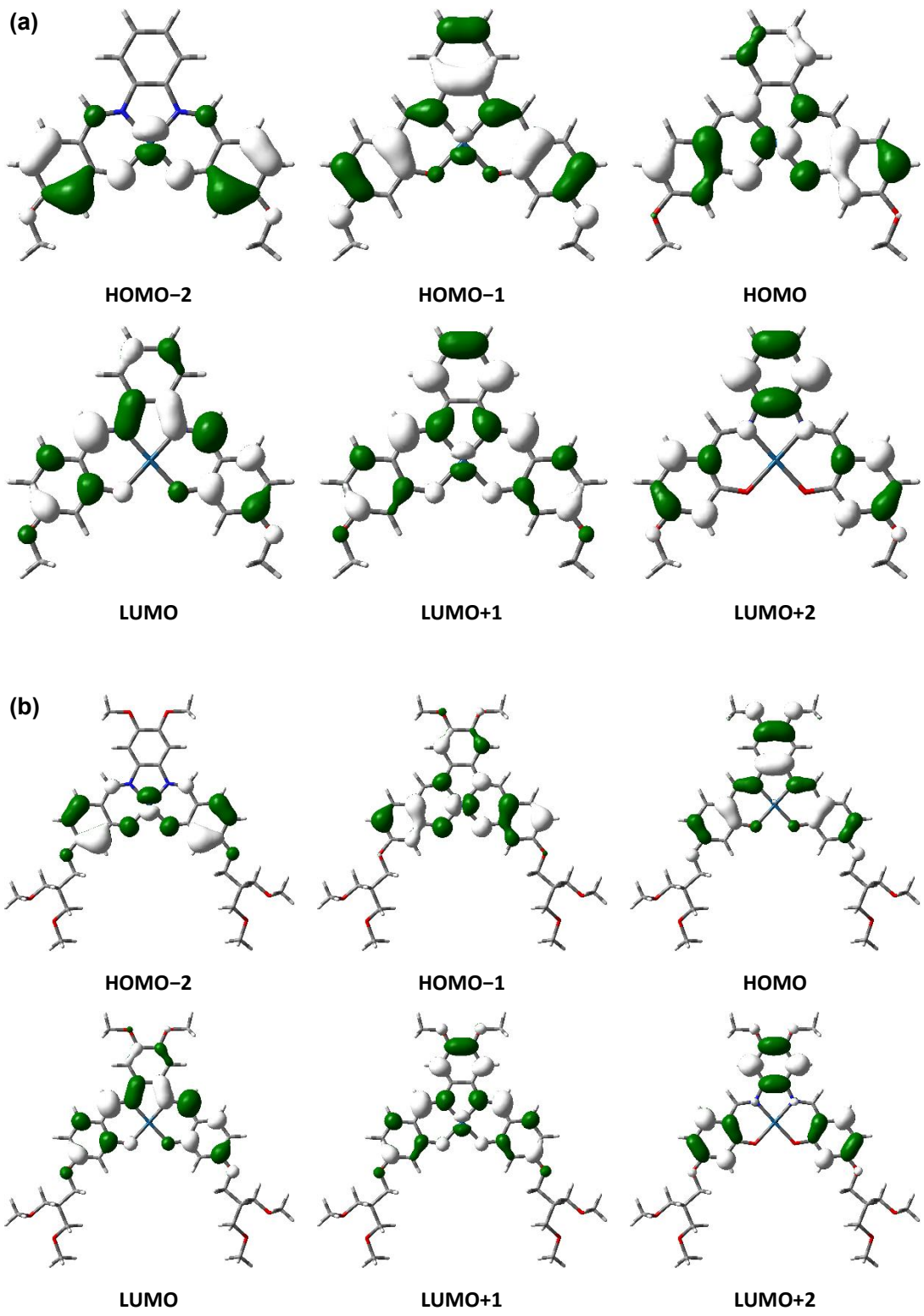

Figure S16. Spatial plots (isovalue = 0.03) of selected molecular orbitals of (a) **1** and (b) **7** at the ground-state (S_0) geometry.

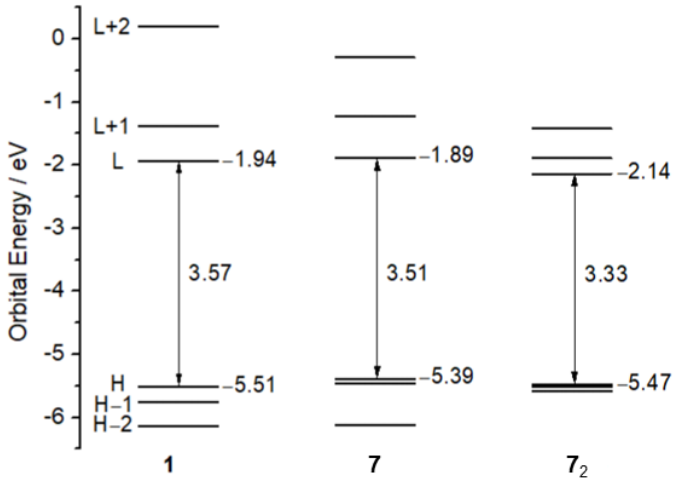

Figure S17. Orbital energy diagram of **1**, **7** and the dimer $\mathbf{7}_2$, with H=HOMO and L=LUMO.

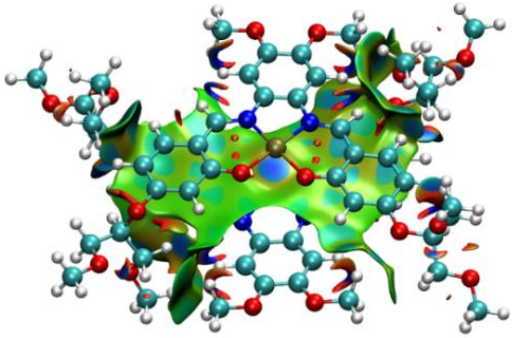

Figure S18. Isosurface plot of noncovalent interactions calculated in the dimer of **7** in *n*-hexane solution, with a Pt···Pt internuclear distance of 3.397 Å. The range of $\lambda_2 \times \rho(\mathbf{r})$ used for the plots is −0.020 to + 0.020 au at s = 0.5 au.

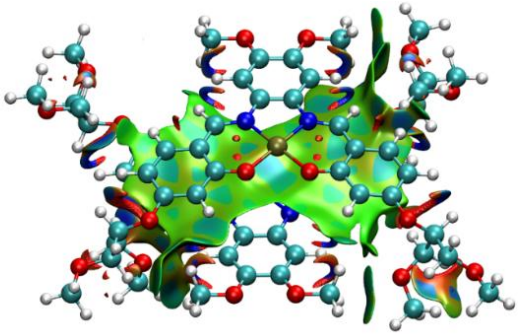

Figure S19. Isosurface plot of noncovalent interactions calculated in the dimer of **7** in dichloromethane solution, with a Pt···Pt internuclear distance of 3.678 Å. The range of $\lambda_2 \times \rho(\mathbf{r})$ used for the plots is −0.020 to + 0.020 au at s = 0.5 au.

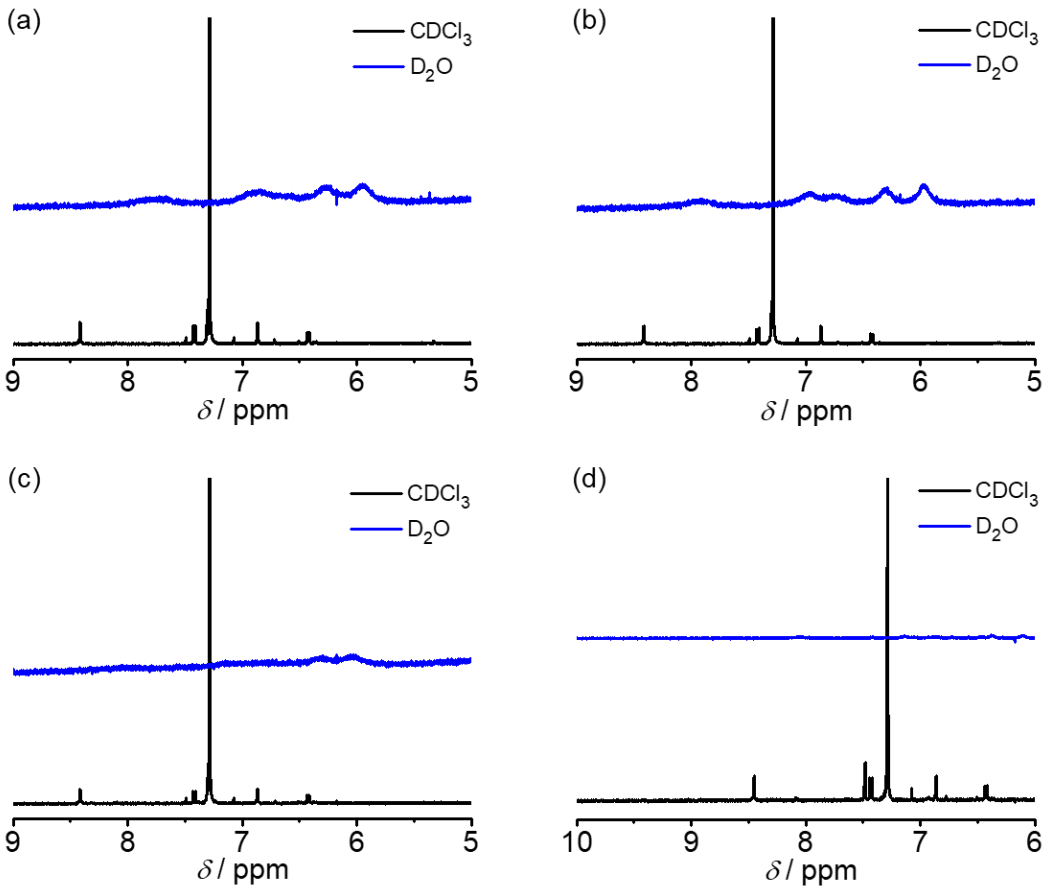

Figure S20. Partial ^{1}H NMR spectra of (a) **2**, (b) **3**, (c) **4** and (d) **6** in $CDCl_3$ and D_2O ([Pt] = 2.0×10^{-4} M) at 298 K.

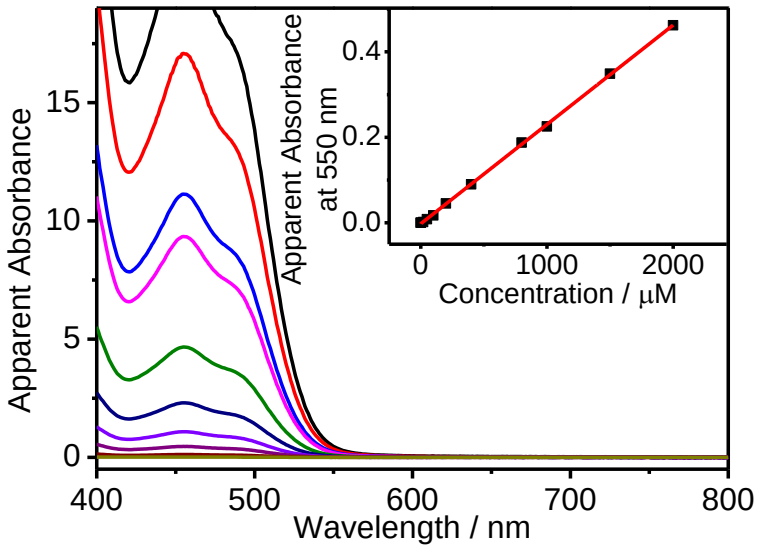

Figure S21. Electronic absorption spectra of **2** in water at various concentrations (2.0 to 2000 μM). Inset: Plot of absorbance at 550 nm against concentration. The apparent absorbance values have been obtained by correcting to a 1-cm path length equivalence.

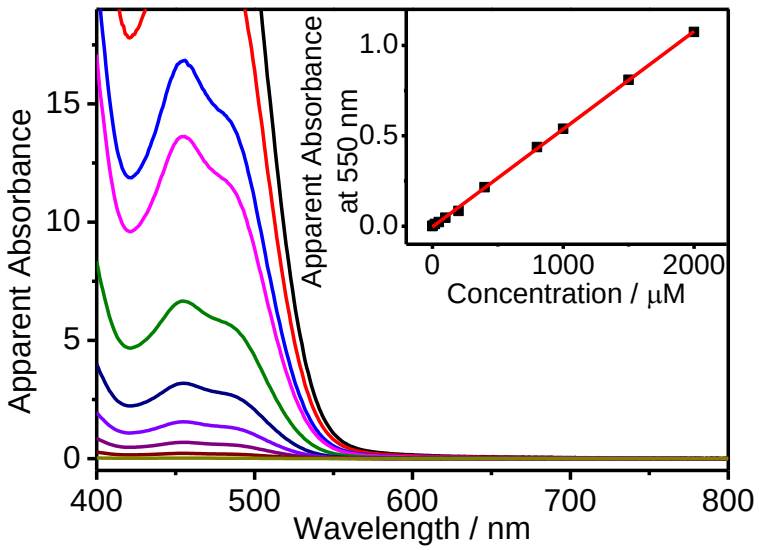

Figure S22. Electronic absorption spectra of **3** in water at various concentrations (2.0 to 2000 μM). Inset: Plot of absorbance at 550 nm against concentration. The apparent absorbance values have been obtained by correcting to a 1-cm path length equivalence.

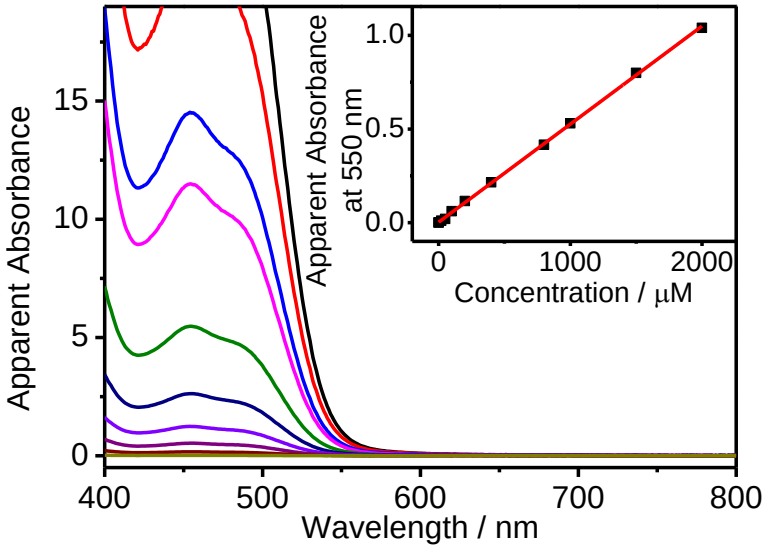

Figure S23. Electronic absorption spectra of **4** in water at various concentrations (2.0 to 2000 μM). Inset: Plot of absorbance at 550 nm against concentration. The apparent absorbance values have been obtained by correcting to a 1-cm path length equivalence.

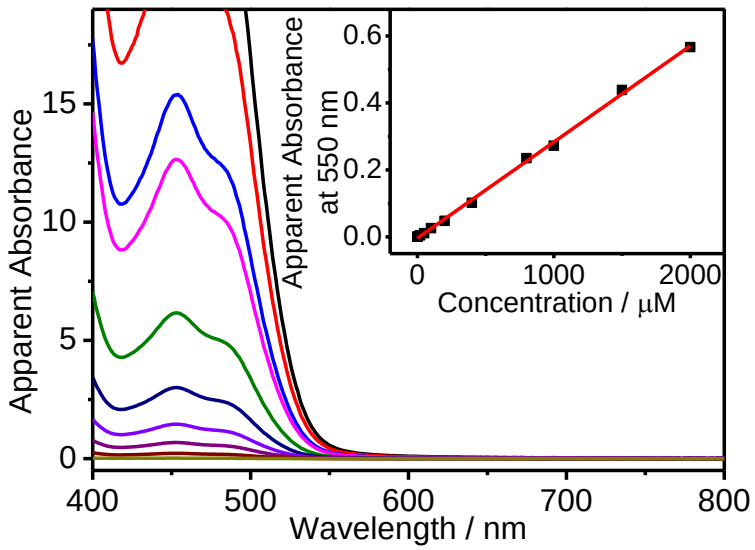

Figure S24. Electronic absorption spectra of **6** in water at various concentrations (2.0 to 2000 μM). Inset: Plot of absorbance at 550 nm against concentration. The apparent absorbance values have been obtained by correcting to a 1-cm path length equivalence.

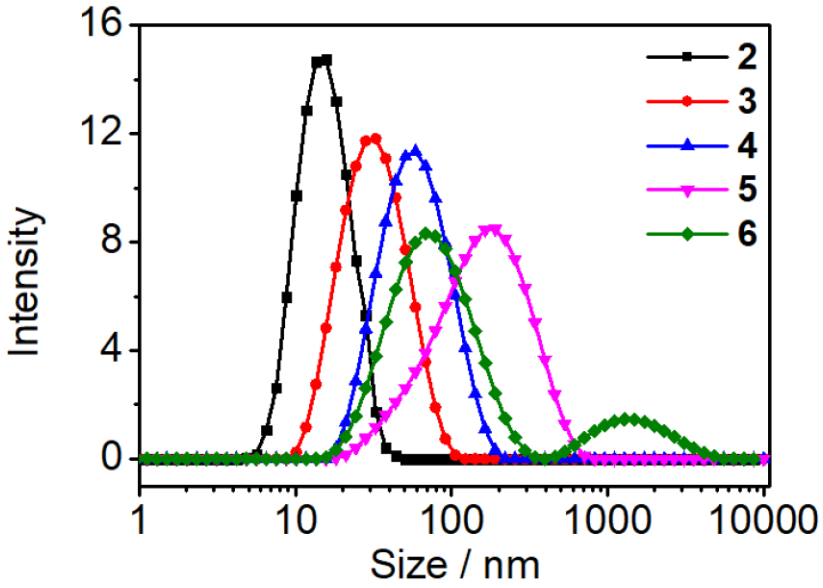

Figure S25. DLS results of complexes **2**–**6** in water at a concentration of 5.0×10^{-4} M at 298 K.

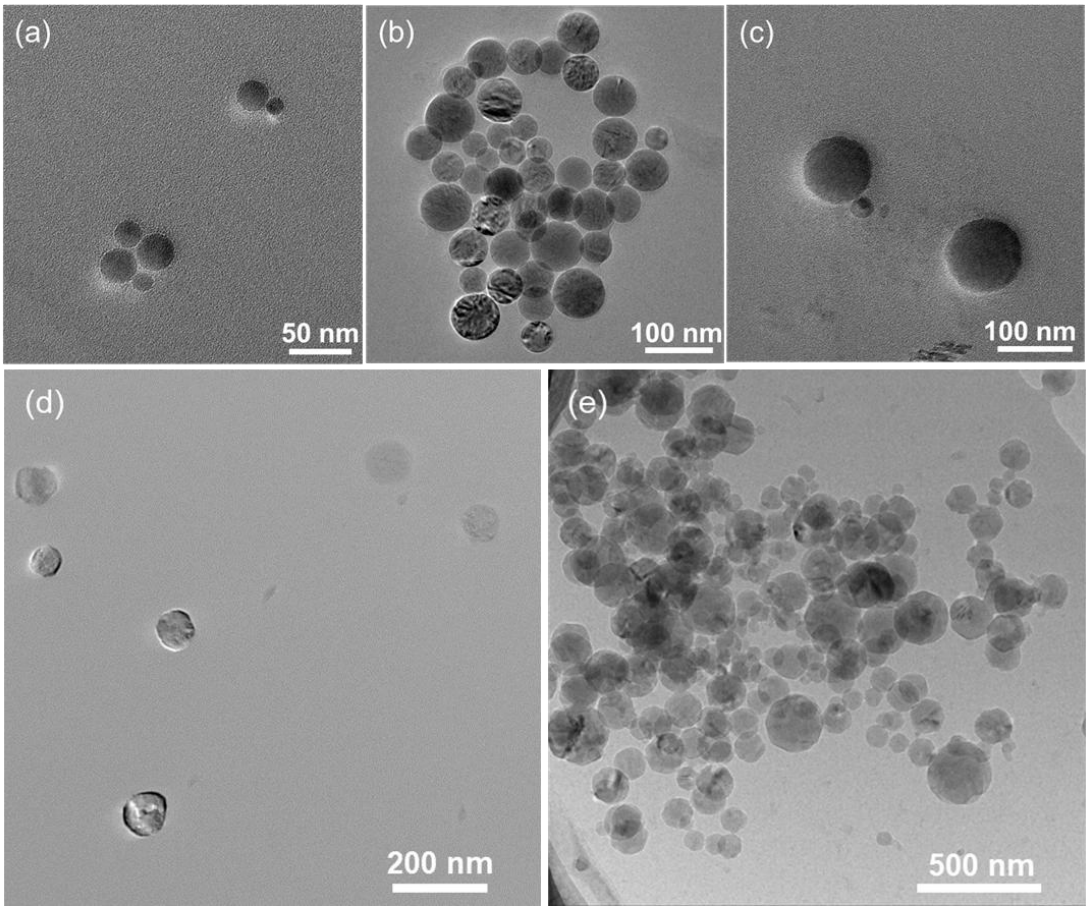

Figure S26. TEM images of (a) **2**, (b) **3**, (c) **4** and (d) **6** in water at a concentration of 5.0×10^{-4} M at 298 K. (e) Cryo-TEM image of **6** in water at a concentration of 5.0×10^{-4} M at 298 K.

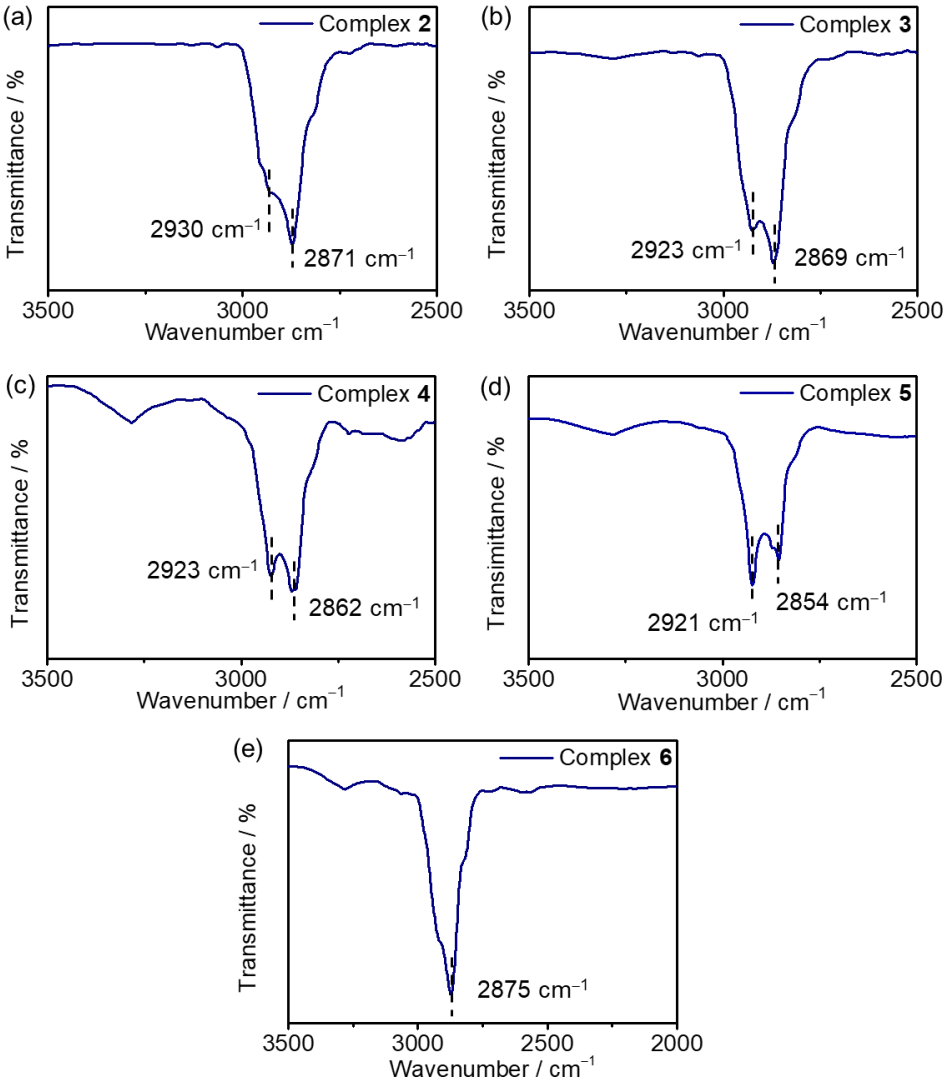

Figure S27. FT-IR spectra of assemblies prepared from (a) **2**, (b) **3**, (c) **4**, (d) **5** and (e) **6** in water at 298 K in CaF_2 pellet.

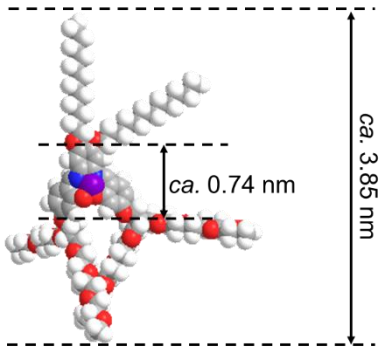

Figure S28. Computer-generated molecular model of **5**. Atom color code: white, H; grey, C; red, O; blue, N; purple, Pt.

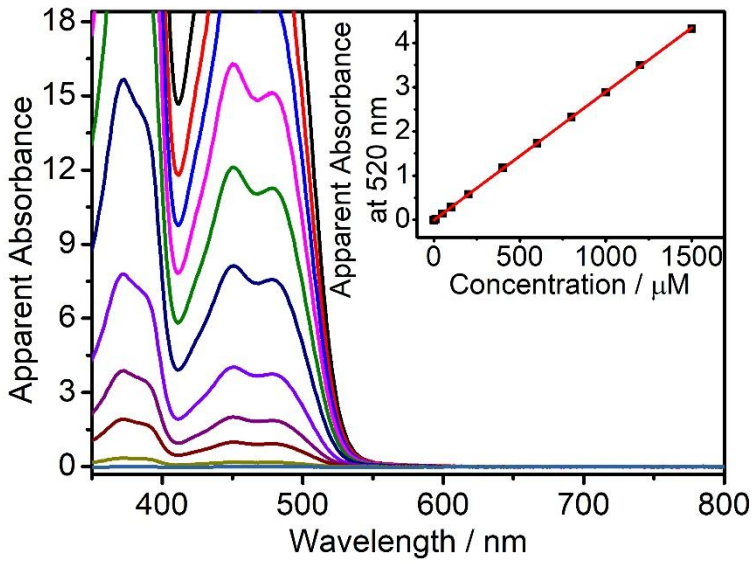

Figure S29. Electronic absorption spectra of **2** in DMSO solutions at various concentrations (1.0 to 1500 μM). Inset: Plot of absorbance at 520 nm against concentration. The apparent absorbance values have been obtained by correcting to a 1-cm path length equivalence.

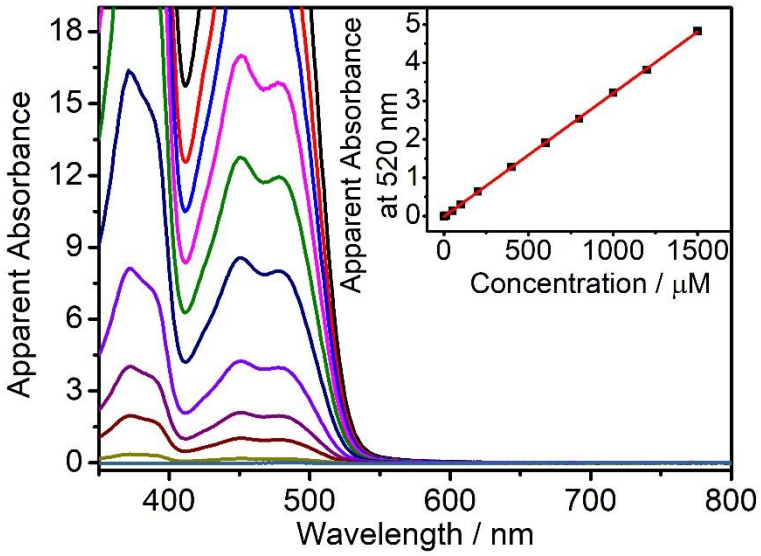

Figure S30. Electronic absorption spectra of **3** in DMSO solutions at various concentrations (1.0 to 1500 μM). Inset: Plot of absorbance at 520 nm against concentration. The apparent absorbance values have been obtained by correcting to a 1-cm path length equivalence.

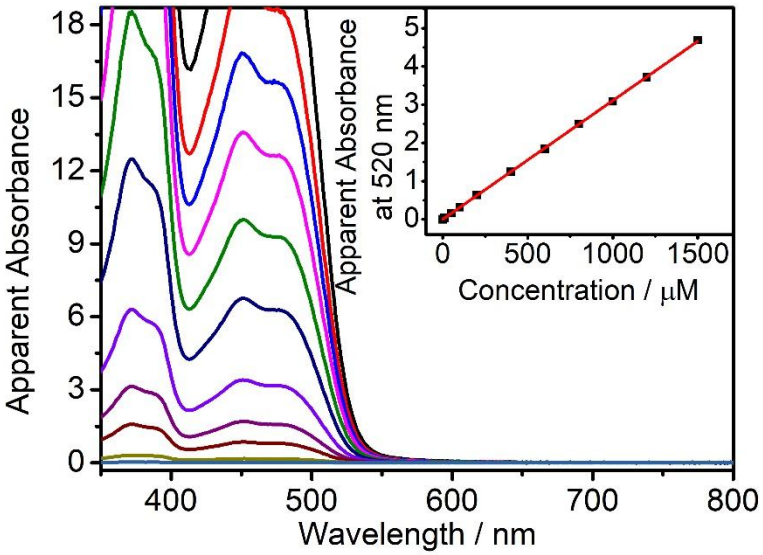

Figure S31. Electronic absorption spectra of **4** in DMSO solutions at various concentrations (1.0 to 1500 μM). Inset: Plot of absorbance at 520 nm against concentration. The apparent absorbance values have been obtained by correcting to a 1-cm path length equivalence.

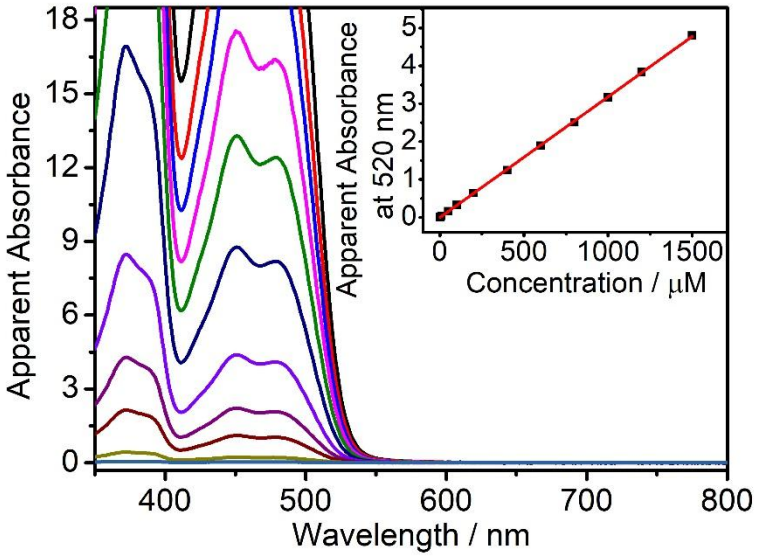

Figure S32. Electronic absorption spectra of **5** in DMSO solutions at various concentrations (1.0 to 1500 μM). Inset: Plot of absorbance at 520 nm against concentration. The apparent absorbance values have been obtained by correcting to a 1-cm path length equivalence.

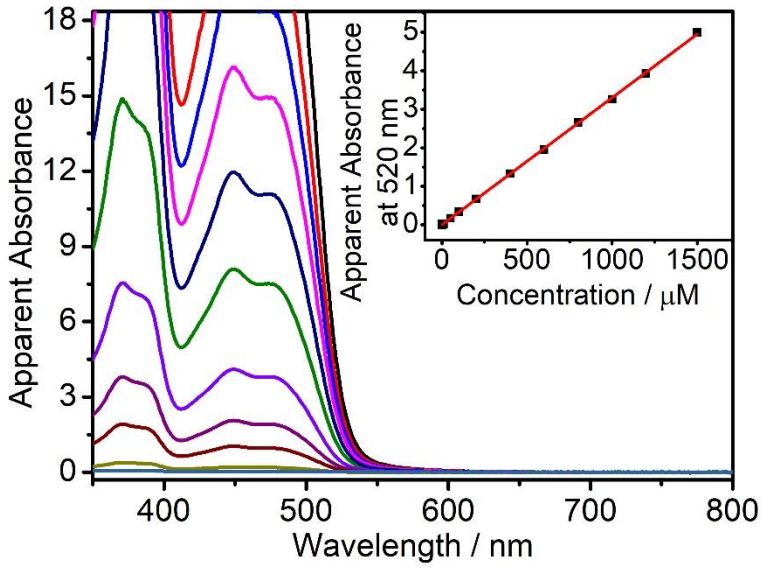

Figure S33. Electronic absorption spectra of **6** in DMSO solutions at various concentrations (1.0 to 1500 μM). Inset: Plot of absorbance at 520 nm against concentration. The apparent absorbance values have been obtained by correcting to a 1-cm path length equivalence.

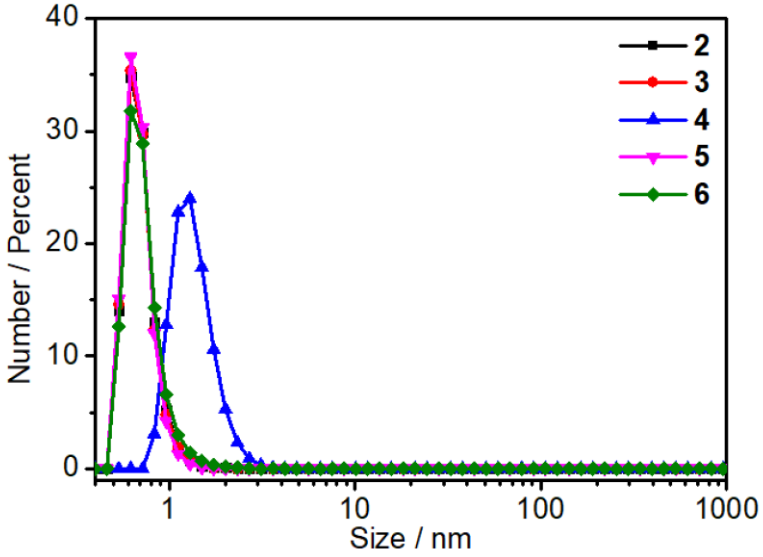

Figure S34. DLS results of complexes **2**–**6** in DMSO solutions at a concentration of 1.0×10^{-3} M at 298 K.

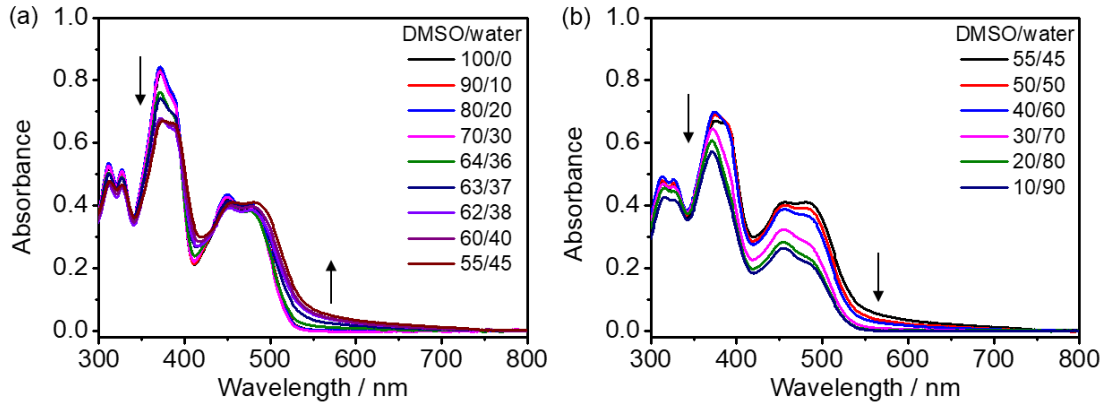

Figure S35. UV–Vis absorption spectral changes of **2** in DMSO solutions upon increasing water content from (a) 0 to 45 % (v/v) and (b) 45 to 90 % (v/v) at 298 K ([Pt] = 2.0×10^{-5} M).

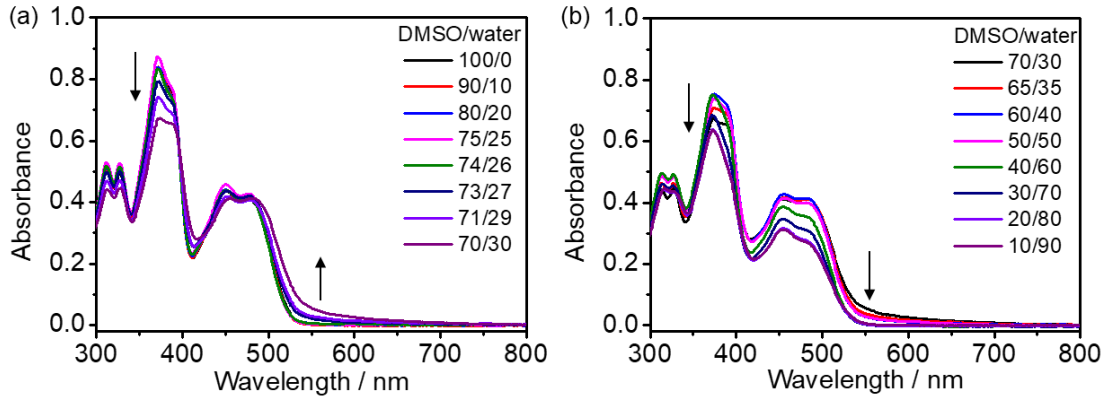

Figure S36. UV–Vis absorption spectral changes of **3** in DMSO solutions upon increasing water content from (a) 0 to 30 % (v/v) and (b) 30 to 90 % (v/v) at 298 K ([Pt] = 2.0×10^{-5} M).

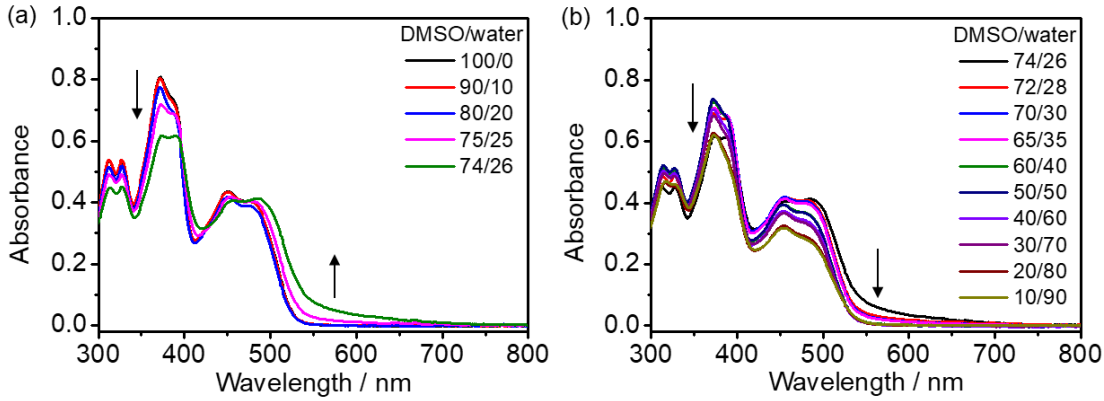

Figure S37. UV–Vis absorption spectral changes of **4** in DMSO solutions upon increasing water content from (a) 0 to 26 % (v/v) and (b) 26 to 90 % (v/v) at 298 K ([Pt] = 2.0×10^{-5} M).

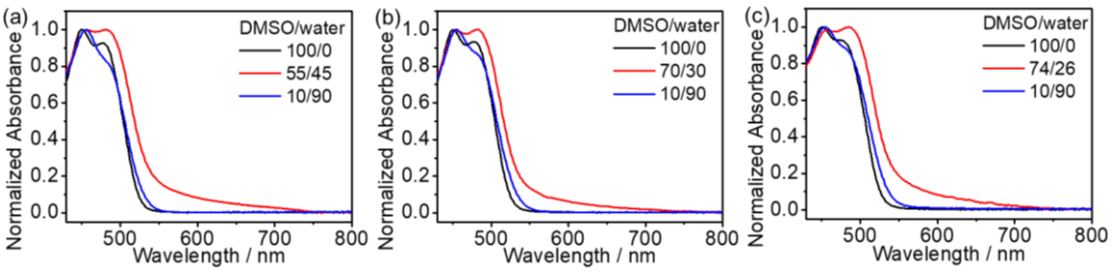

Figure S38. Normalized UV–vis absorption spectral changes of (a) **2**, (b) **3** and (c) **4** in DMSO–water (v/v) solutions in the concentration regime of 2.0×10^{-5} M.

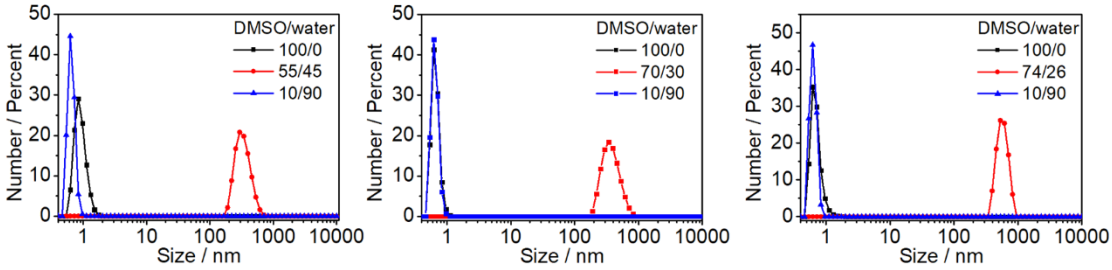

Figure S39. DLS results of (a) **2**, (b) **3** and (c) **4** in DMSO–water (v/v) solutions at a concentration of 2.0×10^{-5} M at 298 K.

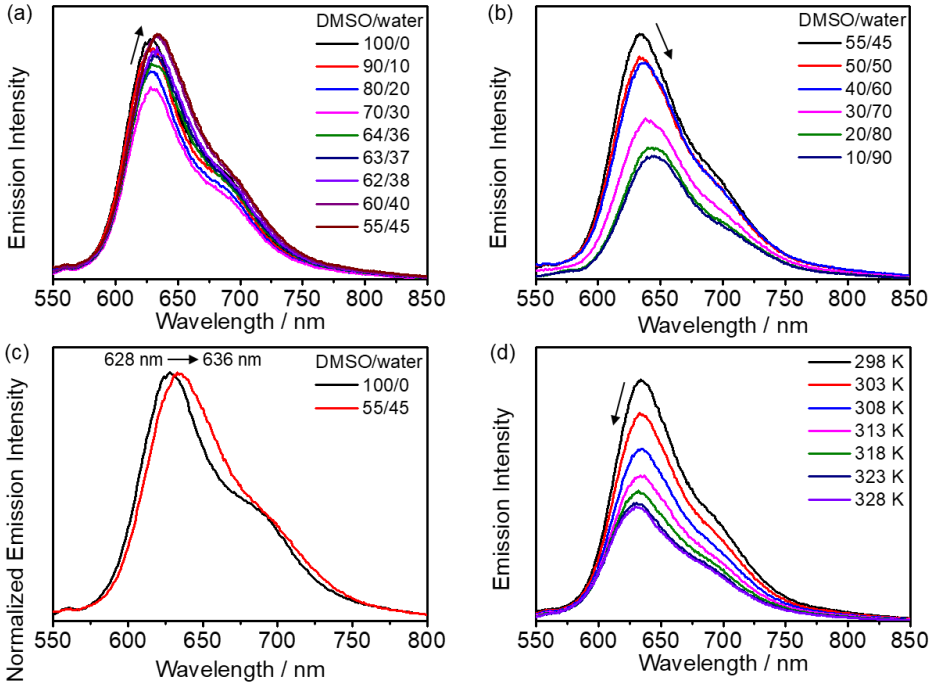

Figure S40. Emission spectral changes of **2** in DMSO solutions upon increasing water content from (a) 0 to 45 % (v/v) and (b) 45 to 90 % (v/v) at 298 K. (c) Normalized emission spectra of **2** in DMSO and 45 % water–DMSO (v/v) solutions at 298 K. (d) Variable-temperature emission spectral changes of **2** in 45 % water–DMSO (v/v) solutions. ([Pt] = 2.0×10^{-5} M)

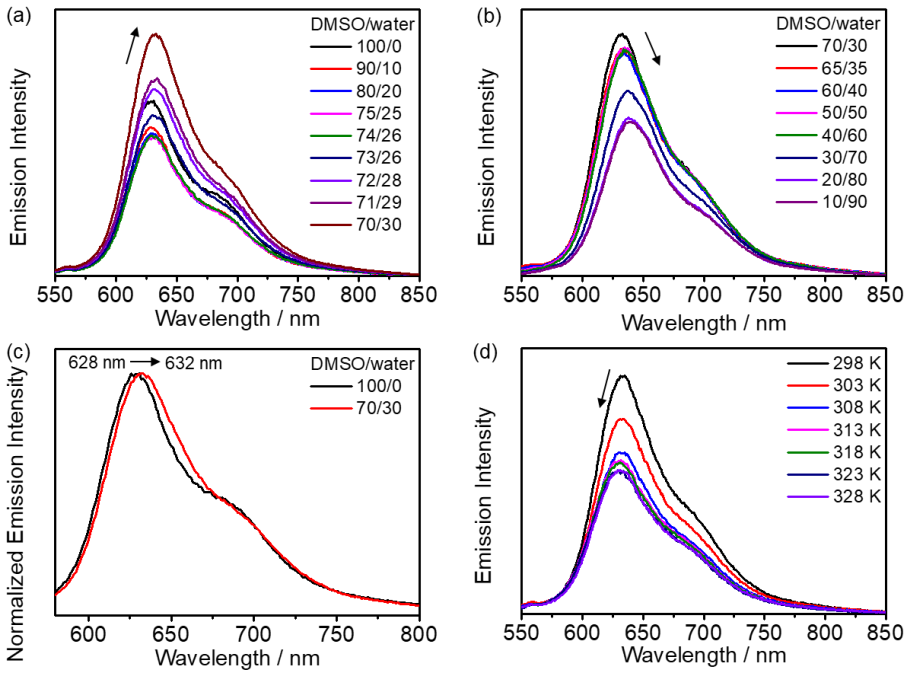

Figure S41. Emission spectral changes of **3** in DMSO solutions upon increasing water content from (a) 0 to 30 % (v/v) and (b) 30 to 90 % (v/v) at 298 K. (c) Normalized emission spectra of **3** in DMSO and 30 % water–DMSO (v/v) solutions at 298 K. (d) Variable-temperature emission spectral changes of **3** in 30 % water–DMSO (v/v) solutions ([Pt] = 2.0×10^{-5} M).

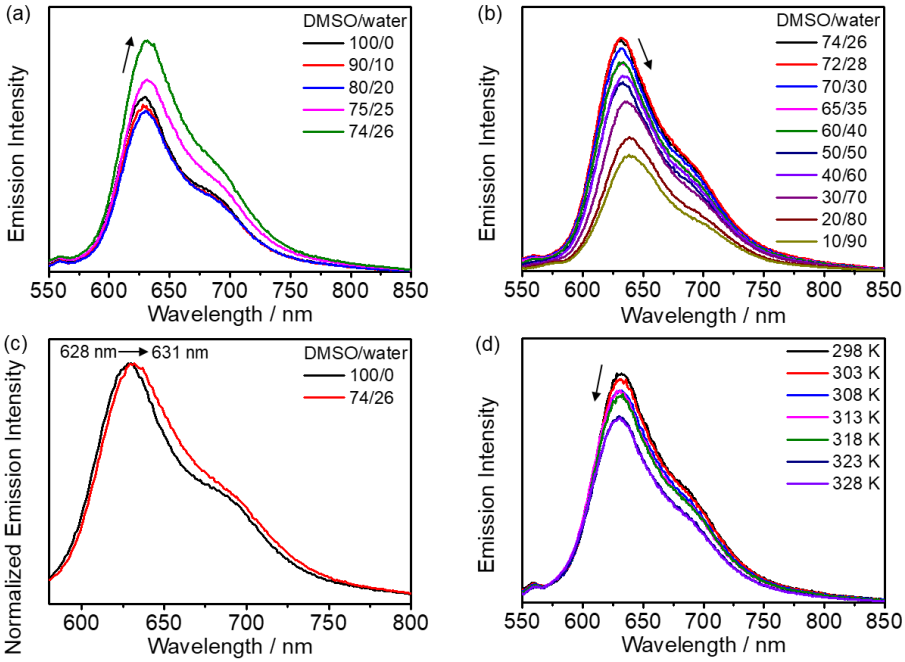

Figure S42. Emission spectral changes of **4** in DMSO solutions upon increasing water content from (a) 0 to 26 % (v/v) and (b) 26 to 90 % (v/v) at 298 K. (c) Normalized emission spectra of **4** in DMSO and 26 % water–DMSO (v/v) solutions at 298 K. (d) Variable-temperature emission spectral changes of **4** in 26 % water–DMSO (v/v) solutions. ([Pt] = 2.0×10^{-5} M)

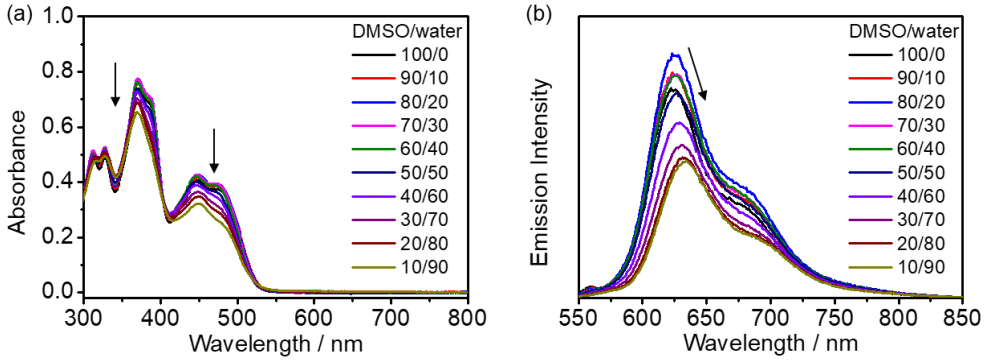

Figure S43. (a) UV–Vis absorption and (b) emission spectral changes of **6** in DMSO solutions upon increasing water content from 0 to 90 % (v/v) at a concentration of 2.0×10^{-5} M at 298 K.

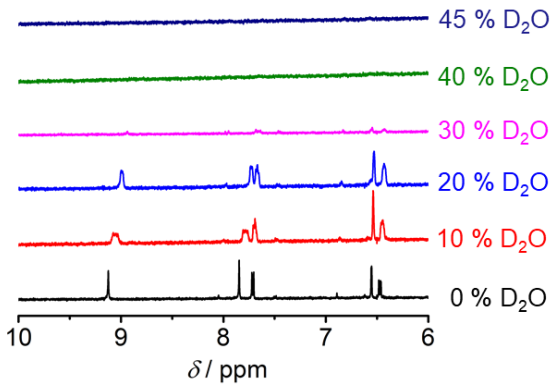

Figure S44. ^{1}H NMR spectral traces of **2** upon increasing D_2O content in DMSO-d_6 from 0 to 45 % (v/v) at 298 K ([Pt] = ~10^{-4} M).

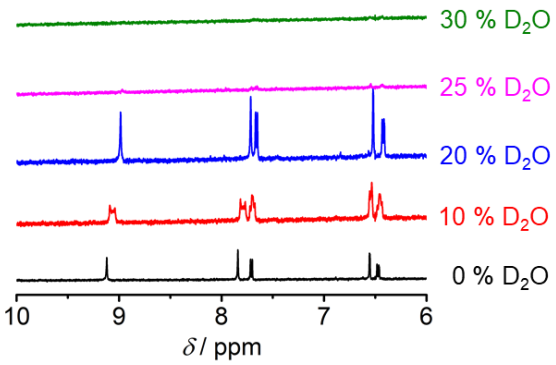

Figure S45. ^{1}H NMR spectral traces of **3** upon increasing D_2O content in DMSO-d_6 from 0 to 30 % (v/v) at 298 K ([Pt] = ~10^{-4} M).

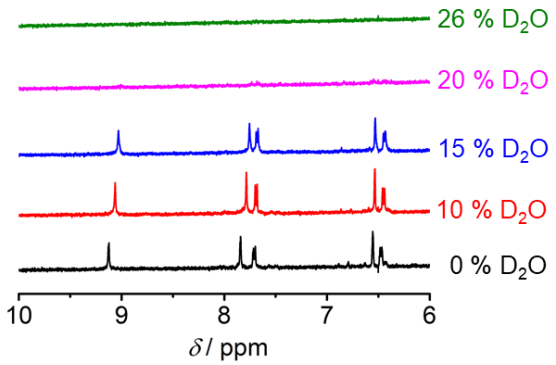

Figure S46. ^{1}H NMR spectral traces of **4** upon increasing D_2O content in DMSO-d_6 from 0 to 26 % (v/v) at 298 K ([Pt] = ~10^{-4} M).

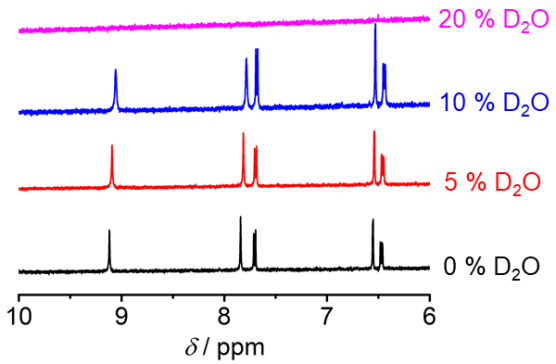

Figure S47. ^{1}H NMR spectral traces of **5** upon increasing D_2O content in DMSO-d_6 from 0 to 20 % (v/v) at 298 K ([Pt] = ~10^{-4} M).

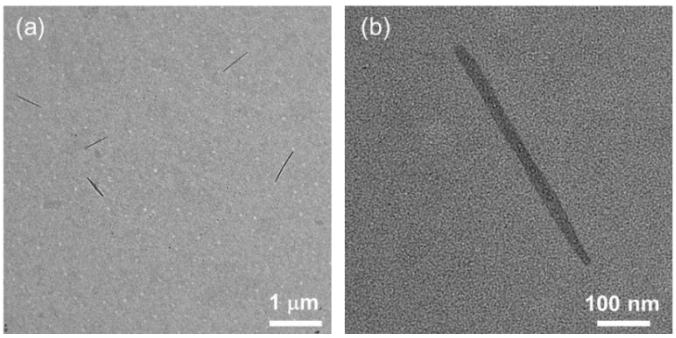

Figure S48. TEM images of **2** prepared from the 45 % water–DMSO (water:DMSO = 45:55, v/v) solution at a concentration of 2.0 × 10^{-5} M at 298 K at (a) lower magnification and (b) higher magnification.

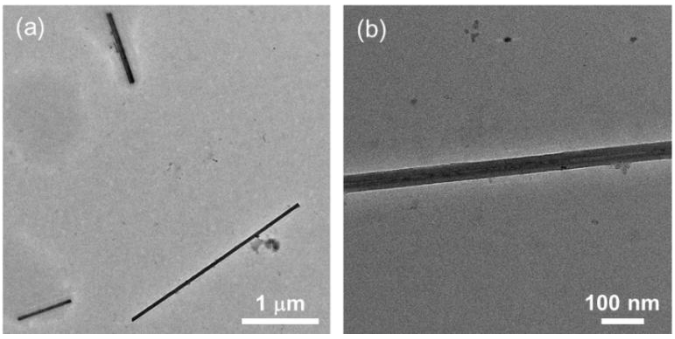

Figure S49. TEM images of **3** prepared from the 30 % water–DMSO (water:DMSO = 30:70, v/v) solution at a concentration of 2.0 × 10^{-5} M at 298 K at (a) lower magnification and (b) higher magnification.

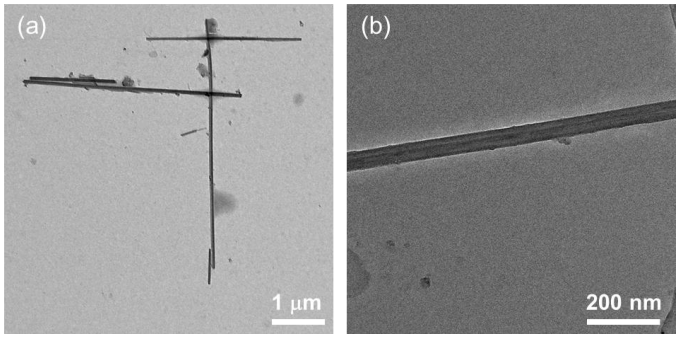

Figure S50. TEM images of **4** prepared from the 26 % water–DMSO (water:DMSO = 26:74, v/v) solution at a concentration of 2.0×10^{-5} M at 298 K at (a) lower magnification and (b) higher magnification.

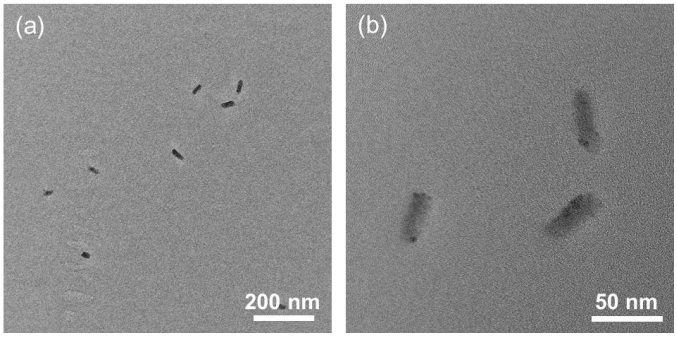

Figure S51. TEM images of **5** prepared from the 90 % water–DMSO (water:DMSO = 90:10, v/v) solution at a concentration of 2.0×10^{-5} M at 298 K at (a) lower magnification and (b) higher magnification.

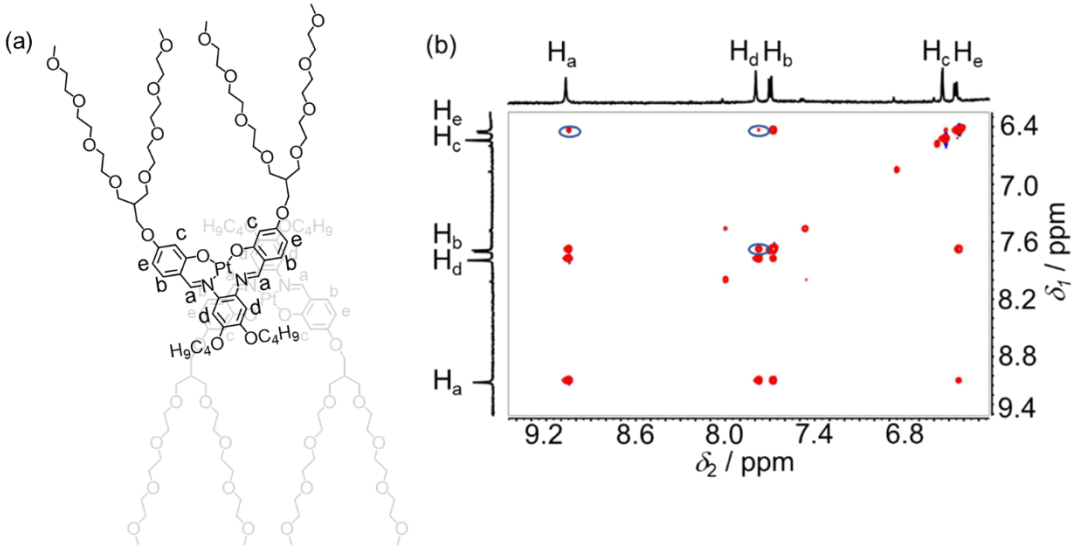

Figure S52. (a) Proposed stacking mode of complex **2** in DMSO upon increasing H_2O content. (b) Partial ^1H–^1H NOESY NMR spectrum of complex **2** in DMSO-d_6 upon the addition of 10 % D_2O (v/v) at 298 K.

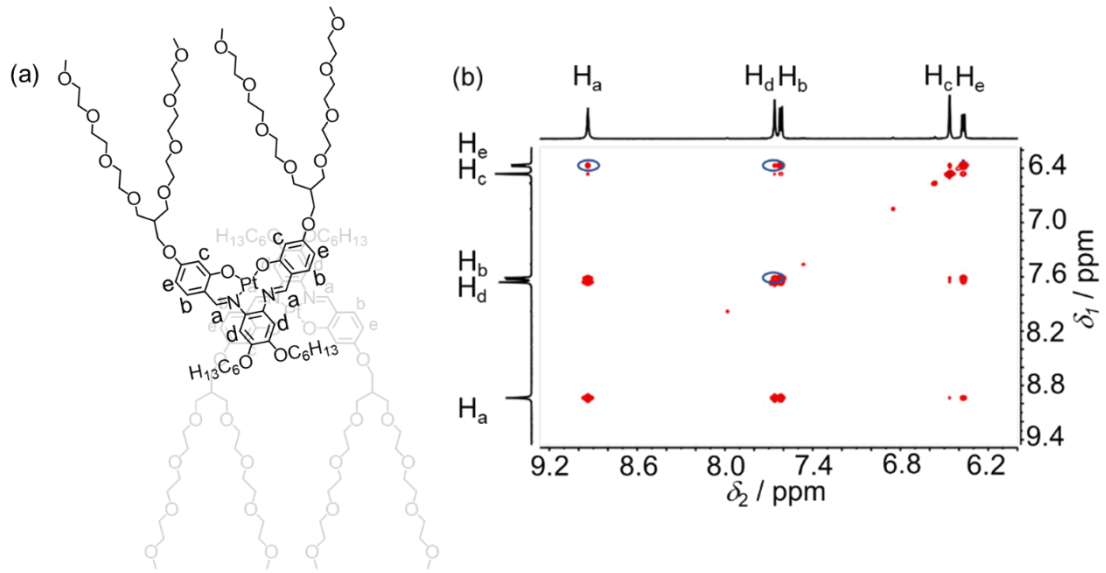

Figure S53. (a) Proposed stacking mode of complex **3** in DMSO upon increasing H_2O content. (b) Partial ^1H–^1H NOESY NMR spectrum of complex **3** in DMSO-d_6 upon the addition of 10 % D_2O (v/v) at 298 K.

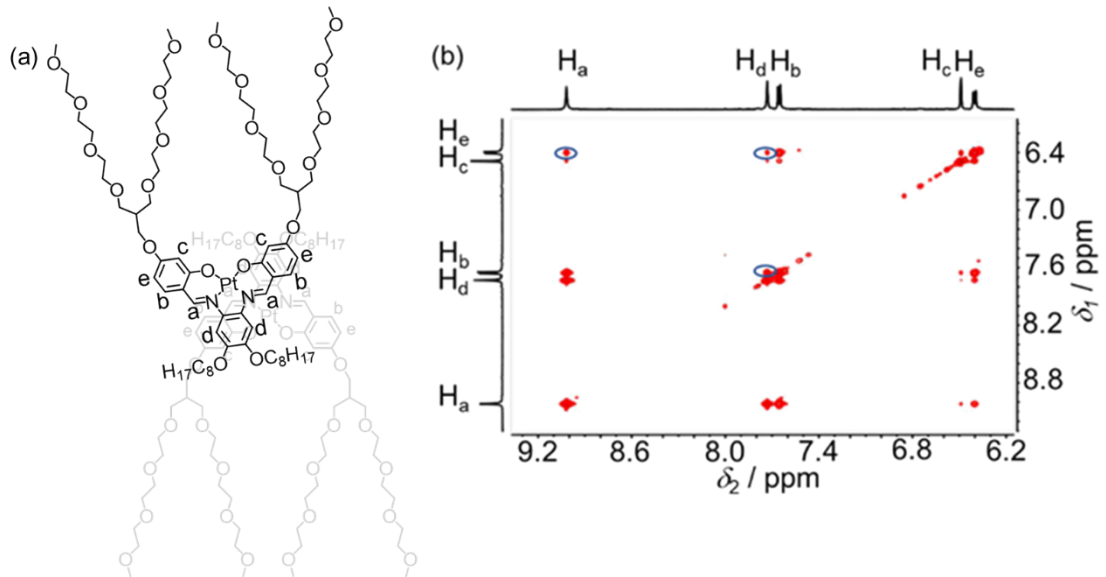

Figure S54. (a) Proposed stacking mode of complex **4** in DMSO upon increasing H_2O content. (b) Partial ^1H–^1H NOESY NMR spectrum of complex **4** in DMSO-d_6 upon the addition of 10 % D_2O (v/v) at 298 K.

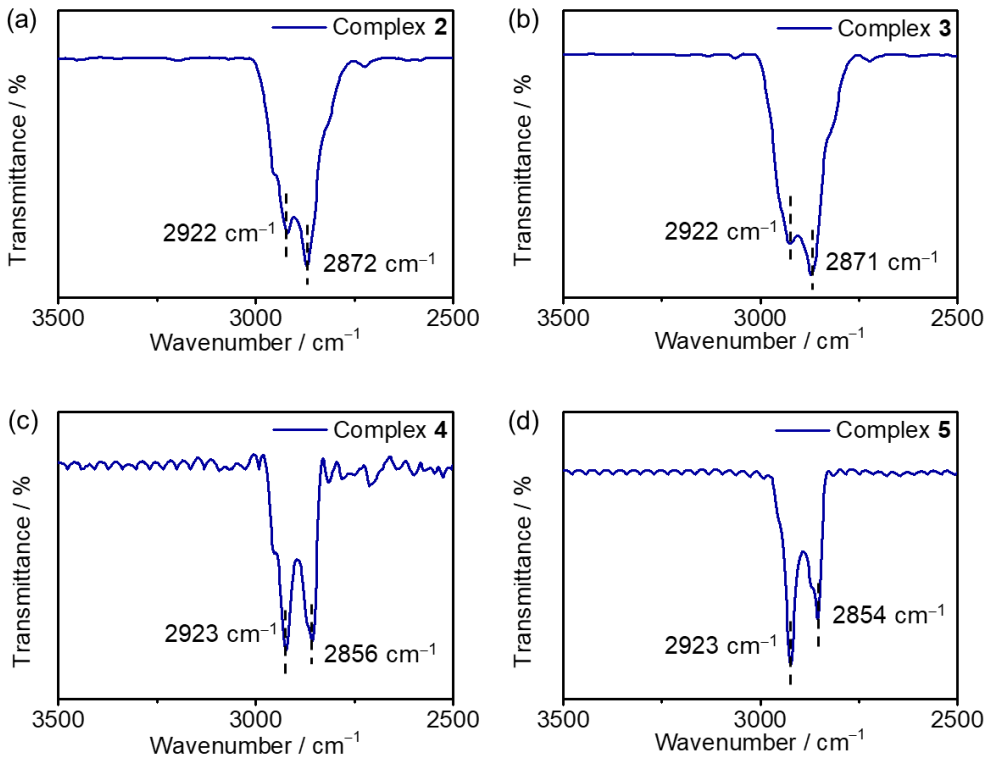

Figure S55. FT-IR spectra of assemblies prepared from (a) **2** in 45 % water–DMSO (water:DMSO = 45:55, v/v) solution, (b) **3** in 30 % water–DMSO (water:DMSO = 30:70, v/v) solution, (c) **4** in 26 % water–DMSO (water:DMSO = 26:74, v/v) solution and (d) **5** in 20 % water–DMSO (water:DMSO = 20:80, v/v) solution at 298 K in CaF_2 pellet.

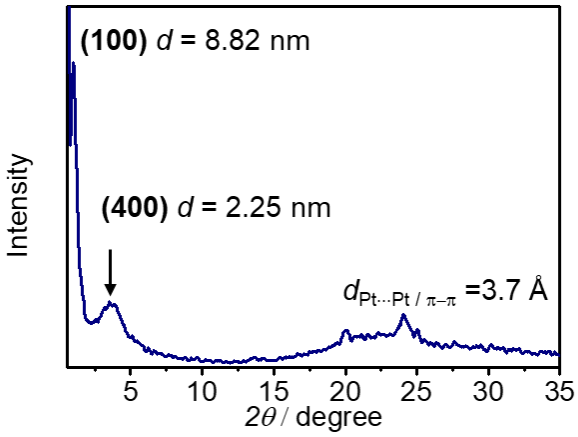

Figure S56. X-Ray diffraction (XRD) pattern of a thin film prepared from **5** in 20 % water–DMSO (water:DMSO = 20:80, v/v) solution at 298 K.

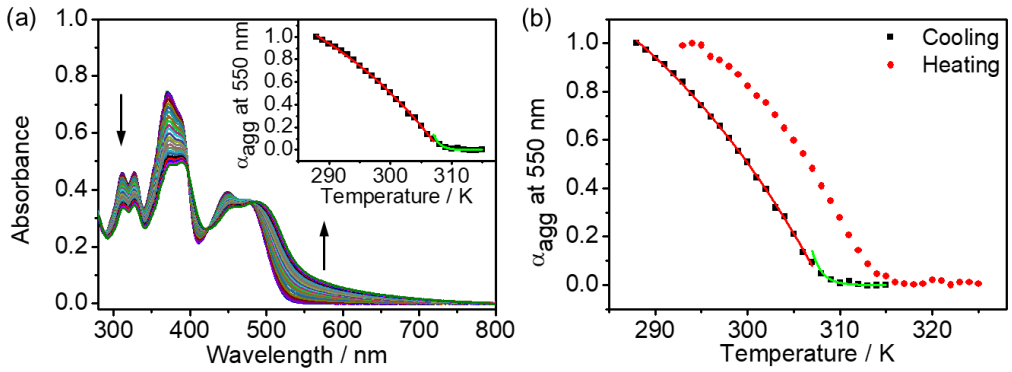

Figure S57. (a) UV–Vis absorption spectral traces on cooling a solution of **2** in 45 % water–DMSO (water:DMSO = 45:55, v/v) mixture at a cooling rate of 0.5 K min^{-1}. Inset: A plot of degree of aggregation at 580 nm as a function of temperature with the curve fitted at the elongation (red line) and nucleation (green line) regime based on the nucleation−elongation model. (b) Plots of degree of aggregation monitored at 580 nm against temperature for the heating and cooling of **2** in the temperature range from 325 to 288 K.

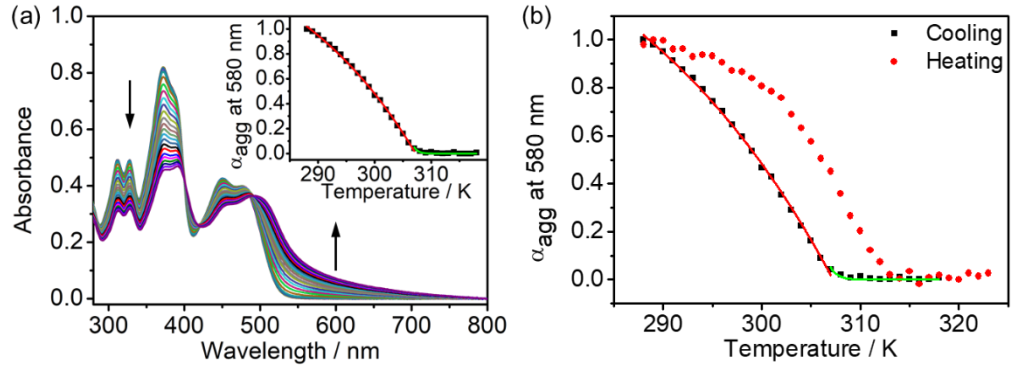

Figure S58. UV–Vis absorption spectral traces on cooling a solution of **3** in 30 % water–DMSO (water:DMSO = 30:70, v/v) mixture at a cooling rate of 0.5 K min^{-1}. Inset: A plot of degree of aggregation at 580 nm as a function of temperature with the curve fitted at the elongation (red line) and nucleation (green line) regime based on the nucleation−elongation model. (b) Plots of degree of aggregation monitored at 580 nm against temperature for the heating and cooling of **3** in the temperature range from 323 to 288 K.

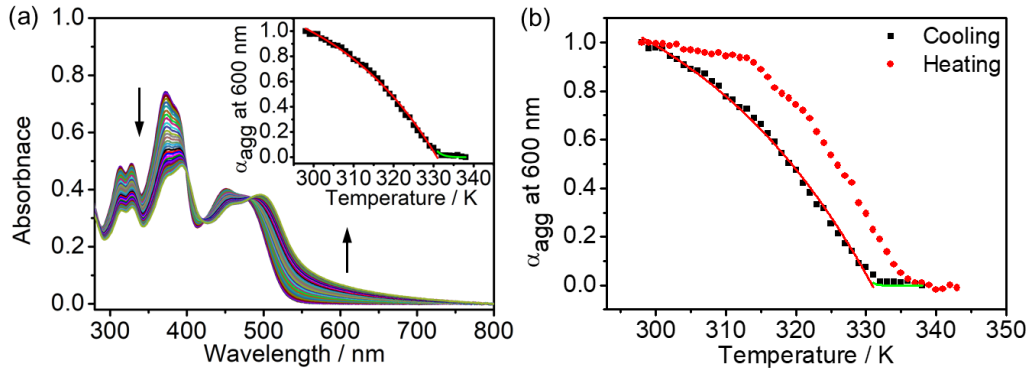

Figure S59. UV–Vis absorption spectral traces on cooling a solution of **4** in 26 % water–DMSO (water:DMSO = 26:74, v/v) mixture at a cooling rate of 0.5 K min^{-1}. Inset: A plot of degree of aggregation at 600 nm as a function of temperature with the curve fitted at the elongation (red line) and nucleation (green line) regime based on the nucleation–elongation model. (b) Plots of degree of aggregation monitored at 600 nm against temperature for the heating and cooling of **4** in the temperature range from 343 to 298 K.

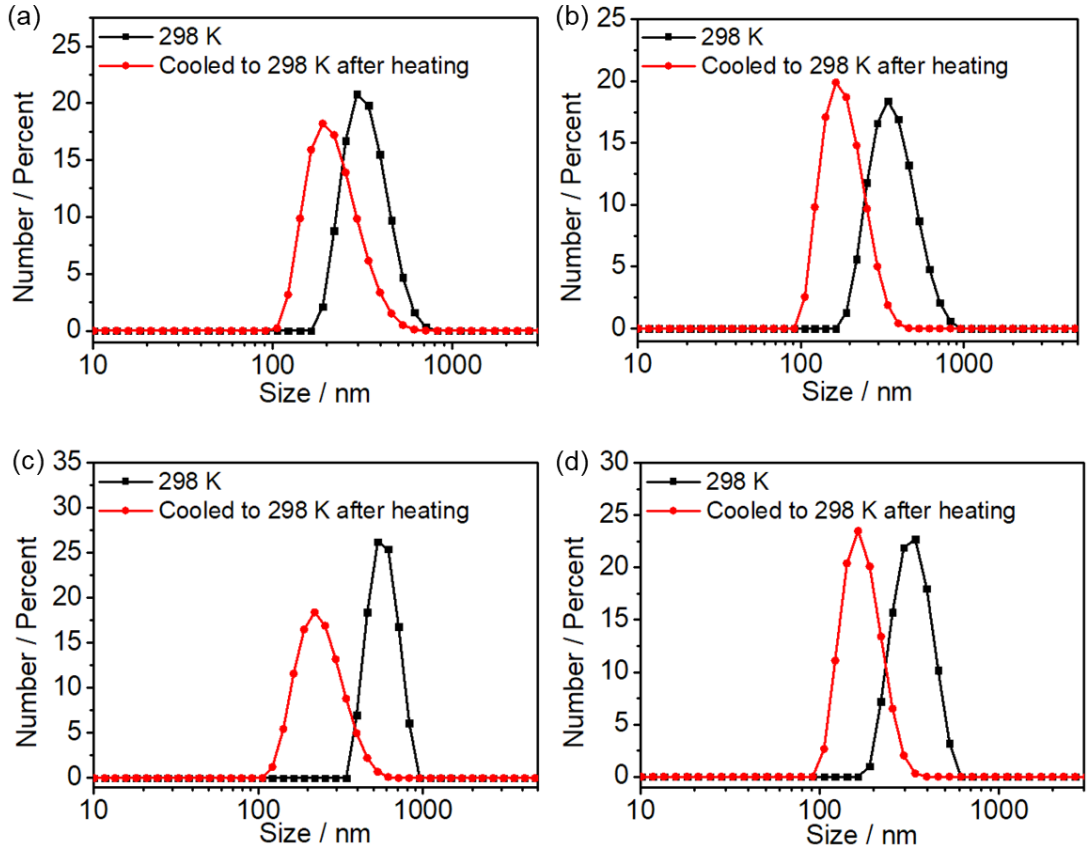

Figure S60. DLS results of (a) **2**, (b) **3**, (c) **4** and (d) **5** in DMSO–water (v/v) solutions at a concentration of 2.0×10^{-5} M at 298 K and after cooling to 298 K after heat treatment.

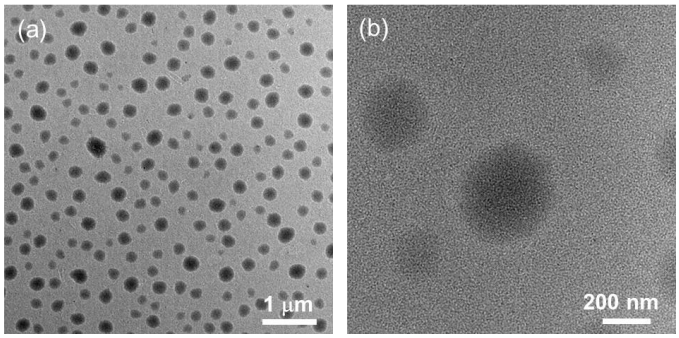

Figure S61. TEM images of **2** prepared from the 45 % water–DMSO (water:DMSO = 45:55, v/v) solution at a concentration of 2.0×10^{-5} M after cooling to 298 K after heat treatment at (a) lower magnification and (b) higher magnification.

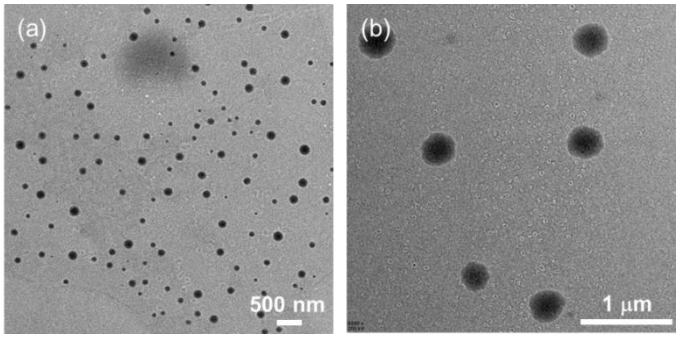

Figure S62. TEM images of **3** prepared from the 30 % water–DMSO (water:DMSO = 30:70, v/v) solution at a concentration of 2.0×10^{-5} M after cooling to 298 K after heat treatment at (a) lower magnification and (b) higher magnification.

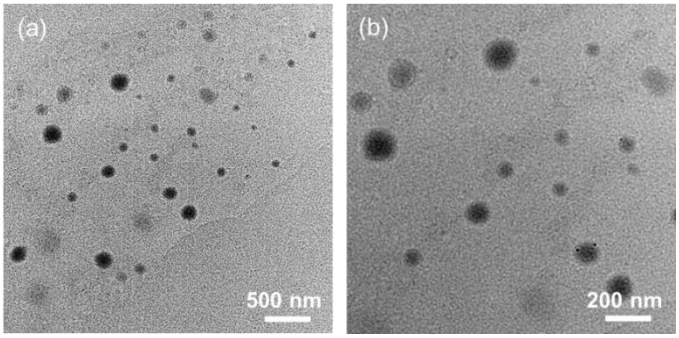

Figure S63. TEM images of **4** prepared from the 26 % water–DMSO (water:DMSO = 26:74, v/v) solution at a concentration of 2.0×10^{-5} M after cooling to 298 K after heat treatment at (a) lower magnification and (b) higher magnification.

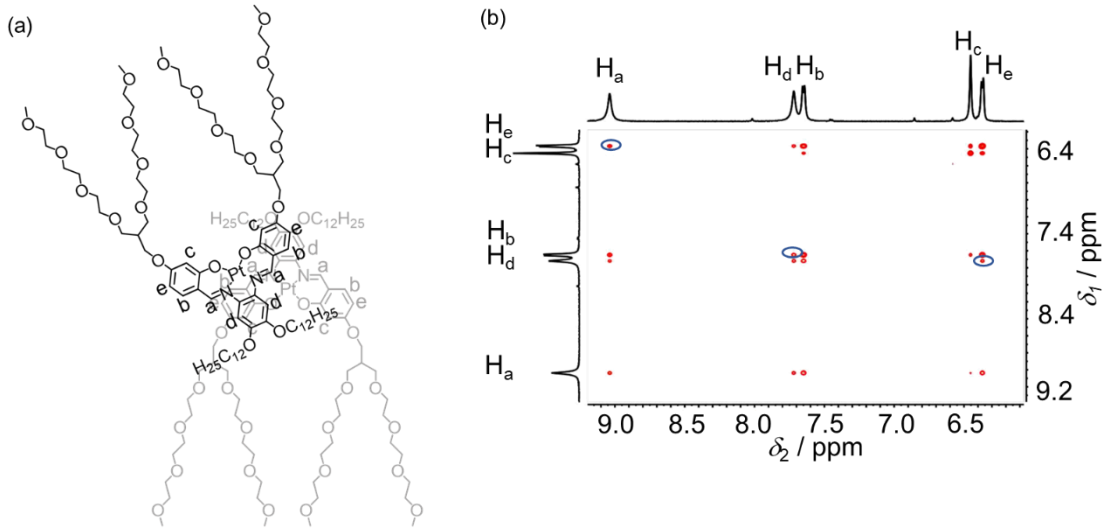

Figure S64. (a) Proposed stacking mode of **5** in DMSO–water mixture after cooling to 298 K after heat treatment. (b) Partial ^{1}H–^{1}H NOESY NMR spectrum of complex **5** in 10 % D_2O–DMSO-d_6 (D_2O:DMSO-d_6 = 10:90, v/v) solution after cooling to 298 K after heat treatment.

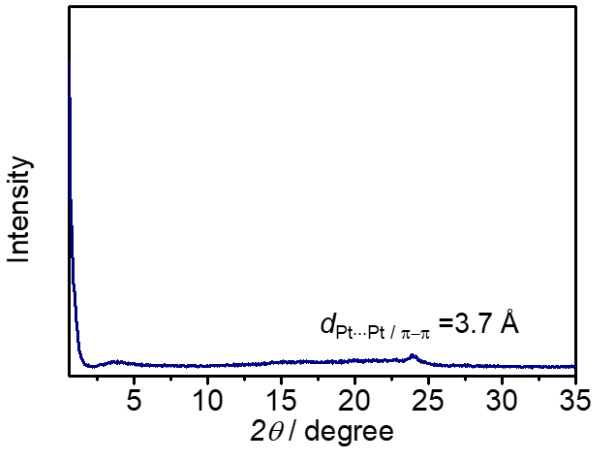

Figure S65. X-Ray diffraction (XRD) pattern of a thin film prepared from **5** in 20 % water–DMSO (water:DMSO = 20:80, v/v) solution after cooling to 298 K after heat treatment.

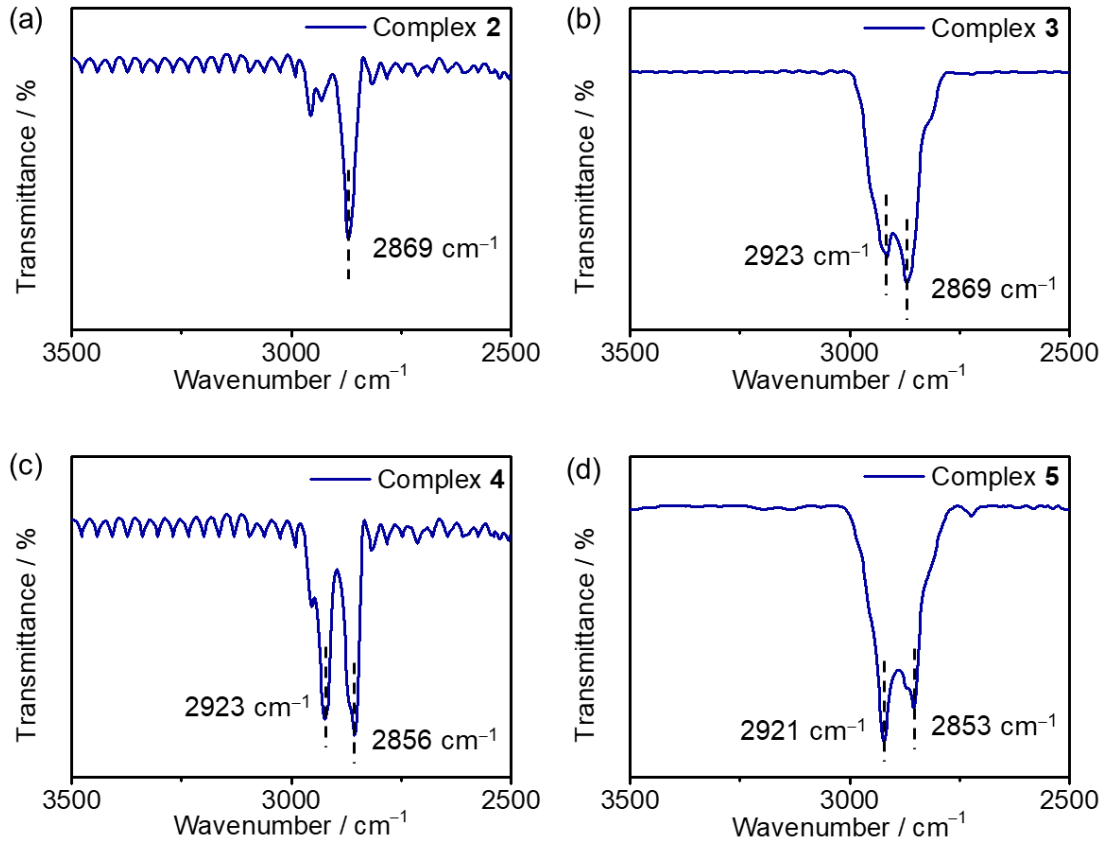

Figure S66. FT-IR spectra of assemblies prepared from (a) **2** in 45 % water–DMSO (water:DMSO = 45:55, v/v) solution, (b) **3** in 30 % water–DMSO (water:DMSO = 30:70, v/v) solution, (c) **4** in 26 % water–DMSO (water:DMSO = 26:74, v/v) solution and (d) **5** in 20 % water–DMSO (water:DMSO = 20:80, v/v) solution after cooling to 298 K after heat treatment in CaF_2 pellet.

Photophysical data

Table S1 Photophysical data of complexes **1**–**6** in dichloromethane solutions (10^{-5} M) at 298 K

Complex	Absorption	Emission	
	λ_{abs} / nm (ε / dm^3 mol^{-1} cm^{-1})	λ_{em} / nm	τ / μs
1	313 (20730), 373 (28510), 390 sh (25470), 443 (16910), 496 sh (8720)	576,[a] 627 sh[a]	5.57
2	313 (15850), 329 (14340), 373 (23910), 388 sh (23000), 453 (12040), 484 sh (11140)	631,[a] 688 sh[a]	3.65
3	313 (13910), 329 (13190), 373 (22260), 388 sh (21320), 454 (11410), 481 sh (10700)	631,[a] 689 sh[a]	3.73
4	314 (15010), 329 (14620), 373 (22220), 387 sh (21080), 453 (11760), 479 sh (10960)	631,[a] 687 sh[a]	3.68
5	313 (13990), 329 (13250), 374 (23040), 389 sh (22120), 454 (11790), 483 sh (11050)	631,[a] 689 sh[a]	3.71
6	314 (14750), 329 (11490), 372 (21810), 387 sh (21020), 450 (11850), 478 sh (10740)	624,[a] 679 sh[a]	4.48

[a] Excitation wavelength at 480 nm in the degassed dichloromethane solution at 298 K.

Crystallographic Data

Table S2 Selection bond lengths [Å] and bond angles [°] with estimated standard deviations (esds) in parentheses for complex **1**

Pt(1)–N(1)	1.970(14)	Pt(1)–N(2)	1.951(15)
Pt(1)–O(1)	1.987(13)	Pt(1)–O(2)	1.998(11)
C(1)–N(1)	1.45(4)	C(9)–N(2)	1.40(2)
C(17)–N(1)	1.29(3)	C(18)–N(2)	1.30(2)
N(1)–Pt(1)–N(2)	84.1(10)	N(1)–Pt(1)–O(1)	95.1(9)
N(2)–Pt(1)–O(2)	94.5(8)	O(1)–Pt(1)–O(2)	86.3(8)
N(1)–Pt(1)–O(2)	178.0(12)	N(2)–Pt(1)–O(1)	178.1(6)

Table S3 Crystal and structure determination data of complex **1**

Empirical formula	$C_{22}H_{18}N_2O_4Pt$
Formula weight	569.47
Temperature	289 K
Wavelength	0.71073A
Crystal system, space group	orthorhombic, $Pna2_1$
Unit cell dimensions	a = 15.502(7) Å α = 90°. b = 20.082(8) Å β = 90°. c = 5.971(2) Å γ = 90°.
Volume	1858.70(13) Å^3
Z	4
Density(calculated)	2.035 g cm^{-3}
Absorption coefficient	7.582 mm^{-1}
F(000)	1096
Crystal size	0.25 × 0.1 × 0.09 mm^3
θ range for data collection	5.256 to 55.014°
Limiting indices	$-20 \le h \le 20$, $-26 \le k \le 26$, $-7 \le l \le 7$
Reflections collected / unique	42950 / 4266 [*R(int)* = 0.1122, *R(sigma)* = 0.0544]
Completeness to θ = 25.242°	99.8 %
Absorption correction	Semi-empirical from equivalents
Max. and min. transmission	0.522 and 0.746
Refinement method	Full-matrix least-squares on F^2
Data / restraints / parameters	4266 / 1 / 264
Goodness-of-fit on F^2	1.104
Final *R* indices [$I > 2\sigma(I)$]	R_1 = 0.0493, wR_2 = 0.1152
R indices (all data)	R_1 = 0.0822, wR_2 = 0.1407
Largest diff. peak and hole	3.85 and –1.85 eÅ^{-3}
Flack parameter	–0.027(11)

Table S4. The first twenty singlet (S_n) excited states computed by TDDFT/SMD (**1** and **7**: CH_2Cl_2, $\mathbf{7}_2$: water) at the optimized ground-state geometries for the complexes described.

Complex	S_n	Excitation[a] (Coefficient)[b]	Vertical excitation wavelength / nm	f [c]
1	S_1	H→L (0.70)	451	0.130
	S_2	H−1→L (0.66)	398	0.499
	S_3	H→L+1 (0.65)	378	0.018
	S_4	H−2→L (0.66)	357	0.394
	S_5	H−1→L+1 (0.67)	336	0.360
	S_6	H−4→L (0.70)	326	0.000
	S_7	H−3→L (0.50)	310	0.213
		H−2→L+1 (−0.44)		
	S_8	H−2→L+1 (0.54)	299	0.263
		H−3→L (0.44)		
	S_9	H−6→L (0.70)	295	0.000
	S_{10}	H→L+4 (0.50)	293	0.000
		H−4→L+1 (−0.46)		
	S_{11}	H−4→L+1 (0.52)	287	0.001
		H→L+4 (0.43)		
	S_{12}	H−3→L+1 (0.51)	274	0.019
		H−8→L (0.32)		
		H−7→L (−0.32)		
	S_{13}	H−5→L (0.63)	272	0.120
	S_{14}	H−7→L (0.45)	264	0.022
		H−3→L+1 (0.45)		
	S_{15}	H−6→L+1 (0.68)	264	0.000
7	S_1	H−1→L (0.70)	452	0.133
	S_2	H→L (0.69)	437	0.480
	S_3	H−1→L+1 (0.64)	366	0.006
	S_4	H→L+1 (0.68)	354	0.586
	S_5	H–2→L (0.64)	353	0.482
	S_6	H−5→L (0.70)	325	0.000
	S_7	H−3→L (0.65)	309	0.441
	S_8	H−4→L (0.69)	306	0.025
	S_9	H−11→L (0.70)	293	0.000
	S_{10}	H−1→L+4 (0.64)	293	0.000
	S_{11}	H−2→L+1 (0.65)	293	0.076
	S_{12}	H−5→L+1 (0.67)	280	0.002
	S_{13}	H−10→L (0.43)	273	0.033
		H−8→L (−0.38)		
	S_{14}	H−12→L (0.61)	272	0.091
	S_{15}	H−6→L (0.54)	270	0.001
		H−7→L (0.43)		

7$_2$	S_1	H→L (0.63)	487	0.025
	S_2	H−1→L (0.67)	462	0.029
	S_3	H−2→L (0.60)	456	0.179
	S_4	H−3→L (0.50)	447	0.120
		H→L+1 (−0.45)		
	S_5	H→L+1 (0.50)	428	0.010
		H−3→L (0.47)		
	S_6	H−1→L+1 (0.51)	420	0.077
		H−2→L+1 (0.37)		
	S_7	H−2→L+1 (0.53)	414	0.056
		H−1→L+1 (−0.36)		
	S_8	H−4→L (0.52)	406	0.262
	S_9	H−3→L+1 (0.60)	400	0.165
	S_{10}	H→L+2 (0.42)	386	0.100
		H−5→L (−0.41)		
	S_{11}	H−4→L+1 (0.63)	380	0.007
	S_{12}	H−6→L (0.46)	373	0.007
		H−5→L (0.32)		
	S_{13}	H→L+2 (0.43)	370	0.333
	S_{14}	H−2→L+2 (0.41)	363	0.030
		H→L+3 (−0.34)		
	S_{15}	H→L+3 (0.36)	363	0.012

[a] The orbitals involved in the excitation (H = HOMO and L = LUMO).

[b] The coefficients in the configuration interaction (CI) expansion that are less than 0.3 are not listed.

[c] Oscillator strengths.

Table S5. Dynamic light scattering data of complexes **2**–**6** in various solvent compositions at 298 K

Complex	Medium	Hydrodynamic diameter / nm
2	DMSO	–,[b] –[c]
	45 % water–DMSO (45:55, v/v)	324.9,[c] – ,[d] 225.9[e]
	90 % water–DMSO (90:10, v/v)	–[c]
	water	14.61[a]
3	DMSO	–,[b] –[c]
	30 % water–DMSO (30:70, v/v)	360.7,[c] –,[d] 187.7[e]
	90 % water–DMSO (90:10, v/v)	–[c]
	water	30.44[a]
4	DMSO	–,[b] –[c]
	26 % water–DMSO (26:74, v/v)	545.6,[c] –,[d] 246.4[e]
	90 % water–DMSO (90:10, v/v)	–[c]
	water	58.77[c]
5	DMSO	–,[b] –[c]
	20 % water–DMSO (20:80, v/v)	309.5,[c] –,[d] 175.2[e]
	90 % water–DMSO (90:10, v/v)	26.63[c]
	water	190.1[a]
6	DMSO	–[b]
	water	68.06, 1281[a]

[a]At a concentration of 5.0×10^{-4} M.

[b]At a concentration of 1.0×10^{-3} M.

[c]At a concentration of 2.0×10^{-5} M.

[d]Heated to 333 K at a concentration of 2.0×10^{-5} M.

[e]Cooled to 298 K after heating at a concentration of 2.0×10^{-5} M.

Table S6. Summary of intermolecular distances estimated from $^{1}H-^{1}H$ NOESY experiments of complexes **2**–**4** at 298 K

Complex	Proton−Proton	Distances / Å
2	H_a-H_e	3.50
	H_b-H_d	3.43
	H_d-H_e	2.88
3	H_a-H_e	2.83
	H_b-H_d	3.58
	H_d-H_e	3.37
4	H_a-H_e	2.98
	H_b-H_d	2.59
	H_d-H_e	3.50

Table S7. Summary of intermolecular distances estimated from $^{1}H-^{1}H$ NOESY experiments of **5** after cooling to 298 K after heat treatment

Complex	Proton−Proton	Distances / Å
5	H_a-H_e	2.60
	H_b-H_d	2.58
	H_d-H_e	2.74

Table S8. Cartesian coordinates of the optimized S_0 state geometry of **1**

Pt	-6E-06	0.1818	0.000323	H	-4.51709	-4.64739	-0.89559
O	-1.35857	-1.28541	0.000626	H	-5.97193	-5.16499	-0.0012
N	1.304501	1.64624	0.0001	H	-4.51743	-4.64798	0.894094
O	1.358538	-1.28541	0.000691	C	2.641995	-1.07873	0.00025
N	-1.30454	1.646227	0.000082	C	3.273484	0.213992	0.000168
C	-2.60107	1.459353	0.0003	C	3.466394	-2.22873	0.000062
H	-3.23883	2.341284	0.000562	H	2.964879	-3.18919	0.000178
C	-0.70501	2.925441	-0.00011	C	4.845885	-2.12415	-0.00024
C	0.704955	2.925454	-0.0001	C	4.696501	0.267368	-0.00017
C	2.601019	1.459392	0.000325	H	5.170118	1.24609	-0.00031
H	3.238782	2.341338	0.000639	C	5.475903	-0.85399	-0.00042
C	-0.69782	5.337112	-0.00072	H	6.559134	-0.80259	-0.00078
H	-1.24476	6.274794	-0.00098	O	5.685115	-3.17238	-0.00045
C	-2.64199	-1.07877	0.000265	C	5.12627	-4.47624	-0.0006
C	-4.69654	0.267322	-5.4E-05	H	4.517253	-4.64757	-0.89533
H	-5.17015	1.24604	-0.00014	H	4.517656	-4.64796	0.894342
C	-3.46639	-2.22879	0.000048	H	5.97215	-5.16495	-0.00093
H	-2.96489	-3.18924	0.000139	C	0.697848	5.337109	-0.00072
C	-4.84586	-2.12419	-0.00019	H	1.244803	6.274782	-0.001
C	-5.47593	-0.85405	-0.00027	C	-1.39773	4.138767	-0.00043
H	-6.55916	-0.80269	-0.00051	H	-2.48171	4.158332	-0.00049
C	-3.27352	0.21395	0.0002	C	1.397728	4.138745	-0.00043
O	-5.68508	-3.17243	-0.00047	H	2.481695	4.158239	-0.00051

Table S9. Cartesian coordinates of the optimized T_1 state geometry of **1**

Pt	0.000003	0.227092	0.000107	H	-4.37662	-4.69805	-0.89483
O	-1.33892	-1.21476	0.000147	H	-5.80868	-5.2737	-0.00036
N	1.312238	1.667949	0.000011	H	-4.37673	-4.69825	0.894423
O	1.338919	-1.21476	0.000168	C	2.642753	-1.05942	0.000077
N	-1.31223	1.667947	0.000017	C	3.293255	0.220835	0.000039
C	-2.63526	1.476218	0.000063	C	3.409532	-2.24255	0.000034
H	-3.27121	2.355801	0.000091	H	2.865338	-3.17969	0.000076
C	-0.71088	2.928891	-5.2E-05	C	4.794383	-2.19225	-5.6E-05
C	0.710878	2.928893	-5.6E-05	C	4.710558	0.219571	-2.1E-05
C	2.635263	1.476216	0.000062	H	5.224436	1.177186	-0.00004
H	3.271213	2.355799	0.000095	C	5.44857	-0.94066	-7.1E-05
C	-0.6998	5.346239	-0.00021	H	6.533574	-0.91734	-0.00013
H	-1.24632	6.284199	-0.00027	O	5.603276	-3.27125	-0.00013
C	-2.64275	-1.05942	0.000068	C	4.992972	-4.54922	-0.00022
C	-4.71056	0.219573	-1.5E-05	H	4.37661	-4.69805	-0.89482
H	-5.22443	1.177189	-0.00003	H	4.376731	-4.69824	0.894435
C	-3.40953	-2.24256	0.000027	H	5.808672	-5.2737	-0.00035
H	-2.86534	-3.1797	0.000062	C	0.69978	5.346242	-0.00021
C	-4.79438	-2.19225	-5.5E-05	H	1.246295	6.284205	-0.00028
C	-5.44857	-0.94066	-6.5E-05	C	-1.39949	4.148538	-0.00013

H	-6.53357	-0.91734	-0.00012	H	-2.48356	4.168476	-0.00013
C	-3.29326	0.220838	0.00004	C	1.399477	4.148545	-0.00014
O	-5.60328	-3.27125	-0.00012	H	2.483551	4.168491	-0.00014
C	-4.99298	-4.54922	-0.00023				

Table S10. Cartesian coordinates of the optimized S_0 state geometry of **7**

Pt	-0.02749	-1.48354	-0.10303	C	2.549774	-7.9574	0.181828
O	-1.35674	0.00936	-0.17818	H	3.004438	-7.51829	-0.71458
N	1.249042	-2.97277	-0.02592	H	2.952311	-7.46241	1.074119
O	1.359288	-0.04315	-0.12123	H	2.790098	-9.02071	0.222127
N	-1.36075	-2.92447	-0.08815	C	-2.84955	-7.86178	0.008752
C	-2.65119	-2.71373	-0.12468	H	-3.28924	-7.35553	0.876827
H	-3.30734	-3.58236	-0.11319	H	-3.23237	-7.40521	-0.91211
C	-0.77956	-4.21009	-0.03481	H	-3.1284	-8.91624	0.029201
C	0.618623	-4.2357	0.002116	C	6.358376	4.057524	-0.26883
C	2.546974	-2.81122	-0.00591	H	6.962839	3.850244	-1.16062
H	3.167645	-3.70439	0.037023	C	5.809028	5.474494	-0.40853
C	-0.83638	-6.62573	0.036426	H	4.858418	5.460045	-0.97186
C	-2.64461	-0.17472	-0.19528	H	5.580753	5.891433	0.587457
C	-4.72215	-1.4809	-0.20669	C	7.22244	3.878976	0.970516
H	-5.21396	-2.45048	-0.19528	H	6.606017	4.060365	1.870579
C	-3.44707	0.990299	-0.23633	H	7.580421	2.839131	1.029798
H	-2.92681	1.940586	-0.24995	C	-6.19983	4.297004	-0.24752
C	-4.82817	0.911076	-0.25934	H	-6.79522	4.185199	-1.16217
C	-5.48156	-0.34525	-0.24778	C	-7.09205	4.055331	0.961038
H	-6.56537	-0.37697	-0.26889	H	-7.50227	3.034025	0.924651
C	-3.30028	-1.45378	-0.17583	H	-6.4821	4.125663	1.880891
O	-5.64822	1.975882	-0.2941	C	-5.59486	5.698013	-0.26405
C	-5.07372	3.277151	-0.27601	H	-4.63221	5.690564	-0.80681
H	-4.43144	3.384752	0.609525	H	-5.37486	6.026061	0.766422
H	-4.45313	3.419505	-1.16944	O	8.306606	4.770551	0.931362
C	2.639259	-0.2755	-0.10077	O	6.74374	6.278871	-1.08174
C	3.245339	-1.5774	-0.04079	O	-6.48289	6.588217	-0.89054
C	3.485642	0.857792	-0.1422	O	-8.12956	5.001243	0.98791
H	3.001906	1.825897	-0.19182	C	9.125358	4.637829	2.062834
C	4.862871	0.727345	-0.12426	H	9.546901	3.623528	2.149293
C	4.665548	-1.65749	-0.02045	H	9.947786	5.351565	1.962532
H	5.119909	-2.64434	0.026638	H	8.578919	4.858445	2.993857
C	5.467919	-0.55156	-0.05964	C	6.307407	7.6082	-1.1788
H	6.549913	-0.62355	-0.046	H	7.070813	8.168013	-1.72614
O	5.722479	1.760189	-0.16808	H	5.352556	7.690304	-1.72315
C	5.195601	3.079922	-0.23958	H	6.174335	8.07058	-0.18779
H	4.550318	3.268467	0.630245	C	-5.99978	7.904595	-0.86514
H	4.587488	3.185543	-1.14641	H	-5.02831	7.997681	-1.37736
C	0.5842	-6.65144	0.080252	H	-6.72887	8.534784	-1.38192
C	-1.50071	-5.41272	-0.01923	H	-5.87841	8.277925	0.164178

H	-2.58194	-5.40258	-0.05351	C	-8.97316	4.810441	2.092542
C	1.293853	-5.46326	0.060437	H	-9.75753	5.57102	2.046023
H	2.375055	-5.49162	0.088237	H	-9.44571	3.815182	2.082469
O	1.13724	-7.87829	0.138021	H	-8.4326	4.919541	3.046463
O	-1.43524	-7.832	0.052757				

Table S11. Cartesian coordinates of the optimized T_1 state geometry of **7**

Pt	-0.05324	-1.56821	-0.09176	C	2.424346	-8.0485	0.131317
O	-1.34043	-0.08044	-0.14853	H	2.877812	-7.61081	-0.76644
N	1.207028	-3.05463	-0.02939	H	2.843588	-7.56563	1.022569
O	1.336428	-0.17574	-0.1246	H	2.647233	-9.11592	0.162515
N	-1.415	-2.96401	-0.06774	C	-2.97419	-7.86454	0.025985
C	-2.73128	-2.7267	-0.092	H	-3.39423	-7.35514	0.901984
H	-3.39928	-3.58215	-0.07628	H	-3.36197	-7.39729	-0.88752
C	-0.85258	-4.23869	-0.02635	H	-3.26931	-8.91459	0.045391
C	0.557094	-4.28738	-0.00403	C	6.254433	4.038736	-0.27479
C	2.536434	-2.91011	-0.009	H	6.868211	3.846015	-1.16348
H	3.140164	-3.8112	0.033755	C	5.673012	5.442558	-0.41707
C	-0.94248	-6.65921	0.033271	H	4.720904	5.405382	-0.97697
C	-2.6498	-0.19233	-0.16062	H	5.439135	5.857809	0.578303
C	-4.7604	-1.39684	-0.15767	C	7.116146	3.880952	0.968999
H	-5.30765	-2.33576	-0.14021	H	6.489522	4.041882	1.865959
C	-3.3749	1.016096	-0.20047	H	7.503255	2.851622	1.027337
H	-2.7976	1.932817	-0.21802	C	-5.95007	4.471263	-0.25388
C	-4.76042	1.014372	-0.21962	H	-6.52967	4.386384	-1.18147
C	-5.45803	-0.21203	-0.19836	C	-6.88373	4.292273	0.933908
H	-6.54316	-0.19779	-0.21372	H	-7.3473	3.294158	0.897236
C	-3.34433	-1.44848	-0.13608	H	-6.29429	4.340472	1.868446
O	-5.53137	2.12229	-0.26009	C	-5.2631	5.83398	-0.26688
C	-4.88534	3.386836	-0.24921	H	-4.28642	5.762594	-0.77924
H	-4.25075	3.472	0.645322	H	-5.0554	6.161986	0.766161
H	-4.24212	3.484697	-1.13339	O	8.1744	4.803616	0.939295
C	2.634611	-0.37788	-0.1054	O	6.587276	6.265561	-1.09614
C	3.239004	-1.67865	-0.04519	O	-6.07653	6.767471	-0.93066
C	3.442778	0.776653	-0.1485	O	-7.86942	5.292866	0.924463
H	2.931593	1.730947	-0.19737	C	8.988305	4.692625	2.076518
C	4.824835	0.678021	-0.13028	H	9.437352	3.690407	2.165276
C	4.655222	-1.72585	-0.0245	H	9.791277	5.429075	1.982842
H	5.134867	-2.69992	0.023203	H	8.429222	4.896949	3.003772
C	5.43435	-0.59307	-0.0648	C	6.122815	7.585299	-1.19257
H	6.517815	-0.65392	-0.04996	H	6.871566	8.160311	-1.74439
O	5.67248	1.72818	-0.17382	H	5.163756	7.646815	-1.73224
C	5.115975	3.032476	-0.25068	H	5.985092	8.046065	-0.20143
H	4.460534	3.209881	0.614744	C	-5.51435	8.052083	-0.90838
H	4.509659	3.124412	-1.16108	H	-4.52491	8.07787	-1.39327
C	0.48072	-6.70811	0.059316	H	-6.18836	8.71793	-1.4544

C	-1.5888	-5.43653	-0.00864	H	-5.39931	8.432551	0.11906
H	-2.66998	-5.41002	-0.03011	C	-8.7496	5.159711	2.008726
C	1.209545	-5.53218	0.038775	H	-9.49005	5.961124	1.935342
H	2.290379	-5.57837	0.053331	H	-9.27527	4.191478	1.995656
O	1.013214	-7.94515	0.101684	H	-8.22804	5.249343	2.975171
O	-1.55936	-7.85674	0.051375				

Table S12. Cartesian coordinates of the optimized S_0 state geometry of the dimer $\mathbf{7}_2$ in aqueous solution

C	3.345899	2.211771	1.811267	H	-3.56078	6.88535	-0.96468
H	2.907065	3.204956	1.79592	H	-3.33451	-7.38198	0.5075
O	-1.46821	1.488115	1.62028	H	2.496572	-7.49287	0.351292
N	-1.57878	-1.46117	1.444959	H	-6.64075	1.271263	0.81625
C	4.722896	2.064988	1.828984	H	6.388778	0.681966	1.877532
O	0.87579	-6.33207	0.641447	H	6.863272	-0.31316	-1.5967
C	4.491746	-0.31773	1.824495	H	-6.17277	-1.78038	-2.04909
H	4.932589	-1.31102	1.811023	O	-5.41	3.742087	0.795739
C	5.308527	0.785459	1.849778	O	5.517316	3.190323	1.853673
O	-1.66229	-6.27633	0.710903	O	6.131398	-2.92978	-1.1986
C	3.066293	-0.22562	1.781373	O	-4.90238	-4.1694	-1.63693
C	2.375201	-1.44439	1.701734	C	-6.76031	3.862216	0.346862
H	2.969332	-2.35061	1.720572	H	-7.03248	3.01029	-0.28524
C	1.08927	-3.98639	1.121774	C	-6.26412	-4.28418	-1.20979
H	2.16913	-4.01438	1.08654	H	-6.93483	-3.80809	-1.93614
C	0.415779	-2.76084	1.358423	C	7.510298	-2.74605	-0.8727
Pt	-0.20981	-0.05714	1.617069	H	7.996218	-2.07856	-1.59387
C	2.486631	1.099065	1.799631	C	6.268176	3.398173	0.648467
O	1.193448	1.35257	1.801917	H	6.594542	2.432574	0.240816
N	1.015574	-1.58443	1.593319	C	7.502159	4.195758	0.990245
C	0.364521	-5.12546	0.900368	H	8.108219	3.639393	1.720957
C	-1.08961	-5.09235	0.923276	H	8.10185	4.317768	0.075266
C	-1.76496	-3.90352	1.131156	C	5.36074	4.078416	-0.36389
H	-2.84655	-3.89576	1.117963	H	4.383335	3.57842	-0.35122
C	-1.04181	-2.72214	1.319017	H	5.205759	5.131585	-0.08875
C	2.294551	-6.44614	0.57503	C	-6.76099	5.125318	-0.49946
H	2.750185	-6.175	1.53277	H	-6.05451	4.999158	-1.33364
H	2.696015	-5.81045	-0.22122	H	-6.42121	5.977331	0.107043
C	-3.08801	-6.3392	0.703666	C	-7.71419	3.926251	1.520477
H	-3.49656	-5.70229	-0.08502	H	-8.74277	3.984927	1.13521
H	-3.48585	-6.03794	1.676698	H	-7.6337	3.007131	2.119905
C	-2.7587	1.351051	1.415506	C	7.688167	-2.17388	0.52037
C	-3.49212	2.53242	1.243357	H	8.766218	-2.13516	0.733276
H	-2.96173	3.47838	1.271182	H	7.300096	-1.14718	0.57435
C	-4.85837	2.523163	0.997968	C	8.10936	-4.13469	-1.01977

C	-5.57005	1.305787	0.973547	H	7.896101	-4.51337	-2.03013
C	-4.86552	0.138548	1.155561	H	7.645314	-4.81884	-0.29461
H	-5.40051	-0.80676	1.133593	C	-6.49273	-3.64281	0.151176
C	-3.45968	0.094112	1.350556	H	-6.34049	-2.56187	0.08288
C	-2.87973	-1.19744	1.372019	H	-7.53751	-3.81291	0.434404
H	-3.56835	-2.03445	1.291154	C	-6.51027	-5.78265	-1.21339
C	-2.95907	-2.91247	-1.7879	H	-6.29913	-6.1841	-2.21535
H	-2.40371	-3.83626	-1.66695	H	-5.82445	-6.27111	-0.5048
O	1.75459	-1.4783	-1.63975	O	-8.06985	5.334035	-0.97593
N	1.367122	1.430422	-1.59166	O	-7.40343	5.055242	2.30585
C	-4.34502	-2.94523	-1.80059	O	5.955482	3.973423	-1.63942
O	-1.76298	5.977649	-1.01965	O	7.124293	5.450252	1.513148
C	-4.40977	-0.57377	-2.05367	O	7.018574	-2.99758	1.45073
H	-4.97126	0.35154	-2.14852	O	9.497059	-4.03311	-0.80113
C	-5.09199	-1.76474	-1.98568	O	-5.60311	-4.14257	1.131758
O	0.795567	6.227507	-0.7526	O	-7.85219	-6.0081	-0.85054
C	-3.00036	-0.48553	-1.96791	C	-8.15579	6.518353	-1.7409
C	-2.47413	0.833124	-1.88234	H	-7.49418	6.477897	-2.61777
H	-3.20736	1.635961	-1.9116	H	-9.18994	6.616255	-2.07869
C	-1.59685	3.59361	-1.43236	H	-7.8877	7.400726	-1.14296
H	-2.67137	3.491874	-1.50421	C	-8.28336	5.178374	3.402626
C	-0.76395	2.473945	-1.55785	H	-9.32486	5.295761	3.070716
Pt	0.239552	-0.16594	-1.69715	H	-8.22641	4.301862	4.063786
C	-2.24663	-1.70338	-1.87061	H	-7.98623	6.067195	3.964062
O	-0.93769	-1.78234	-1.82849	C	5.173908	4.614491	-2.62684
N	-1.21619	1.150407	-1.74764	H	5.68106	4.480235	-3.585
C	-1.04756	4.838516	-1.17673	H	4.168159	4.175392	-2.6902
C	0.358545	4.978333	-1.03754	H	5.074505	5.689249	-2.42
C	1.180323	3.873309	-1.17697	C	8.250724	6.252012	1.797233
H	2.249015	3.980795	-1.04814	H	7.886076	7.202377	2.193874
C	0.622468	2.619194	-1.45237	H	8.902852	5.779019	2.545298
C	-3.17784	5.875912	-1.11701	H	8.844047	6.4453	0.892028
H	-3.4802	5.517212	-2.10739	C	7.306407	-2.61222	2.77918
H	-3.58143	5.21216	-0.34583	H	7.008974	-1.57199	2.971366
C	2.192817	6.392716	-0.55262	H	6.739596	-3.27089	3.441189
H	2.546508	5.780111	0.284796	H	8.378314	-2.71551	2.99907
H	2.755431	6.137957	-1.45776	C	10.12709	-5.29447	-0.88143
C	3.01439	-1.11272	-1.5891	H	9.99329	-5.74692	-1.87414
C	3.969854	-2.12894	-1.4221	H	11.19326	-5.14006	-0.70076
H	3.628113	-3.15127	-1.2931	H	9.731506	-5.98828	-0.12632
C	5.329975	-1.85535	-1.395	C	-6.22052	-4.98479	2.08781
C	5.805241	-0.54083	-1.5823	H	-5.44371	-5.30577	2.785545
C	4.881947	0.469475	-1.70949	H	-6.99776	-4.44578	2.645611
H	5.230163	1.495001	-1.81121	H	-6.67264	-5.87044	1.62445

C	3.484859	0.240642	-1.68459	C	-8.12681	-7.38801	-0.72453
C	2.669069	1.40406	-1.66663	H	-9.17723	-7.48842	-0.44249
H	3.195846	2.353205	-1.71178	H	-7.9572	-7.91837	-1.67201
H	2.338485	7.447525	-0.31885	H	-7.50009	-7.85006	0.051272

Table S13. Cartesian coordinates of the optimized T_1 state geometry of the dimer $\mathbf{7}_2$ in aqueous solution

C	-3.34578	-2.212	1.811336	H	3.560856	-6.88528	-0.96456
H	-2.90688	-3.20516	1.796041	H	3.33403	7.382075	0.50703
O	1.468284	-1.48816	1.620278	H	-2.49698	7.492512	0.350881
N	1.57878	1.461125	1.44505	H	6.640867	-1.27112	0.816591
C	-4.72279	-2.06526	1.829105	H	-6.38871	-0.68228	1.877499
O	-0.87613	6.331825	0.641052	H	-6.86326	0.313254	-1.59674
C	-4.49171	0.317469	1.824412	H	6.172776	1.780446	-2.04838
H	-4.93256	1.310748	1.810824	O	5.410182	-3.74193	0.795683
C	-5.30846	-0.78575	1.849765	O	-5.51717	-3.19061	1.853906
O	1.661951	6.276261	0.71057	O	-6.13138	2.929868	-1.19879
C	-3.06625	0.225395	1.78135	O	4.90224	4.169458	-1.63655
C	-2.37523	1.444202	1.701856	C	6.760486	-3.86195	0.346745
H	-2.96932	2.35045	1.720831	H	7.032616	-3.00989	-0.28518
C	-1.08944	3.98619	1.121616	C	6.263979	4.284399	-1.20947
H	-2.1693	4.014069	1.0864	H	6.934702	3.808284	-1.93578
C	-0.41588	2.760681	1.358353	C	-7.51029	2.746195	-0.87289
Pt	0.209839	0.057058	1.617064	H	-7.99621	2.078621	-1.59398
C	-2.48655	-1.09927	1.799665	C	-6.26807	-3.3986	0.648761
O	-1.19336	-1.35269	1.801955	H	-6.59461	-2.43305	0.24111
N	-1.0156	1.584285	1.593405	C	-7.50192	-4.19636	0.990622
C	-0.36477	5.125269	0.900094	H	-8.10808	-3.64004	1.721289
C	1.089364	5.092254	0.923037	H	-8.10158	-4.31854	0.075649
C	1.764778	3.903482	1.131045	C	-5.36063	-4.07871	-0.36367
H	2.846375	3.895799	1.117895	H	-4.38326	-3.57864	-0.35102
C	1.04171	2.722073	1.318987	H	-5.20556	-5.13189	-0.08863
C	-2.29489	6.445812	0.574677	C	6.761156	-5.12489	-0.49982
H	-2.75049	6.174695	1.532445	H	6.054631	-4.99859	-1.33394
H	-2.69636	5.810054	-0.22152	H	6.421431	-5.97702	0.106538
C	3.087652	6.339304	0.703388	C	7.714383	-3.9262	1.520336
H	3.496354	5.702292	-0.08513	H	8.74296	-3.98474	1.135056
H	3.485473	6.038301	1.676506	H	7.633848	-3.00722	2.119964
C	2.758782	-1.35103	1.415569	C	-7.68821	2.174193	0.520252
C	3.492221	-2.53237	1.243309	H	-8.76627	2.135451	0.733105
H	2.961892	-3.47836	1.271002	H	-7.30008	1.147523	0.574389
C	4.858487	-2.52304	0.997995	C	-8.10935	4.134816	-1.02016
C	5.570151	-1.30566	0.973764	H	-7.89602	4.513364	-2.03055
C	4.865589	-0.13845	1.155837	H	-7.64534	4.819045	-0.29506

H	5.400577	0.806858	1.134207	C	6.492715	3.643316	0.151607
C	3.459723	-0.09406	1.35074	H	6.34098	2.562284	0.083715
C	2.879723	1.197467	1.372163	H	7.537404	3.813947	0.434858
H	3.568301	2.034511	1.291348	C	6.509976	5.782904	-1.21327
C	2.959005	2.912462	-1.78765	H	6.298735	6.184214	-2.21525
H	2.403623	3.836247	-1.66676	H	5.824141	6.271358	-0.50468
O	-1.75457	1.478276	-1.63965	O	8.070001	-5.33348	-0.97638
N	-1.36712	-1.43046	-1.59169	O	7.403682	-5.05538	2.305465
C	4.344959	2.945264	-1.8002	O	-5.95543	-3.97366	-1.63917
O	1.763013	-5.97767	-1.01979	O	-7.12383	-5.45074	1.513618
C	4.409779	0.573807	-2.05328	O	-7.01871	2.998062	1.450532
H	4.971295	-0.35149	-2.14807	O	-9.49705	4.03326	-0.8016
C	5.091988	1.764784	-1.98515	O	5.602878	4.14302	1.132017
O	-0.79554	-6.22754	-0.75265	O	7.851898	6.008548	-0.85052
C	3.000358	0.485536	-1.96772	C	8.155976	-6.51773	-1.74146
C	2.47414	-0.83312	-1.88222	H	7.494296	-6.47726	-2.61828
H	3.207405	-1.63593	-1.91131	H	9.19011	-6.61553	-2.07933
C	1.596847	-3.59364	-1.43249	H	7.887997	-7.40017	-1.14357
H	2.671366	-3.49191	-1.50437	C	8.283674	-5.17875	3.402166
C	0.763939	-2.47398	-1.55793	H	9.325155	-5.29605	3.070176
Pt	-0.23956	0.165912	-1.69718	H	8.226752	-4.30238	4.063527
C	2.246591	1.703375	-1.87045	H	7.986578	-6.0677	3.963421
O	0.937649	1.78232	-1.8284	C	-5.17387	-4.61462	-2.62666
N	1.216184	-1.15043	-1.74769	H	-5.68112	-4.4804	-3.58478
C	1.047572	-4.83855	-1.17684	H	-4.16817	-4.17541	-2.6901
C	-0.35853	-4.97837	-1.03762	H	-5.07433	-5.68937	-2.41985
C	-1.18032	-3.87335	-1.17705	C	-8.25011	-6.25269	1.797753
H	-2.249	-3.98087	-1.04817	H	-7.88529	-7.20297	2.194448
C	-0.62248	-2.61923	-1.45242	H	-8.90232	-5.77977	2.545793
C	3.17788	-5.87587	-1.11699	H	-8.8434	-6.44614	0.892561
H	3.480325	-5.51722	-2.10737	C	-7.30658	2.612884	2.779028
H	3.581359	-5.21205	-0.34582	H	-7.00934	1.57262	2.971311
C	-2.19277	-6.39277	-0.55256	H	-6.73962	3.271505	3.440955
H	-2.5464	-5.78015	0.28487	H	-8.37847	2.716401	2.998937
H	-2.75546	-6.13804	-1.45766	C	-10.1271	5.294617	-0.88197
C	-3.01437	1.112726	-1.58899	H	-9.9932	5.747038	-1.87469
C	-3.96982	2.128963	-1.42198	H	-11.1933	5.140229	-0.70138
H	-3.62806	3.151284	-1.29294	H	-9.73153	5.988445	-0.12687
C	-5.32995	1.855399	-1.39499	C	6.220101	4.985268	2.088164
C	-5.80522	0.540893	-1.58227	H	5.443092	5.306559	2.785538
C	-4.88194	-0.46943	-1.70943	H	6.997012	4.44619	2.646361
H	-5.23018	-1.49495	-1.81114	H	6.672585	5.870732	1.624804
C	-3.48485	-0.24064	-1.68453	C	8.126327	7.388496	-0.72454
C	-2.66908	-1.40408	-1.66654	H	9.176753	7.489055	-0.44257

H	-3.19587	-2.35322	-1.71167	H	7.956581	7.918828	-1.67201
H	-2.3384	-7.44757	-0.31876	H	7.499586	7.85046	0.051294

Table S14. Cartesian coordinates of the optimized S_0 state geometry of the dimer $\mathbf{7}_2$ in *n*-hexane

C	-3.24157	-2.30099	1.893567	H	3.696007	-6.75	-1.17039
H	-2.78443	-3.28285	1.951483	H	3.268427	7.419516	0.482036
O	1.5522	-1.47191	1.577046	H	-2.62142	7.502327	0.895195
N	1.577013	1.457121	1.323811	H	6.662768	-1.16472	0.537136
C	-4.61262	-2.1751	1.858656	H	-6.30611	-0.8222	1.79283
O	-0.95467	6.389301	1.007013	H	-6.91133	0.230715	-1.59697
C	-4.42318	0.205491	1.721942	H	6.060693	2.001764	-2.21626
H	-4.8782	1.189799	1.635457	O	5.50303	-3.6675	0.677891
C	-5.22484	-0.90652	1.79112	O	-5.3773	-3.30913	1.903928
O	1.60894	6.349475	0.835258	O	-6.21606	2.857097	-1.23206
C	-3.00885	0.12361	1.727572	O	4.737238	4.335203	-1.71315
C	-2.31385	1.358734	1.59823	C	6.898861	-3.77392	0.442979
H	-2.94457	2.241564	1.518339	H	7.238498	-2.99688	-0.25371
C	-1.08214	3.989808	1.293907	C	6.069737	4.459831	-1.24045
H	-2.16131	4.014405	1.360175	H	6.786178	4.049645	-1.9661
C	-0.39805	2.771261	1.376672	C	-7.5454	2.659733	-0.77606
Pt	0.249245	0.031346	1.577954	H	-8.10617	2.005587	-1.45794
C	-2.3903	-1.1697	1.829175	C	-6.18044	-3.52207	0.745434
O	-1.11569	-1.39706	1.839356	H	-6.57826	-2.56716	0.375764
N	-1.02246	1.518887	1.540129	C	-7.35278	-4.39722	1.121851
C	-0.38639	5.170564	1.110315	H	-7.90126	-3.9249	1.952846
C	1.029955	5.146313	1.015935	H	-8.03135	-4.45326	0.254216
C	1.70879	3.940409	1.100697	C	-5.3169	-4.12729	-0.35206
H	2.787868	3.931765	0.999767	H	-4.3421	-3.61571	-0.35259
C	0.996769	2.74326	1.272341	H	-5.14771	-5.19357	-0.14398
C	-2.36269	6.450065	1.023027	C	7.077757	-5.12534	-0.22824
H	-2.77454	6.094695	1.976918	H	6.428489	-5.17337	-1.11838
H	-2.80221	5.86971	0.201196	H	6.76466	-5.91697	0.467677
C	3.010329	6.37469	0.665667	C	7.693233	-3.66154	1.730553
H	3.32773	5.762144	-0.18518	H	8.765258	-3.69087	1.477147
H	3.533144	6.026025	1.564199	H	7.486295	-2.69259	2.213324
C	2.810482	-1.31463	1.318934	C	-7.605	2.063964	0.620168
C	3.577834	-2.48867	1.170616	H	-8.66367	2.048725	0.920881
H	3.072191	-3.44074	1.285365	H	-7.23617	1.027623	0.616316
C	4.927127	-2.45702	0.870544	C	-8.16844	4.044516	-0.8252
C	5.602519	-1.22181	0.74877	H	-8.02785	4.466407	-1.83267
C	4.868591	-0.06658	0.89743	H	-7.65077	4.696522	-0.10566
H	5.369259	0.889914	0.781124	C	6.303564	3.773495	0.09784
C	3.480861	-0.04973	1.160041	H	6.376297	2.683853	-0.02439
C	2.852787	1.230217	1.170546	H	7.271574	4.134747	0.476257

H	3.508417	2.08289	0.996178	C	6.307115	5.958596	-1.15238
C	2.823489	3.029072	-1.87344	H	6.002952	6.42694	-2.10116
H	2.235779	3.926483	-1.7214	H	5.686475	6.384144	-0.34873
O	-1.83323	1.468754	-1.68975	O	8.428944	-5.25032	-0.57759
N	-1.38029	-1.42257	-1.66466	O	7.340191	-4.7218	2.573972
C	4.20222	3.101536	-1.90071	O	-5.98123	-3.94336	-1.57904
O	1.881781	-5.893	-1.23227	O	-6.89427	-5.67108	1.483409
C	4.335291	0.739023	-2.22166	O	-6.83878	2.85305	1.495728
H	4.923326	-0.16617	-2.34804	O	-9.52867	3.911325	-0.51062
C	4.982495	1.94753	-2.12885	O	5.258882	4.094853	0.984514
O	-0.66829	-6.22824	-0.98486	O	7.671018	6.154828	-0.89427
C	2.932419	0.605165	-2.11119	C	8.724684	-6.51915	-1.09684
C	2.436314	-0.7246	-2.03401	H	8.150507	-6.73144	-2.01251
H	3.18468	-1.51243	-2.09957	H	9.789836	-6.53457	-1.34118
C	1.638938	-3.50969	-1.58478	H	8.516358	-7.31695	-0.36762
H	2.710112	-3.36792	-1.62818	C	8.025242	-4.67525	3.795158
C	0.776634	-2.41027	-1.68788	H	9.116415	-4.74021	3.657286
Pt	-0.29271	0.204062	-1.7707	H	7.803861	-3.75239	4.354063
C	2.13791	1.798394	-1.97546	H	7.695278	-5.53076	4.389882
O	0.845679	1.838073	-1.90443	C	-5.33089	-4.59435	-2.63903
N	1.194109	-1.07409	-1.8514	H	-5.89778	-4.3888	-3.55028
C	1.133379	-4.77921	-1.36364	H	-4.3023	-4.22568	-2.78036
C	-0.2687	-4.96411	-1.23207	H	-5.29112	-5.68321	-2.48361
C	-1.11833	-3.87614	-1.33908	C	-7.94435	-6.52823	1.837426
H	-2.18146	-4.01681	-1.19729	H	-7.50687	-7.49594	2.095748
C	-0.6043	-2.59491	-1.57653	H	-8.50494	-6.15259	2.707794
C	3.2844	-5.74816	-1.30387	H	-8.65554	-6.67169	1.008039
H	3.599251	-5.36033	-2.2823	C	-7.08445	2.534099	2.841866
H	3.670791	-5.09475	-0.51266	H	-6.84751	1.483681	3.069178
C	-2.04011	-6.4364	-0.73639	H	-6.44217	3.173654	3.452743
H	-2.38323	-5.86398	0.135044	H	-8.13429	2.719356	3.116304
H	-2.65503	-6.17594	-1.60836	C	-10.1806	5.151344	-0.44984
C	-3.07082	1.084639	-1.64122	H	-10.1389	5.683958	-1.41271
C	-4.04705	2.087703	-1.47176	H	-11.2276	4.960924	-0.20045
H	-3.71589	3.115148	-1.36682	H	-9.74545	5.804523	0.322438
C	-5.39802	1.796839	-1.42377	C	5.548944	3.708687	2.306899
C	-5.85541	0.471043	-1.59199	H	4.675292	3.946617	2.918943
C	-4.92047	-0.52715	-1.72431	H	5.748667	2.629834	2.386223
H	-5.26163	-1.55732	-1.81334	H	6.420009	4.251848	2.702046
C	-3.52687	-0.27928	-1.72284	C	7.984523	7.509918	-0.7085
C	-2.68357	-1.42103	-1.72165	H	9.057427	7.574864	-0.51138
H	-3.19144	-2.3826	-1.7526	H	7.752594	8.109512	-1.60206
H	-2.15236	-7.50173	-0.52946	H	7.440185	7.94133	0.145899

Table S15. Cartesian coordinates of the optimized T_1 state geometry of the dimer $\mathbf{7}_2$ in *n*-hexane

C	-3.25413	-2.28067	1.848607	H	3.770622	-6.74258	-1.2301
H	-2.77805	-3.25506	1.878002	H	3.199895	7.446204	0.415643
O	1.51858	-1.44481	1.515468	H	-2.6337	7.508695	0.738433
N	1.574257	1.486558	1.304226	H	6.661625	-1.18782	0.60599
C	-4.62945	-2.17591	1.856213	H	-6.33025	-0.83516	1.874962
O	-0.98155	6.374522	0.882223	H	-6.87706	0.179871	-1.56064
C	-4.47043	0.222482	1.789112	H	6.082017	2.039441	-2.17233
H	-4.94277	1.200496	1.742938	O	5.463853	-3.67851	0.66475
C	-5.24728	-0.90523	1.842214	O	-5.39357	-3.31435	1.895217
O	1.562225	6.335181	0.754722	O	-6.20394	2.81467	-1.20373
C	-3.04282	0.172536	1.750339	O	4.744365	4.369224	-1.6889
C	-2.37601	1.397426	1.651776	C	6.862166	-3.79776	0.456951
H	-2.99329	2.286654	1.616035	H	7.226342	-3.00787	-0.21252
C	-1.12968	3.996001	1.226422	C	6.06952	4.49612	-1.19455
H	-2.20884	4.014282	1.265503	H	6.796759	4.079343	-1.90531
C	-0.43788	2.759273	1.346379	C	-7.54481	2.609225	-0.78712
Pt	0.232625	0.063757	1.534467	H	-8.07549	1.936875	-1.47512
C	-2.42192	-1.14034	1.802611	C	-6.15805	-3.5377	0.714098
O	-1.14132	-1.35117	1.799421	H	-6.54023	-2.58364	0.324295
N	-1.01945	1.563987	1.534183	C	-7.34666	-4.40385	1.06035
C	-0.43647	5.157555	1.028535	H	-7.91741	-3.9221	1.870689
C	1.006832	5.137638	0.951827	H	-7.99908	-4.4638	0.173032
C	1.702249	3.943823	1.062263	C	-5.26644	-4.15676	-0.35283
H	2.782123	3.947304	0.970784	H	-4.28576	-3.65802	-0.32041
C	1.004951	2.74395	1.239378	H	-5.11869	-5.22498	-0.13862
C	-2.39204	6.455956	0.889177	C	7.040669	-5.13361	-0.24484
H	-2.80789	6.122329	1.848144	H	6.4136	-5.14952	-1.15192
H	-2.82945	5.862402	0.076805	H	6.700439	-5.93927	0.421688
C	2.971722	6.39792	0.613319	C	7.630398	-3.72658	1.763292
H	3.317914	5.777052	-0.21874	H	8.707422	-3.7568	1.532109
H	3.476533	6.078844	1.531104	H	7.419161	-2.76955	2.267388
C	2.789417	-1.29687	1.285557	C	-7.64109	2.036062	0.616172
C	3.541564	-2.47593	1.130778	H	-8.70975	1.991236	0.876586
H	3.019621	-3.42242	1.215107	H	-7.23906	1.012416	0.644548
C	4.901526	-2.46077	0.866021	C	-8.18328	3.984666	-0.88075
C	5.595134	-1.23486	0.787566	H	-8.01853	4.389377	-1.8917
C	4.873699	-0.07098	0.940783	H	-7.69548	4.656604	-0.15882
H	5.391195	0.880422	0.857199	C	6.279079	3.817031	0.150708
C	3.47767	-0.03482	1.167103	H	6.326717	2.725074	0.037948
C	2.8701	1.248646	1.177296	H	7.251907	4.159885	0.533808
H	3.53233	2.097736	1.021163	C	6.310341	5.994712	-1.11439
C	2.838153	3.048894	-1.85173	H	6.024242	6.456133	-2.07224

H	2.243465	3.943992	-1.71407	H	5.678142	6.429837	-0.32477
O	-1.80649	1.453058	-1.61867	O	8.398408	-5.26771	-0.56478
N	-1.33413	-1.43436	-1.61175	O	7.252939	-4.80683	2.570221
C	4.216292	3.130486	-1.87336	O	-5.88731	-3.96635	-1.60237
O	1.951853	-5.89409	-1.27223	O	-6.90738	-5.67775	1.44624
C	4.363575	0.76723	-2.18139	O	-6.93583	2.86431	1.50589
H	4.958074	-0.13433	-2.30269	O	-9.55054	3.839938	-0.60371
C	5.003648	1.980163	-2.09034	O	5.235487	4.168606	1.027945
O	-0.59183	-6.24173	-0.98925	O	7.670018	6.188127	-0.83448
C	2.962174	0.624107	-2.07333	C	8.688294	-6.52317	-1.11829
C	2.475978	-0.71056	-1.99975	H	8.133877	-6.69643	-2.05421
H	3.230505	-1.49207	-2.06636	H	9.758852	-6.54723	-1.33709
C	1.695368	-3.50719	-1.59325	H	8.450215	-7.34122	-0.42131
H	2.765037	-3.362	-1.65581	C	7.910947	-4.79678	3.806843
C	0.82731	-2.40955	-1.6681	H	9.004664	-4.86377	3.691416
Pt	-0.25832	0.199783	-1.71817	H	7.681624	-3.88816	4.385549
C	2.160932	1.811849	-1.93709	H	7.563961	-5.66624	4.370902
O	0.868825	1.844293	-1.84938	C	-5.21363	-4.62918	-2.63985
N	1.235823	-1.06974	-1.82226	H	-5.75154	-4.42172	-3.56818
C	1.198039	-4.78114	-1.37885	H	-4.17728	-4.27298	-2.7537
C	-0.20108	-4.9733	-1.22797	H	-5.19076	-5.71777	-2.47881
C	-1.05653	-3.88808	-1.31101	C	-7.97273	-6.52508	1.775973
H	-2.11694	-4.03541	-1.15668	H	-7.54951	-7.49316	2.05606
C	-0.55115	-2.60194	-1.54055	H	-8.55715	-6.13832	2.625648
C	3.353222	-5.74146	-1.351	H	-8.65981	-6.672	0.926957
H	3.659996	-5.34289	-2.3278	C	-7.20603	2.544479	2.846682
H	3.740461	-5.09373	-0.55571	H	-6.92809	1.507681	3.089574
C	-1.95954	-6.45901	-0.72564	H	-6.61114	3.216636	3.470392
H	-2.29484	-5.89645	0.155161	H	-8.27087	2.683552	3.089491
H	-2.58631	-6.19362	-1.58751	C	-10.2188	5.072284	-0.58429
C	-3.04268	1.061693	-1.57207	H	-10.1556	5.588356	-1.55505
C	-4.02756	2.05829	-1.41779	H	-11.2704	4.873202	-0.36197
H	-3.70555	3.088714	-1.31724	H	-9.81455	5.744627	0.188376
C	-5.37665	1.758189	-1.37974	C	5.499135	3.761711	2.35009
C	-5.8231	0.428063	-1.54671	H	4.626383	4.019341	2.955426
C	-4.88078	-0.56408	-1.66678	H	5.665319	2.676723	2.420947
H	-5.21273	-1.59652	-1.76242	H	6.381661	4.274922	2.759506
C	-3.48891	-0.30531	-1.65197	C	7.98732	7.544019	-0.66151
C	-2.63835	-1.44057	-1.65265	H	9.056983	7.606235	-0.44693
H	-3.14078	-2.40467	-1.68052	H	7.773811	8.132584	-1.56691
H	-2.06386	-7.52679	-0.5273	H	7.430857	7.989597	0.17772

Table S16. Cartesian coordinates of the optimized S_0 state geometry of the dimer $\mathbf{7}_2$ in dichloromethane

C	-4.11863	2.367403	-1.46362	H	2.981078	7.382618	0.66987
H	-3.746	3.38673	-1.46299	H	3.32626	-6.72528	-0.83354
O	0.730644	1.911135	-1.78433	H	-2.57902	-7.3165	-0.28365
N	1.001038	-1.00508	-1.58912	H	5.95804	1.950562	-1.67904
C	-5.48421	2.141353	-1.38871	H	-7.05189	0.613356	-1.37434
O	-1.04088	-6.08711	-0.69315	H	-5.90029	-1.66633	1.682445
C	-5.08964	-0.21453	-1.48296	H	7.060888	-0.84059	1.033643
H	-5.46386	-1.23301	-1.48786	O	4.637526	4.360518	-1.53556
C	-5.99016	0.821882	-1.41855	O	-6.25083	3.249335	-1.30241
O	1.526152	-5.82793	-0.89289	O	-4.61677	-4.10097	1.67724
C	-3.68802	-0.03304	-1.5246	O	6.149196	-3.40711	1.247368
C	-2.89879	-1.21663	-1.45959	C	6.002894	4.510637	-1.15592
H	-3.4521	-2.15126	-1.37753	H	6.649721	3.886032	-1.78394
C	-1.41954	-3.7317	-1.10536	C	7.238626	-3.4663	0.326593
H	-2.49227	-3.84573	-1.00127	H	7.964002	-2.66623	0.521627
C	-0.85658	-2.46813	-1.33783	C	-5.926	-4.30218	1.160603
Pt	-0.44819	0.314463	-1.62064	H	-6.67586	-3.79267	1.781183
C	-3.18601	1.314569	-1.54834	C	-7.65737	3.130727	-1.10516
O	-1.93124	1.645726	-1.63532	H	-8.07501	2.347815	-1.74983
N	-1.59411	-1.26975	-1.457	C	-8.27892	4.441129	-1.53304
C	-0.60123	-4.83979	-0.95257	H	-8.00666	4.644388	-2.58098
C	0.810352	-4.69726	-1.05084	H	-9.37349	4.331539	-1.48298
C	1.360905	-3.44773	-1.28094	C	-7.93877	2.798112	0.35322
H	2.437067	-3.34431	-1.32379	H	-7.3423	1.924739	0.661582
C	0.533437	-2.32596	-1.41898	H	-7.639	3.650477	0.980361
C	-2.43817	-6.26303	-0.53129	C	6.182871	4.112543	0.303305
H	-2.98051	-6.03211	-1.4552	H	5.645994	3.171585	0.498951
H	-2.83413	-5.6398	0.277931	H	5.751337	4.88889	0.951916
C	2.937002	-5.71589	-0.97455	C	6.377803	5.951942	-1.41487
H	3.337379	-5.06147	-0.19255	H	7.461005	6.059555	-1.24752
H	3.251312	-5.33698	-1.95359	H	6.171142	6.195853	-2.46858
C	2.028358	1.843788	-1.76112	C	-6.08349	-3.8246	-0.27401
C	2.726978	3.065845	-1.70908	H	-7.01659	-4.26487	-0.65477
H	2.152055	3.984529	-1.67069	H	-6.19006	-2.73344	-0.31753
C	4.108635	3.118798	-1.6501	C	-6.13474	-5.80342	1.279746
C	4.875455	1.933153	-1.70877	H	-5.90127	-6.12049	2.307727
C	4.20815	0.732148	-1.76317	H	-5.44122	-6.32199	0.598742
H	4.784196	-0.18961	-1.77229	C	6.746965	-3.33836	-1.10822
C	2.79704	0.628151	-1.76343	H	6.221833	-2.38088	-1.2211
C	2.264105	-0.68891	-1.67966	H	7.619043	-3.31824	-1.77306
H	2.997991	-1.49228	-1.66038	C	7.890146	-4.80537	0.61568
C	4.087788	-2.41109	1.623771	H	8.195975	-4.83834	1.672767

H	3.667361	-3.40672	1.71882	H	7.151255	-5.60558	0.453996
O	-0.68946	-1.735	2.086529	O	7.558655	3.96011	0.535035
N	-0.86485	1.179597	1.785876	O	5.650676	6.789218	-0.55299
C	5.433889	-2.26201	1.34825	O	-9.31258	2.533169	0.469638
O	1.400222	6.195956	1.037033	O	-7.83572	5.471801	-0.68994
C	5.173828	0.115707	1.346027	O	-4.97548	-4.24325	-1.03771
H	5.595945	1.11173	1.242395	O	-7.47051	-6.07773	0.950461
C	6.002275	-0.97418	1.222319	O	5.854427	-4.37609	-1.45113
O	-1.17326	6.035158	1.143235	O	8.994999	-4.94757	-0.23889
C	3.780456	0.009795	1.580092	C	7.833338	3.669151	1.883275
C	3.039954	1.226494	1.55653	H	7.355632	2.729797	2.202603
H	3.623894	2.131823	1.400136	H	8.916597	3.563794	1.983739
C	1.669875	3.815908	1.389292	H	7.490394	4.473523	2.551325
H	2.747885	3.889147	1.339598	C	5.955815	8.146044	-0.75523
C	1.052997	2.570846	1.572846	H	7.02411	8.352276	-0.58751
Pt	0.538927	-0.18684	1.88686	H	5.697339	8.474428	-1.77332
C	3.222053	-1.30455	1.743819	H	5.369114	8.726573	-0.03875
O	1.970183	-1.56663	1.974557	C	-9.68899	2.290355	1.802145
N	1.743821	1.343166	1.66418	H	-10.7641	2.092771	1.810351
C	0.904992	4.960883	1.242833	H	-9.16519	1.416911	2.220446
C	-0.51292	4.870735	1.297934	H	-9.48172	3.157014	2.447954
C	-1.11936	3.641127	1.494016	C	-8.42033	6.705351	-1.02071
H	-2.19932	3.58174	1.517423	H	-8.03346	7.451533	-0.32167
C	-0.34326	2.482697	1.63224	H	-8.16618	7.016356	-2.04577
C	2.802518	6.324626	0.864128	H	-9.51763	6.673769	-0.93401
H	3.345159	6.031185	1.771679	C	-5.22823	-4.16845	-2.42289
H	3.164043	5.739035	0.012956	H	-5.50603	-3.15179	-2.73638
C	-2.58779	5.988854	1.147923	H	-4.30939	-4.45487	-2.94103
H	-2.97183	5.360101	0.335122	H	-6.03493	-4.85462	-2.71876
H	-2.97485	5.620684	2.106077	C	-7.73625	-7.45849	0.936313
C	-1.9803	-1.6341	1.97059	H	-7.55804	-7.91781	1.920386
C	-2.70168	-2.83966	1.908573	H	-8.78916	-7.58786	0.672993
H	-2.14672	-3.77093	1.930949	H	-7.11641	-7.98364	0.193774
C	-4.07731	-2.86565	1.767577	C	6.393154	-5.30499	-2.3666
C	-4.81919	-1.66387	1.751081	H	5.661183	-6.10866	-2.48349
C	-4.12808	-0.47489	1.805041	H	6.568853	-4.84557	-3.35079
H	-4.68298	0.458893	1.756899	H	7.339624	-5.73205	-2.01089
C	-2.71564	-0.40064	1.885809	C	9.655837	-6.17362	-0.03951
C	-2.14054	0.900531	1.812396	H	10.49242	-6.21403	-0.74168
H	-2.84879	1.723795	1.74206	H	10.04696	-6.26109	0.985295
H	-2.92287	7.015904	0.996297	H	8.99071	-7.02963	-0.22865

Table S17. Cartesian coordinates of the optimized T_1 state geometry of the dimer $\mathbf{7}_2$ in dichloromethane

C	-4.13451	2.35605	-1.42805	H	2.873616	7.40865	0.602002
H	-3.77196	3.378997	-1.42608	H	3.396702	-6.67242	-0.85612
O	0.719745	1.948657	-1.71867	H	-2.50023	-7.32611	-0.30819
N	1.015878	-0.97067	-1.57343	H	5.948075	2.025339	-1.71909
C	-5.49839	2.117427	-1.36483	H	-7.05158	0.574575	-1.35846
O	-0.97568	-6.07841	-0.71285	H	-5.89914	-1.74896	1.716294
C	-5.08057	-0.23439	-1.45103	H	7.058405	-0.86613	1.013277
H	-5.44476	-1.25642	-1.45635	O	4.612139	4.422448	-1.52427
C	-5.99163	0.793376	-1.39552	O	-6.27611	3.218918	-1.2891
O	1.587546	-5.79285	-0.91199	O	-4.56987	-4.16335	1.672494
C	-3.68061	-0.0398	-1.48377	O	6.120012	-3.43085	1.216438
C	-2.88086	-1.21672	-1.42173	C	5.976889	4.58052	-1.14415
H	-3.42602	-2.15603	-1.33849	H	6.629617	3.978549	-1.78806
C	-1.3781	-3.72289	-1.10206	C	7.223912	-3.49453	0.316145
H	-2.44939	-3.84852	-0.99655	H	7.94981	-2.69797	0.524569
C	-0.8275	-2.45181	-1.32341	C	-5.86934	-4.38338	1.142863
Pt	-0.44448	0.337068	-1.5786	H	-6.63536	-3.90157	1.766439
C	-3.19079	1.31217	-1.50137	C	-7.68251	3.087553	-1.10017
O	-1.93832	1.65552	-1.57406	H	-8.08842	2.297528	-1.74363
N	-1.57584	-1.25904	-1.42907	C	-8.31424	4.38965	-1.53824
C	-0.54882	-4.82447	-0.96156	H	-8.03846	4.590141	-2.58581
C	0.861173	-4.66782	-1.06049	H	-9.40791	4.269863	-1.49319
C	1.399362	-3.41132	-1.28145	C	-7.96998	2.759045	0.357956
H	2.474415	-3.29616	-1.32184	H	-7.36956	1.890866	0.673138
C	0.560921	-2.2965	-1.40907	H	-7.67929	3.615904	0.983311
C	-2.37052	-6.26908	-0.54678	C	6.166258	4.153027	0.305473
H	-2.91914	-6.03473	-1.46603	H	5.668576	3.186138	0.475437
H	-2.76888	-5.65699	0.269709	H	5.700588	4.895383	0.970347
C	2.997518	-5.66587	-0.98944	C	6.330549	6.032663	-1.37046
H	3.38924	-5.01442	-0.20088	H	7.411956	6.153042	-1.20186
H	3.310955	-5.27485	-1.96377	H	6.117895	6.29809	-2.41773
C	2.018526	1.888367	-1.73155	C	-6.03124	-3.88408	-0.28388
C	2.709542	3.114935	-1.68836	H	-6.9587	-4.32897	-0.67309
H	2.12849	4.028961	-1.63664	H	-6.15041	-2.79354	-0.3088
C	4.091213	3.177507	-1.64749	C	-6.04858	-5.89039	1.234503
C	4.865271	1.998996	-1.73041	H	-5.81215	-6.22064	2.257664
C	4.205383	0.793524	-1.78452	H	-5.34274	-6.38326	0.547172
H	4.787841	-0.12368	-1.81191	C	6.761972	-3.36226	-1.12829
C	2.795586	0.67895	-1.76028	H	6.231536	-2.40823	-1.24508
C	2.274894	-0.6436	-1.67825	H	7.64709	-3.3315	-1.77539
H	3.015456	-1.44101	-1.67563	C	7.866556	-4.83562	0.615704
C	4.066828	-2.40205	1.593193	H	8.149328	-4.87128	1.679092

H	3.633449	-3.3921	1.691131	H	7.130062	-5.63431	0.436459
O	-0.68505	-1.72087	2.105431	O	7.546097	4.052401	0.540659
N	-0.87784	1.197691	1.780205	O	5.592149	6.838863	-0.48787
C	5.418813	-2.27318	1.31826	O	-9.34272	2.485799	0.467668
O	1.336641	6.157247	0.951945	O	-7.88538	5.429131	-0.69832
C	5.184287	0.110224	1.328163	O	-4.91822	-4.27628	-1.0544
H	5.621129	1.100283	1.227621	O	-7.37758	-6.1865	0.895669
C	5.998074	-0.99116	1.200309	O	5.884661	-4.40407	-1.49774
O	-1.20023	5.987943	1.064658	O	8.989958	-4.97898	-0.21463
C	3.781928	0.029903	1.560742	C	7.825641	3.725023	1.879595
C	3.065967	1.245656	1.542274	H	7.387725	2.754833	2.161284
H	3.644641	2.148738	1.373513	H	8.911889	3.66387	1.984144
C	1.666337	3.809123	1.344447	H	7.443729	4.488878	2.573639
H	2.742181	3.896496	1.2933	C	5.87695	8.204554	-0.65876
C	1.064516	2.549223	1.538058	H	6.942804	8.421826	-0.4902
Pt	0.530416	-0.17073	1.881971	H	5.60962	8.553318	-1.66774
C	3.217381	-1.28992	1.727022	H	5.285331	8.759404	0.073879
O	1.962884	-1.54145	1.982941	C	-9.72432	2.240763	1.798285
N	1.724883	1.371207	1.642018	H	-10.7982	2.036489	1.801034
C	0.886098	4.928092	1.182006	H	-9.19717	1.370711	2.21934
C	-0.57062	4.827793	1.239654	H	-9.52582	3.108789	2.445045
C	-1.1781	3.616222	1.450329	C	-8.48262	6.654428	-1.03701
H	-2.25701	3.555663	1.475008	H	-8.10684	7.408256	-0.34008
C	-0.39709	2.448696	1.602859	H	-8.22831	6.963537	-2.06263
C	2.742481	6.346272	0.804133	H	-9.5798	6.610906	-0.95418
H	3.268563	6.081246	1.727959	C	-5.17174	-4.18193	-2.438
H	3.136105	5.764072	-0.03332	H	-5.46291	-3.16403	-2.73491
C	-2.62183	5.98093	1.082345	H	-4.24919	-4.44769	-2.96062
H	-3.01956	5.349155	0.280508	H	-5.96934	-4.87366	-2.74565
H	-2.99918	5.63205	2.049871	C	-7.61461	-7.57186	0.857842
C	-1.98041	-1.64197	1.9793	H	-7.43057	-8.04369	1.834943
C	-2.67663	-2.85706	1.904409	H	-8.6636	-7.71888	0.588107
H	-2.10137	-3.77636	1.918857	H	-6.98126	-8.07205	0.109428
C	-4.05493	-2.91447	1.771516	C	6.451225	-5.32574	-2.4033
C	-4.81717	-1.72662	1.774903	H	5.725461	-6.13116	-2.54461
C	-4.15245	-0.52265	1.834591	H	6.651838	-4.86013	-3.37986
H	-4.72875	0.398538	1.798051	H	7.389355	-5.75141	-2.02467
C	-2.73398	-0.40973	1.899533	C	9.645054	-6.20548	-0.00073
C	-2.19501	0.89154	1.82959	H	10.4965	-6.2471	-0.68479
H	-2.90661	1.707868	1.7586	H	10.01408	-6.29303	1.032281
H	-2.92616	7.014854	0.92013	H	8.983424	-7.06109	-0.2037

References

(1) Gaussian 16, Revision C.01, M. J. Frisch, G. W. Trucks, H. B. Schlegel, G. E. Scuseria, M. A. Robb, J. R. Cheeseman, G. Scalmani, V. Barone, G. A. Petersson, H. Nakatsuji, X. Li, M. Caricato, A. V. Marenich, J. Bloino, B. G. Janesko, R. Gomperts, B. Mennucci, H. P. Hratchian, J. V. Ortiz, A. F. Izmaylov, J. L. Sonnenberg, D. Williams-Young, F. Ding, F. Lipparini, F. Egidi, J. Goings, B. Peng, A. Petrone, T. Henderson, D. Ranasinghe, V. G. Zakrzewski, J. Gao, N. Rega, G. Zheng, W. Liang, M. Hada, M. Ehara, K. Toyota, R. Fukuda, J. Hasegawa, M. Ishida, T. Nakajima, Y. Honda, O. Kitao, H. Nakai, T. Vreven, K. Throssell, J. A. Montgomery, Jr., J. E. Peralta, F. Ogliaro, M. J. Bearpark, J. J. Heyd, E. N. Brothers, K. N. Kudin, V. N. Staroverov, T. A. Keith, R. Kobayashi, J. Normand, K. Raghavachari, A. P. Rendell, J. C. Burant, S. S. Iyengar, J. Tomasi, M. Cossi, J. M. Millam, M. Klene, C. Adamo, R. Cammi, J. W. Ochterski, R. L. Martin, K. Morokuma, O. Farkas, J. B. Foresman and D. J. Fox, Gaussian, Inc., Wallingford CT, 2019.

(2) J. P. Perdew, M. Ernzerhof and K. Burke, Rationale for mixing exact exchange with density functional approximations, *J. Chem. Phys.*, 1996, **105**, 9982–9985.

(3) C. Adamo and V. Barone, Toward reliable density functional methods without adjustable parameters: the PBE0 model, *J. Chem. Phys.*, 1999, **110**, 6158–6170.

(4) A. V. Marenich, C. J. Cramer and D. G. Truhlar, Universal solvation model based on solute electron density and on a continuum model of the solvent defined by the bulk dielectric constant and atomic surface tensions, *J. Phys. Chem. B*, 2009, **113**, 6378–6396.

(5) D. Andrae, U. Häußermann, M. Dolg, H. Stoll and H. PreuB, Energy-adjusted *ab initio* pseudopotentials for the second and third row transition elements, *Theor. Chim. Acta*, 1990, **77**, 123–141.

(6) A.W. Ehlers, M. Böhme, S. Dapprich, A. Gobbi, A. Höllwarth, V. Jonas, K. F. Köhler, R. Stegmann, A. Veldkamp, G. A. Frenking, Set of *f*-polarization functions for pseudo-potential basis sets of the transition metals Sc–Cu, Y–Ag and La–Au, *Chem. Phys. Lett.*, 1993, **208**, 111–114.

(7) P. C. Hariharan and J. A. Pople, The influence of polarization functions on molecular orbital hydrogenation energies, *Theoret. Chim. Acta*, 1973, **28**, 213–222.

(8) J. D. Dill and J. A. Pople, Self-consistent molecular orbital methods. XV. extended gaussian-type basis sets for lithium, beryllium, and boron, *J. Chem. Phys.*, 1975, **62**, 2921–2923.

(9) M. M. Francl, W. J. Pietro, W. J. Hehre, J. S. Binkley, M. S. Gordon, D. J. DeFrees and J. A. Pople, Self-consistent molecular orbital methods. XXIII. a polarization-type basis set for second-row elements, *J. Chem. Phys.*, 1982, **77**, 3654–3665.

(10) W. J. Hehre, R. Ditchfield and J. A. Pople, Self-conistent molecular orbital methods. XII. further extensions of gaussian-type basis sets for use in molecular orbital studies of organic molecules, *J. Chem. Phys.*, 1972, **56**, 2257–2261.

(11) M. Dolg, P. Pyykkö and N. Runeberg, Calculated structure and optical properties of $Tl_2Pt(CN)_4$, *Inorg. Chem.*, 1996, **35**, 7450–7451.

(12) R. E. Stratmann, G. E. Scuseria and M. J. Frisch, An efficient implementation of time-dependent density functional theory for the calculation of excitation energies of large molecules, *J. Chem. Phys.*, 1998, **109**, 8218–8224.

(13) M. E. Casida, C. Jamorski and K. C. Casida, Molecular excitation energies to high-lying bound states from time-dependent density-functional response theory: characterization and correction of the time-dependent local density approximation ionization threshold, *J. Chem. Phys.*,

1998, **108**, 4439–4449.
(14) R. Bauernschmitt and R. Ahlrichs, Treatment of electronic excitations within the adiabatic approximation of time dependent density functional theory, *Chem. Phys. Lett*, 1996, **256**, 454–464.
(15) T. Lu and F. Chen, Multiwfn: a multifunctional wavefunction analyzer, *J. Comput. Chem.*, 2012, **33**, 580–592.
(16) J. M. Younker and K. D. Dobbs, Correlating experimental photophysical properties of iridium(III) complexes to spin–orbit coupled TDDFT predictions, *J. Phys. Chem. C*, 2013, **117**, 25714–25723.
(17) R. A. Boto, F. Peccati, R. Laplaza, C. Quan, A. Carbone, J.-P. Piquemal, Y. Maday and J. Contreras-Garcia, NCIPLOT4: a new step towards a fast quantification of noncovalent interactions.
(18) J. Contreras-Garcia, E. R. Johnson, S. Keinan, R. Chaudret, J. P. Piquemal, D. N. Beratan and W. Yang, NCIPLOT: a program for plotting noncovalent interaction regions, *J. Chem. Theory Comput.*, 2011, **7**, 625–632.
(19) E. R. Johnson, S. Keinan, P. Mori-Sánchez, J. Contreras-García, A. J. Cohen and W. Yang, Revealing noncovalent interactions, *J. Am. Chem. Soc.*, 2010, **132**, 6498–6506.
(20) W. Humphrey, A. Dalke and K. Schulten, VMD: visual molecular dynamics, *J. Mol. Graphics*, 1996, **14**, 33–38.
(21) M. M. J. Smulders, M. M. L. Nieuwenhuizen, T. F. A. de Greef, P. van der Schoot, A. P. H. J. Schenning and E. W. Meijer, How to distinguish isodesmic from cooperative supramolecular polymerisation, *Chem. Eur. J.*, 2010, **16**, 362–367.
(22) P. A. Korevaar, C. Schaefer, T. F. A. de Greef and E. W. Meijer, Controlling chemical self-assembly by solvent-dependent dynamics, *J. Am. Chem. Soc.*, 2012, **134**, 13482–13491.
(23) T. V. Jones, M. M. Slutsky, R. Laos, T. F. A. de Greef and G. N. Tew, Solution ^{1}H NMR confirmation of folding in short *o*-phenylene ethynylene oligomers, *J. Am. Chem. Soc.*, 2005, **127**, 17235–17240.
(24) S. Schlamp, P. Thoma and B. Weber, New octahedral, head–tail iron(II) complexes with spin crossover properties, *Eur. J. Inorg. Chem.*, 2012, **16**, 2759–2768.
(25) X. de Hatten, D. Asil, R. Friend and J. R. Nitschke, Aqueous self-assembly of an electroluminescent double-helical metallopolymer, *J. Am. Chem. Soc.*, 2012, **134**, 19170–19178.
(26) Y. Xiang, W. Li, Y. Fang, D. Zhang, X. Li and W. Jin, Construction and luminescence property of a highly ordered 2D self-assembled amphiphilic bidentate organoplatinum(II) complex, *RSC Adv.*, 2016, **6**, 27360–27369.
(27) J. Wu, L. You, L. Lan, H. J. Lee, S.T. Chaudhry, R. Li, J.-X. Cheng and J. Mei, Semiconducting polymer nanoparticles for centimeters-deep photoacoustic imaging in the second near-ifrared window, *Adv. Mater.*, 2017, **29**, 1703403.